Map projections

Exploring and analysing different types of distortions caused by map projections

by

Maaike Bukman

to obtain the degree of Bachelor of Science

at the Delft University of Technology,

to be defended publicly on Tuesday July 16, 2024 at 3:00 PM.

Project duration:	February 29, 2024 – July 16, 2024	
Thesis committee:	dr. P.M. Visser,	TU Delft, supervisor
	dr. O. Jaïbi,	TU Delft, supervisor
	dr. B. van den Dries,	TU Delft

Layman's Abstract

Map are tools that project a piece of the curved surface of the Earth onto a flat map. This can be done in various ways with individual strengths and weaknesses. There are some projections, for example, that maintain form properly (Mercator), while others maintain area (Equal-area). Yet no map can ever truly represent the Earth as it is due to distortions in such things as distances and shapes. My thesis examines these distortions, explaining how they can be quantified via ideas including sampling points worldwide. It was observed that among well-known maps like Mercator and Winkel Tripel, Gott-Wagner has lesser distortion overall. However, which projection is best depends on what aspect is most important for its use, whether distance or area must be preserved more accurately.

Abstract

Maps, which have been in used for centuries, are constructed by map projections. A map projection is a transformation of the latitudes and longitudes positions on the globe to the x and y coordinates on a flat map. There are probably over a hundred of different map projections, some more practical than others. A perfect map is impossible to create, so it is essential to determine the next best alternative. The different maps can be classified in five different categories: Conformal, Equal-area, compromise, equidistant and true-direction. To evaluate this, various distortions are considered. The six distortions defined in this thesis are: area (A), isotropy (I), flexion (F), skewness (S), distance (D), and boundary cut (B). These distortions together form a comprehensive set of all distortions that occur due to map projections. Since these distortions are quite difficult to compute directly, they are numerically approximated. To achieve this, the data points of the coordinates need to be sampled, which can be done through various methods. This thesis examines systematic generation and random sampling of points. Additionally, it investigates how many points are needed to achieve a sufficiently homogeneous covering of the globe and a stable solution for the distortion, this is achieved from around 20.000 point on the globe. These methods are then applied to different map projections, including the Mercator, Equirectangular, Winkel Tripel, Gott-Wagner, and Azimuthal Equidistant and the Azimuthal Equidistant split into two-hemispheres.. Among these map projections, the Gott-Wagner projection has the lowest total distortion value and is therefore considered the best overall map projection. However, each distortion has its own advantages and disadvantages, so it is not possible to definitively declare one map projection as the best in all scenarios. Selecting the best map projection depends on minimising the distorting specific to its needs.

List of variables

Latitude	ϕ	The latitude represents a coordinate that specifies the north-south positions of a point on the surface of the sphere. The longitude ranges from $-\frac{\pi}{2}$ to $\frac{\pi}{2}$.
Longitude	λ	The longitude represents a coordinate that specifies the east-west positions of a point on the surface of the sphere. The longitude ranges from $-\pi$ to π.
x-coordinate	x	The x-coordinate represents the location of a point on a flat surface in the horizontal position.
y-coordinate	y	The y-coordinate represents the location of a point on a flat surface in the vertical position.
Transformation matrix	T	The transformation matrix transforms the longitude and latitude coordinates to x, y-coordinates
	a	a is the major axis of a Tissot indicatrix and a singular value of the transformation matrix T.
	b	b is the minor axis of a Tissot indicatrix and a singular value of the transformation matrix T
Jacobian matrix	J	The Jacobian matrix is a matrix that consists of the first-order partial derivatives of a multi variable function.
Hessian matrix	H	The Hessian matrix is a matrix that consists of the second-order partial derivatives of a multi variable function.
	L	The arc length measured on a map, depended on λ, ϕ, α and β.
	β	The arc length measured on a sphere.
	s	The arc length parameter.
Length element	ds	The length element on the unit sphere, thought of as the infinitesimal element of distance on the sphere.
	t	The arc length parameter.
Parameterisation vector	$\vec{r}(t)$	$\vec{r}(t)$ is the standard parameterisation vector of a sphere.
Velocity vector	v	The velocity vector parallel to the globe.
Perpendicular velocity vector	$v_\perp$	The velocity vector perpendicular to the globe.
Acceleration vector	a	The acceleration vector for a trajectory on the plane.
	u	The unit vector for the first derivatives at $t = 0$ of the latitude and longitude.
	$u_\perp$	The unit vector perpendicular to the vector u.
	w	The vector for the second derivatives at $t = 0$ of the latitude and longitude.
Area distortion	A	The area distortion is the distortion that describes the amount of deformation with respect to the area over the whole map.
Isotropy distortion	I	The isotropy distortion is the distortion that describes the amount of deformation with respect to the angles over the whole map.
Local flexion distortion	f	The local flexion distortion measures the change in direction of a straight line in a point on the globe in comparison with the line on the map.
Flexion distortion	F	The flexion distortion is the average of the absolute value of the local flexion distortion.
Local skewness distortion	s	The local skewness distortion measures the change in length of a straight line in a point on the globe in comparison with the line on the map.

Skewness distortion	S	The skewness distortion is the average of the absolute value of the local skewness distortion.
Distance distortion	D	The distance distortion is the value that shows de correlation between the path length between two points on the map and the path length between two points on the sphere.
Boundary cut distortion	B	The boundary cut distortion is the value that measures the length of the border on the globe.
Scaling factor	γ	The scaling factor that the map can be scaled with.
Angle of rotation	α	The angle of rotation of the unit vector to determine the flexion and skewness distortion. To make a full circle α ranges from 0 to 2π.

Contents

1

Introduction

The question of what constitutes the earliest known map is subject to debate. A wall painting from the ancient Anatolian city of Çatalhöyük, dating back to the 7th millennium BCE, is frequently regarded as one of the earliest known maps. However, whether this can be consider a true map is contested [1].The first recognised map is believed to have been created by Thales of Miletus around 600 years BCE, depicting the celestial sphere in a gnomic projection. Later, in approximately 150 B.C., the Greek astronomer and mathematician Hipparchus introduced stereographic and orthographic projections. This transformed the latitudes and longitudes on the globe to x and y coordinates to construct a flat map. After that people probably made hundreds or thousands more projections, some more practical than others. Different maps can be used for different purposes. For example, when measuring distances on a map, the accuracy can be distorted depending on the map projection used. As shown in Figure 1.1, the distances on the Equirectangular map are distorted, while on the Azimuthal Equidistant the distance is accurately presented.

(a) The distances between Madison-Madrid and Madison-Buenos Aires shown on the Equirectangular map and compared to the distances in reality [2]. As can be seen these are not equal to each other on the Equirectangular map.

(b) The distances between Madison-Madrid and Madison-Buenos Aires shown on the Azimuthal Equidistant map and compared to the distances in reality [2]. As can be seen these are equal to each other on the Azimuthal Equidistant.

Figure 1.1: The distances between Madison-Madrid and Madison-Buenos Aires shown on the Equirectangular map and the Azimuthal Equidistant map and compared to the distances in reality. On the Equirectangular map is seems that the two lines are of equal length, in comparison on the Azimuthal Equidistant the different accurate length is shown.

Beside distances, directions are also influenced by the type of map projections. As shown in Figure 1.2, the shortest path is not always represented as a straight line. On the Mercator map, the shortest path is not a straight line, but on the Stereographic, it is [2]. To identify which map projections preserve distances, directions and other qualities, mathematical principles are introduced.

(a) A Mercator map that shows a straight path from New York to Istanbul and the curved shortest path that follows a great circle [2].

(b) A Stereographic map that shows a straight path from New York to Istanbul and the shortest path that follows a great circle [2]. On the Stereographic map the shortest path is by straight line between certain points.

Figure 1.2

The mathematical study of map projections began to advance significantly in the 19th century, largely due to the contributions of Carl Friedrich Gauss and Nicolas Auguste Tissot. Tissot's indicatrices, introduced around 1880, visualise angular and area distortion on maps. Facilitating the classification of different types of map projections [3].
In 1827, Carl Friedrich Gauss published the "Theorema Egregium", latin for "Remarkable Therorem". This theorem has to do with the curvature of surfaces. One of the applications of this theorem that is significant for cartography, is that it implies that no flat map of the Earth can be perfect, not even for a small part of the Earth [4].
However, the need for accurate map projections extends traditional maps. Take for example the music and entertainment arena the sphere close to the Las Vegas Strip. The external surface of the sphere is covered with LED light panels which can show anything, shown in Figure 1.3a. The inside is also covered with a LED screen that wraps around the interior as shown in Figure 1.3b [5]. To display a two-dimensional video effectively on this spherical surface, theory from map projections is used.

(a) The sphere in Las Vegas from the outside, depicting a baseball on the spherical outside of the arena [6].

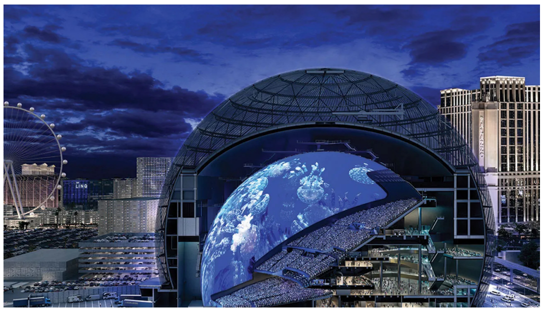

(b) The sphere with how it looks like from the inside, with the LED screen that is a sphere [7].

Figure 1.3

Knowing that there can not be a perfect map, the question is what would be the best map? How can different distortions be measured and how to determine the different kind of maps? This has been studied for quite some time now, but these studies have been mainly focusing on two types of distortions, the area and angle. In

this thesis, the distortions determined by Gott and Goldberg in an article from 2007 will be looked at, which provides six different distortions.
In Chapter 2 the basics of map projections will be explained, such as what are map projections, the different properties of map projections, the different construction methods and some mathematics behind map projections. Chapter 3 explains the distortions determined in the article of Gott and Goldberg from 2007 and looked at in further detail and how to determine them. There will be looked at the six different distortions, the first two being the area (A) and isotropy (I) distortion. Which determine the difference of the area surface on the map in comparison with the area surface on the globe. The isotropy distortion measures the distortion of the angle due to the map projection. The two most important distortions from the article are the flexion (F) and the skewness distortion (S). When drawing a straight line segment on the globe, the flexion distortion measures the change in direction and the skewness measures the change in length. And the last two distortions are the distance (D) and boundary cut (B) distortion, both these distortions are determined to punish cuts in the map. The distance distortion measures the relationship between the path length on the globe in comparison with the path length on the map. Lastly, the boundary cut measures the length of the cut of the map on the globe. In Chapter 4 the data points will be looked at, how these will be determined and how many are needed for an accurate mapping. In Chapter 5 the distortions determined in Chapter 3 are applied to various different map projections. For these map projections the transformation equations, derivatives and Hessian matrices are given and from this the distortions can be determined and plotted over the maps. Lastly, in Chapter 6 a conclusion is drawn and the results of chapter 5 will be looked at. Then in Chapter 7 the results and methods are discussed.
The code used for determining the distortions and generating corresponding maps, with and without those distortions, can be found in the following GitHub repository:
https://github.com/MaaikeBukman/BEP-Mapprojections.git

2

Basics of Map Projections

In this chapter the basics of map projections will be explained. For this first will be introduced the different coordinate systems that are with map projections. The different kind of properties that map projections can be classified as. Also the different methods to construct a map projection. After the mathematics can be introduced among them Tissot's indicatrices and the parameterization of geodesics.

2.1. Geographic coordinate systems

A geographic coordinate system (GCS) describes a three dimensional spherical surface on which a location on the Earth is defined. It consists of an angular unit measure and a prime meridian.
In the spherical system, the horizontal lines are lines of equal latitude, called parallels. The vertical lines are lines of equal longitude, called meridians. These lines together form a grid called the graticular network, as pictured in Figure 2.1.

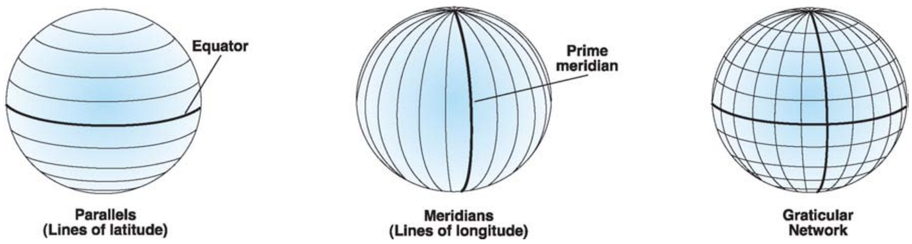

Figure 2.1: A visual representation of parallels and meridians on the sphere, and the construction of the graticular network, where both the parallels and the meridians are visible[8].

The circle of latitude midway in between the poles is called the Equator. Here the latitude is equal to zero. The line of longitude that has value zero is called the prime meridian. In general, for most geographic coordinate systems in Western Europe, the prime meridian goes through Greenwich, England. The origin of the graticular network is where the Equator intersects the prime meridian.
The pair (ϕ, λ) is used to denote latitude and longitude. The values for ϕ and λ can be measured in radian, decimal degrees or degrees, minutes and seconds (DMS). When looking at it from a mathematical approach, radians are most commonly used for angles. The latitude values range from $-90°$ to $90°$, or noted in radians $\phi \in [-\frac{\pi}{2}, \frac{\pi}{2}]$, with $\phi = 0$ being the Equator and $\phi = -\frac{\pi}{2}$ and $\phi = \frac{\pi}{2}$ the South and North Pole, respectively. The longitude values range from $-180°$ to $180°$, or $\lambda \in [-\pi, \pi]$, with $\lambda = 0$ being the prime meridian.

Definition 2.1.1 Circles with a radius equal to the Earth's radius are called great circles. The Equator and all meridians represent great circles. [8]

2.2. Projected coordinate systems

A projected coordinate system is designed for a flat two-dimensional plane. It originated from a geographical coordinate system that describes a three dimensional spherical surface. The location on the surface is determined by x and y coordinates on a grid, that reference to a central location. The x-coordinate specifies the horizontal position and the y-coordinate specifies the vertical position. The coordinates at the centre are given by $(x, y) = (0, 0)$. [8]

2.3. Map projection

A map projection is a transformation of the latitudes and longitudes positions on the globe to the x and y coordinates on a flat map. More precisely, a map projection requires a transformation from a set of two coordinates on the globe to a set of the Cartesian coordinates on the map, $(\phi, \lambda) \to (x, y)$. This is achieved with a transformation matrix T [9]. For map projections, T can be defined as:

$$T = \begin{bmatrix} x_\phi & x_\lambda \\ y_\phi & y_\lambda \end{bmatrix} \begin{bmatrix} \frac{1}{\cos(\phi)} & 0 \\ 0 & 1 \end{bmatrix} = \begin{bmatrix} \frac{x_\phi}{\cos(\phi)} & x_\lambda \\ \frac{y_\phi}{\cos(\phi)} & y_\lambda \end{bmatrix} \tag{2.3.1}$$

where x_ϕ represents the partial derivative of x with respect to ϕ and similarly for x_λ,y_ϕ and y_λ. Let K be the matrix:

$$K = \begin{bmatrix} \frac{1}{\cos(\phi)} & 0 \\ 0 & 1 \end{bmatrix} \tag{2.3.2}$$

2.4. Properties of map projections

A map projection is a transformation from the three-dimensional surface of the Earth to a two-dimensional flat surface. An easy way to visualise this, is to shine a light thought the Earth onto a surface, called the projection surface, as shown in Figure 2.2. Projecting the surface of the Earth onto a map causes distortions in various aspects, like shape, area, distance or direction.

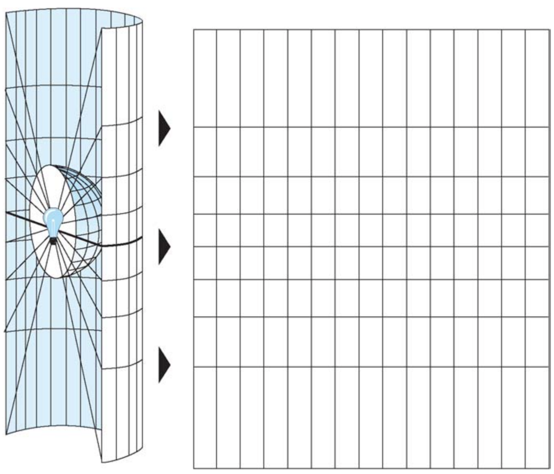

Figure 2.2: A visual representation of a map projection, the globe is projected on the flat paper from inside [8].

There are many different type of maps, each with different type of distortions that are sustained by doing a map projection. Some projections are made to minimise one specific type of distortion, while others aim to minimise multiple type of distortions. The maps that are attained by these projections can be classified into five different categories.

Definition 2.4.1 The classes of map projections are defined as [8][9]:

1. Conformal: conformal projections preserve local shape during the transformation from the globe to a map, but can significantly distort the size of features. Conformal projections are only applicable to small areas on Earth, therefore they are mostly used in topographic maps, navigation charts and weather maps.

2. Equal-area: equal-area projections preserve the size of area between the flat map and the globe, but they can have significant distortion in shape, angle and scale.

3. Compromise or conventional: these projections are neither conformal or equal area, they are designed to balance between the two properties.

4. Equidistant: these projections preserve the distances between certain points, but do not maintain scale correctly by the projection throughout the entire map.

5. True-direction: these projections maintain some of the great circle arcs, giving the directions of all points on the map accurately with relative to the centre. They can also be called azimuthal projections.

2.5. Classification based on construction

There are various methods to obtain a map projection. Three examples of the different types of methods to construct projections are[8]:

1. Conic projections: projection resulting from a projection of the Earth onto a cone. Mostly applicable for small areas only.

2. Cylindrical projections: projection resulting from a projection of the Earth onto a cylinder.

3. Planar projections: projection resulting from a projection onto a plane. Also known as an azimuthal projection.

2.5.1. Conic projections

There are multiple ways to do a conic projection, in the simplest form the conic projection aligns the tangent to the globe along a line of equal latitude, as shown in Figure 2.3. This line is called the standard parallel. The projection involves projecting meridians onto a conical surface and the parallel lines of latitude are projected onto the cone as rings. The cone is then sliced along a meridian to form the final conic projection, resulting in straight lines for the meridians and circular arcs for the parallels. The meridian straight across from the cut line is called the central meridian.

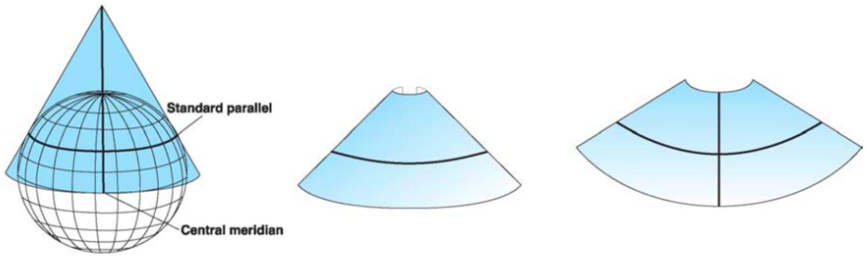

Figure 2.3: A visual representation of a tangent conic projection. There is one standard parallel, where the globe and the cone are tangent to each other [8].

With conic projections, the accuracy decreases as you move further away from the standard parallel. Because of this, cutting of the top can produce a more accurate projection.
A different approach of conic projections is when there are two standard parallels, as shown in Figure 2.4. These projections are called secant projections. The secant conic projection is in general better, with less distortions than the tangent conic projection.

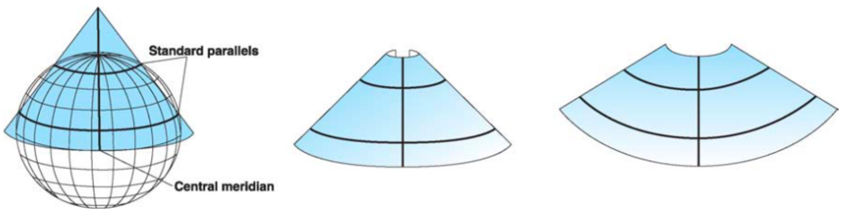

Figure 2.4: A visual representation of a secant conic projection, here in comparison with Figure 2.3 there are two standard parallels. Where the cone is tangent to the globe on two places[8].

A more general method of conic projections is the oblique projection, where the axis of the cone does not line up with the axis that goes straight from the North Pole to the South Pole. So the tip of the cone is not pointing to the north, but is askew and pointing some other way.
The classification of conic projections is bases on the specific projection. When the parallels are equally spaced, the projection is the equidistant North-South but neither conformal nor equal area [8].

2.5.2. Cylindrical projections

Like conic projections, cylindrical projections can have tangent and secant projections. For the normal cylindrical projection, the tangent line is along the Equator, as seen in Figure 2.5. The cylinder is sliced along a meridian to construct the final cylindrical projection. The meridians are equally spaced, while the spacing between parallels increases towards the poles. The cylindrical projections are conformal and display true direction along straight lines.

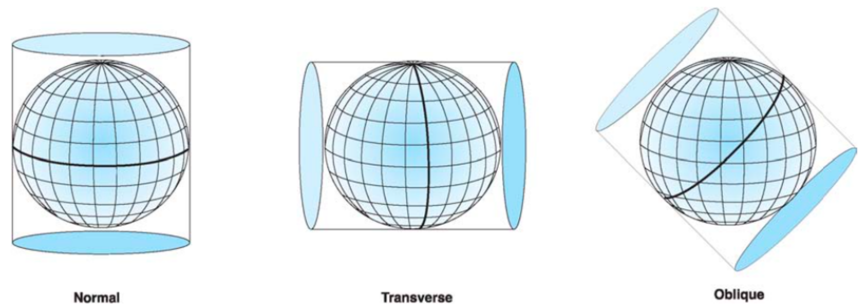

Figure 2.5: A visual representation of cylindrical projections, where in the normal cylindrical projection the cylinder is tangent to the Equator. For the transverse cylindrical projection the cylinder is tangent to a meridian from the North Pole to the South Pole. The oblique projection is when the cylinder is tangent to anywhere in between the equator and the meridians[8].

The cylinder can be rotated for a different type of cylindrical projections. During this, the tangent line changes. An example is the transverse cylindrical projections, where the tangent line is a meridian. The standard lines then run North-South, along this line the scale is accurate.

The oblique cylindrical projection is when the cylinder is anywhere along a great circle line between the Equator and the meridians. In general, the meridians and lines of latitude are then no longer straight lines. In all cylindrical projections, the tangent lines have no distortion and thus are lines of equidistance [8].

2.5.3. Planar projections

Planar projections, also know as azimuthal projections, project the globe onto a flat surface that is tangent to the globe. Usually this flat surface is tangent to the globe at one point but it can also be secant. If the point of contact is the North Pole or South Pole, it is called polar. If the tangent point is at the Equator it is called Equatorial. It can also be any point in between, being called oblique, as shown in Figure 2.6. The point of contact on the globe specifies the aspect and is called the focus of the projections. This is identified by a central longitude and a central latitude.

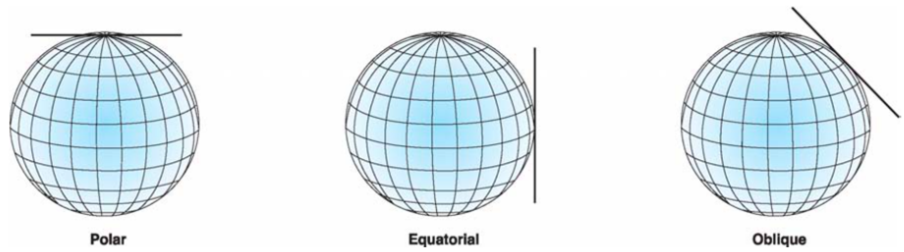

Figure 2.6: A visual representation of planar projections. For a polar planer projection the tangent point is at the North Pole or South pole. For the equatorial planer projection the tangent point is at the Equator and for an oblique planar projection the tangent point is anywhere in between. [8].

For polar projections, the parallels are circles centred on the pole, and meridians are straight lines. The great circles passing through the focus appear as straight lines. This means that the shortest distance from the centre to all other point on the map is are straight lines.
The perspective point may vary for different projections. The point of view determines how the globe is projected onto the flat surface. The perspective point can be the centre of the Earth, a surface point opposite from the focus, or a point external to the globe. This can be seen in Figure 2.7

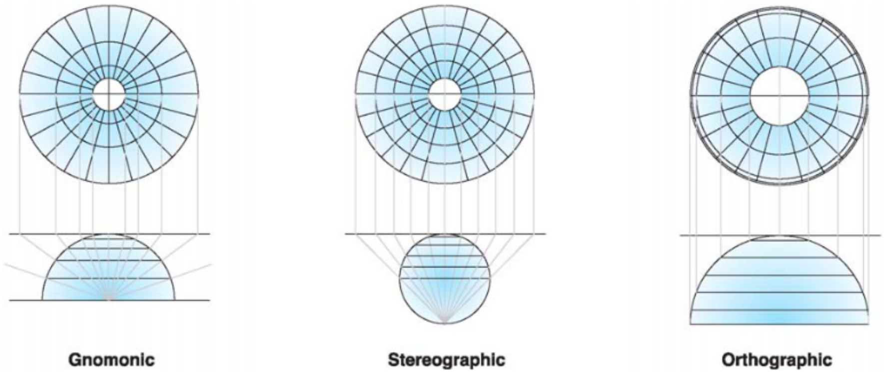

Figure 2.7: A visual representation of different points of perspective. When it is an gnomic projection the perspective point is from the centre of the Earth. A perspective point that is stereographic means that the point of view is from the opposing pole. When the perspective point is orthographic the point of view is orthogonal to [8].

Planar projections are classified by the point of contact called the focus point and point of view called the perspective point [8].

2.6. Geodesics

Definition 2.6.1 A geodesic is defined as the path of shortest distance between any two points on the surface of a spheroid. The path along a meridian between any two points form a geodesic [8].

A geodesic is shown in Figure 2.8.

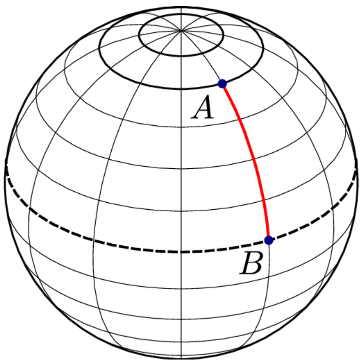

Figure 2.8: A visual representation a geodesic on a sphere, with the red line representing the geodesic from point A to point B [10].

A general geodesic is a great circle on the sphere, thus the Equator is also a geodesic.

2.7. Tissot's Indicatrix

Tissot's indicatrices were presented by Nicolas Auguste Tissot in 1859 and 1871, they are a mathematical way to visualise local distortions on a map . The Tissot's indicatrix is an ellipse that shows the angular and area distortions at the point where it is centred. This ellipse forms when projection a circle of infinitesimal size from the globe onto the map, this results in an ellipse of infinitesimal size whose major and minor semi-axis are the maximum and minimum scale factors at that point, of which also the angular distortion consists of. When an map projection is conformal, the ellipse is a perfect circle, which means that there is no angular distortion. When a map projection does have angular distortion this results in a ellipse, with a major and minor axis, as shown in Figure 2.9. When a map projection has area distortion the Tissot's indicatrices have varying sizes depending on the location on the map, as can be seen in Figure 2.10 which can be used to determine the different distortions. [11]

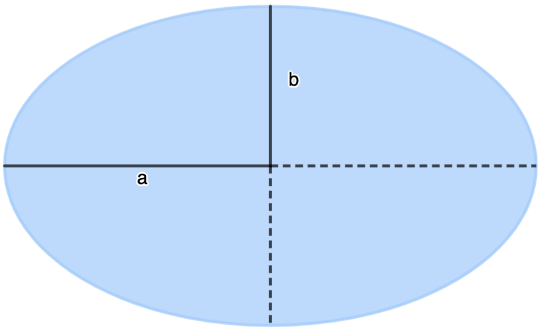

Figure 2.9: A visual representation of an ellipse, with a being the major axis and b being the minor axis. Also, a and b are the singular values of the transformation matrix T

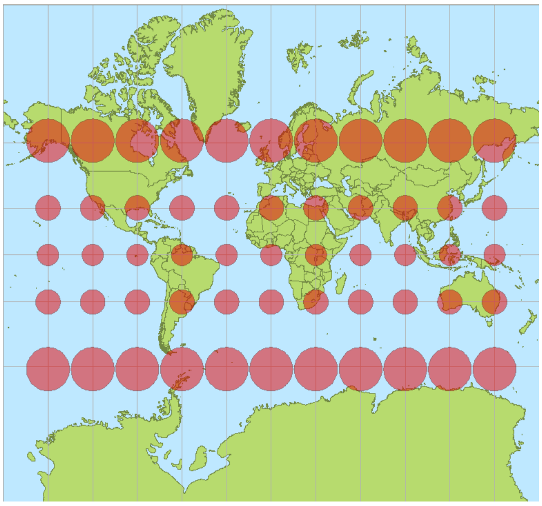

(a) A Mercator projection with the Tissot's indicatrices in red [12]. The Mercator is a conformal map projection and therefore there is no angular distortion which results in that the Tissot's indicatrices are perfect circles. However, as the Tissot's indicatrices do have different sizes the Mercator does have area distortions.

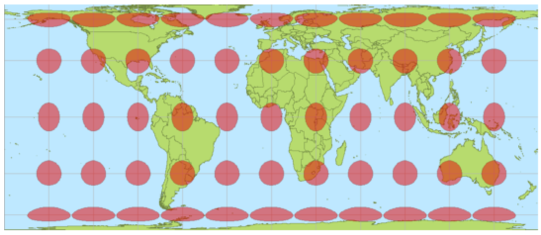

(b) A Behrmann projection with the Tissot's indicatrices in red [12]. The Behrmann projection has no angular distortion around the equator as the Tissot's indicatrices are perfect circles there. While it looks like that the Tissot's indicatrices all have the same areas, which would indicate that there is no area distortion.

Figure 2.10

One way to use Tissot's indicatrices is through the differential geometry of surfaces. The length element ds, thought of as the infinitesimal element of distance on the sphere, can be computed using the first fundamental form:

$$ds^2 = Ed\phi^2 + 2Fd\phi d\lambda + Gd\lambda^2 \tag{2.7.1}$$

where

$$E = \vec{r}_\phi \cdot \vec{r}_\phi, \tag{2.7.2}$$
$$F = \vec{r}_\phi \cdot \vec{r}_\lambda, \tag{2.7.3}$$
$$G = \vec{r}_\lambda \cdot \vec{r}_\lambda, \tag{2.7.4}$$

$\vec{r}_\phi$ represents the partial derivative of the vector $\vec{r}$ in $\mathbb{R}^3$ with respect to ϕ and $\vec{r}_\lambda$ represents the partial derivative of the vector $\vec{r}$ in $\mathbb{R}^3$ with respect to λ. We will use the standard parameterization of the sphere in $\mathbb{R}^3$:

$$\vec{r}(\lambda,\phi) = \begin{bmatrix} \cos\phi\cos\lambda \\ \cos\phi\sin\lambda \\ \sin\phi \end{bmatrix}. \tag{2.7.5}$$

The function for E, F and G follow:

$$E = 1, \tag{2.7.6}$$
$$F = 0, \tag{2.7.7}$$
$$G = \cos^2\phi. \tag{2.7.8}$$

This gives a length element ds on the unit sphere, for which

$$ds^2 = d\phi^2 + \cos^2\phi d\lambda^2. \tag{2.7.9}$$

Remembering that the Tissot's Indicatrix relates how distances on the sphere change when mapped to a planer surface. We want to find a transformation matrix that satisfies the following relations:

$$\begin{bmatrix} dx \\ dy \end{bmatrix} = T \begin{bmatrix} ds(\lambda,0) \\ ds(0,\phi) \end{bmatrix}. \tag{2.7.10}$$

From equation (2.7.9) the following relation can be determined:

$$\begin{bmatrix} d\lambda \\ d\phi \end{bmatrix} = K \begin{bmatrix} ds(\lambda,0) \\ ds(0,\phi) \end{bmatrix}, \qquad \text{with } K = \begin{bmatrix} \frac{1}{\cos\phi} & 0 \\ 0 & 1 \end{bmatrix}. \tag{2.7.11}$$

The distances on the sphere and the distances on the plane are related by the Jacobian Matrix, J:

$$\begin{bmatrix} dx \\ dy \end{bmatrix} = J \begin{bmatrix} d\lambda \\ d\phi \end{bmatrix}, \qquad \text{with } J = \begin{bmatrix} \frac{\partial x}{\partial \lambda} & \frac{\partial x}{\partial \phi} \\ \frac{\partial y}{\partial \lambda} & \frac{\partial y}{\partial \phi} \end{bmatrix}. \tag{2.7.12}$$

Which means that T satisfies:

$$T = \begin{bmatrix} \frac{\partial x}{\partial \lambda} & \frac{\partial x}{\partial \phi} \\ \frac{\partial y}{\partial \lambda} & \frac{\partial y}{\partial \phi} \end{bmatrix} \begin{bmatrix} \frac{1}{\cos\phi} & 0 \\ 0 & 1 \end{bmatrix} = \begin{bmatrix} \frac{\partial x}{\partial \lambda}\frac{1}{\cos\phi} & \frac{\partial x}{\partial \phi} \\ \frac{\partial y}{\partial \lambda}\frac{1}{\cos\phi} & \frac{\partial y}{\partial \phi} \end{bmatrix}. \tag{2.7.13}$$

Applying singular value decomposition to T will allow us to get the singular values a and b, a being the major axis and b the minor axes of the ellipse ($a > b > 0$). The values for a and b are the singular values of the transformation matrix T. These can be attained by the following sequence of equations:

$$ab = \sqrt{\det(T^T T)} = \sqrt{\det(T)\det(T)} = |\det(T)|, \tag{2.7.14}$$

$$a^2 + b^2 = \text{Trace}(T^T T). \tag{2.7.15}$$

Which results in the following equations for a and b:

$$a = \frac{\sqrt{\text{Trace}(T^T T) + 2|\det(T)|} + \sqrt{\text{Trace}(T^T T) - 2|\det(T)|}}{2}, \tag{2.7.16}$$
$$b = \frac{\sqrt{\text{Trace}(T^T T) + 2|\det(T)|} - \sqrt{\text{Trace}(T^T T) - 2|\det(T)|}}{2}. \tag{2.7.17}$$

It can be easily deduced from equations (2.7.14-2.7.15) that this holds. The $|\det(T)|$ and $\mathrm{Trace}(T^T T)$ can be written out knowing that the matrix T is a $(2x2)$ matrix, therefore

$$T = \begin{bmatrix} T_{11} & T_{12} \\ T_{21} & T_{22} \end{bmatrix}, \tag{2.7.18}$$

$$T^T T = \begin{bmatrix} T_{11}^2 + T_{12}^2 & T_{11}T_{12} + T_{21}T_{22} \\ T_{11}T_{12} + T_{21}T_{22} & T_{12}^2 + T_{22}^2 \end{bmatrix}. \tag{2.7.19}$$

Then the Trace of $T^T T$ is

$$\mathrm{Trace}(T^T T) = T_{11}^2 + T_{12}^2 + T_{21}^2 + T_{22}^2. \tag{2.7.20}$$

Also $|\det(T)|$ is given:

$$|\det(T)| = |T_{11}T_{22} - T_{12}T_{21}|. \tag{2.7.21}$$

With knowing T from equation 2.7.13, the following can be result is found

$$\mathrm{Trace}(T^T T) = T_{11}^2 + T_{12}^2 + T_{21}^2 + T_{22}^2 = \frac{x_\lambda^2 + y_\lambda^2}{\cos^2\phi} + x_\phi^2 + y_\phi^2, \tag{2.7.22}$$

$$|\det(T)| = |T_{11}T_{22} - T_{12}T_{21}| = \frac{|x_\lambda y_\phi - y_\lambda x_\phi|}{\cos\phi}. \tag{2.7.23}$$

2.8. Root Mean Square

The root mean square, also know as the quadratic mean and often abbreviated as RMS, is a special case of the generalised mean. In the case of a finite number of values, the root mean square is given by:

$$x_{\mathrm{RMS}} = \sqrt{\frac{1}{n}(x_1^2 + x_2^2 + \ldots + x_n^2)} = \sqrt{\langle x^2 \rangle}, \tag{2.8.1}$$

with $\langle x^2 \rangle$ being the mean of x^2 [13]. When the RMS is taken over continuous function between two values, it is defined as:

$$f_{\mathrm{RMS}} = \sqrt{\frac{1}{T_2 - T_1}\int_{T_1}^{T_2} [f(t)]^2 \, dt}. \tag{2.8.2}$$

In particular when looking at the globe the root mean square over a function g it is given by:

$$g_{\mathrm{RMS}} = \sqrt{\frac{1}{4\pi}\int_{-\pi}^{\pi}\int_{-\frac{\pi}{2}}^{\frac{\pi}{2}} [g]^2 \cos\phi \; d\phi d\lambda}. \tag{2.8.3}$$

2.9. Parameterization of a Geodesic on the Globe

The equation for the velocity vector and acceleration vector on the globe, can be found with the help of a parameterization of a geodesic on the globe. First a circle around the Equator is given by

$$\vec{r}(t) = \begin{bmatrix} \cos t \\ \sin t \\ 0 \end{bmatrix}. \tag{2.9.1}$$

To rotate the circle around the x-axis with angle α, the rotation matrix, R_x is used:

$$R_x(\alpha) = \begin{bmatrix} 1 & 0 & 0 \\ 0 & \cos\alpha & -\sin\alpha \\ 0 & \sin\alpha & \cos\alpha \end{bmatrix}. \tag{2.9.2}$$

To rotate around the y-axis with angle ϕ, the rotation matrix R_y is used:

$$R_y(\phi) = \begin{bmatrix} \cos\phi & 0 & -\sin\phi \\ 0 & 1 & 0 \\ \sin\phi & 0 & \cos\phi \end{bmatrix}. \tag{2.9.3}$$

To get the parameterization that shows the whole globe, these rotation matrices are multiplied and this gives the following result:

$$\vec{r}(t) = R_x(\alpha)\ R_y(\phi) \begin{bmatrix} \cos t \\ \sin t \\ 0 \end{bmatrix} = \begin{bmatrix} \cos\phi\cos t - \sin\alpha\sin\phi\sin t \\ \cos\alpha\sin t \\ \sin\phi\cos t + \sin\alpha\cos\phi\sin t \end{bmatrix}. \tag{2.9.4}$$

To obtain the equations for the $\phi(t)$ and $\lambda(t)$ we compare this with the general geodesic parameterization, $\vec{r}(t)$:

$$\vec{r}(t) = \begin{bmatrix} \cos\lambda(t)\cos\phi(t) \\ \sin\lambda(t)\cos\phi(t) \\ \sin\phi(t) \end{bmatrix}. \tag{2.9.5}$$

This equality is then

$$\begin{bmatrix} \cos\lambda(t)\cos\phi(t) \\ \sin\lambda(t)\cos\phi(t) \\ \sin\phi(t) \end{bmatrix} = \begin{bmatrix} \cos\phi\cos t - \sin\alpha\sin\phi\sin t \\ \cos\alpha\sin t \\ \sin\phi\cos t + \sin\alpha\cos\phi\sin t \end{bmatrix}, \tag{2.9.6}$$

from the following equation is deduced:

$$\sin\phi(t) = \sin\phi_0\cos t + \sin\alpha\cos\phi_0\sin t, \tag{2.9.7}$$

this gives

$$\begin{aligned} \phi(t) =& \arcsin(\sin\phi_0\cos(t) + \sin\alpha\cos\phi_0\sin t) \\ =& \phi_0 + t\sin\alpha - \frac{t^2}{2}\cos^2\alpha\tan\phi_0 + \mathcal{O}(t^3) \end{aligned} \tag{2.9.8}$$

Where it is approximated with the Taylor expansion. When knowing the equation for ϕ the first and second derivative at $t = 0$ can be determined:

$$\dot{\phi} = \sin\alpha, \tag{2.9.9}$$

$$\ddot{\phi} = -\cos^2\alpha\tan\phi. \tag{2.9.10}$$

The same can be done for the λ coordinates:

$$\begin{aligned} \lambda(t) =& \arcsin\left(\frac{\cos\alpha\sin t}{\cos\phi(t)}\right) \\ =& 0 + t\frac{\cos\alpha}{\cos\alpha} + \frac{t^2}{2}\frac{\sin 2\alpha\tan\phi}{\cos\phi} + \mathcal{O}(t^3) \end{aligned} \tag{2.9.11}$$

yielding the derivatives at $t = 0$,

$$\dot{\lambda} = \frac{\cos\alpha}{\cos\phi}, \tag{2.9.12}$$

$$\ddot{\lambda} = \sin 2\alpha\frac{\tan\phi}{\cos\phi}. \tag{2.9.13}$$

Now the velocity and the acceleration can be determined. For this we need the Jacobian and the Hessian matrices:

$$J = \begin{bmatrix} x_\lambda & x_\phi \\ y_\lambda & y_\phi \end{bmatrix}, \tag{2.9.14}$$

$$H_x = \begin{bmatrix} x_{\lambda\lambda} & x_{\phi\lambda} \\ x_{\lambda\phi} & x_{\phi\phi} \end{bmatrix}, \tag{2.9.15}$$

$$H_y = \begin{bmatrix} y_{\lambda\lambda} & y_{\phi\lambda} \\ y_{\lambda\phi} & y_{\phi\phi} \end{bmatrix}, \tag{2.9.16}$$

Matrix, K, is determined in Section 2.7:

$$K = \begin{bmatrix} \frac{1}{\cos\phi} & 0 \\ 0 & 1 \end{bmatrix}. \tag{2.9.17}$$

The velocity parallel to the globe can be determined as followed, using the chain rule:

$$\vec{v} = \begin{bmatrix} \dot{x} \\ \dot{y} \end{bmatrix} = J\,u, \tag{2.9.18}$$

with u being a unit vector on the sphere:

$$u = \begin{bmatrix} \dot{\lambda} \\ \dot{\phi} \end{bmatrix} = K \begin{bmatrix} \cos\alpha \\ \sin\alpha \end{bmatrix} = \begin{bmatrix} \frac{\cos\alpha}{\cos\phi} \\ \sin\alpha \end{bmatrix}. \tag{2.9.19}$$

For the velocity perpendicular to the globe it is as:

$$\vec{v_\perp} = \begin{bmatrix} \dot{x} \\ \dot{y} \end{bmatrix} = J\,u_\perp, \tag{2.9.20}$$

with $u_\perp$ being the unit vector with direction perpendicular to u:

$$u_\perp = K \begin{bmatrix} -\sin\alpha \\ \cos\alpha \end{bmatrix} = \begin{bmatrix} \frac{-\sin\alpha}{\cos\phi} \\ \cos\alpha \end{bmatrix}. \tag{2.9.21}$$

To determine the acceleration for a trajectory in the plane:

$$\vec{a} = \begin{bmatrix} \ddot{x} \\ \ddot{y} \end{bmatrix} = J w + \begin{bmatrix} u^T H_x u \\ u^T H_y u \end{bmatrix}, \tag{2.9.22}$$

with w being:

$$w = \begin{bmatrix} \ddot{\lambda} \\ \ddot{\phi} \end{bmatrix} = K \begin{bmatrix} \sin 2\alpha \\ -\cos^2\alpha \end{bmatrix} \tan\phi = \begin{bmatrix} \frac{\tan\phi \sin 2\alpha}{\cos\phi} \\ -\tan\phi\cos^2\alpha \end{bmatrix}. \tag{2.9.23}$$

3
The Distortions

There are multiple ways to measure the different distortions of a projection. In this chapter the distortion measures that were constructed by Goldberg and Gott in 2007 are described and analysed. In the report from 2007 they introduce scale distortion of flexion (F) and skewness (S) as well as area (A), isotropy (I), distance (D) and boundary cut (B) distortions. These six parameters are determined by [14]:

$$\begin{aligned}
&\text{Area} && = A && = \text{RMS } (\ln\ a_i b_i - \langle \ln\ a_i b_i \rangle) && (3.0.1)\\
&\text{Isotropy} && = I && = \text{RMS } \left(\ln \left(\frac{a_i}{b_i}\right)\right) && (3.0.2)\\
&\text{Flexion} && = F && = \langle |f_i| \rangle && (3.0.3)\\
&\text{Skewness} && = S && = \langle |s_i| \rangle && (3.0.4)\\
&\text{Distance} && = D && = \text{RMS } \left(\ln\ \frac{d_{ij,map}}{d_{ij,globe}}\right) && (3.0.5)\\
&\text{Boundary cut} && = B && = \frac{L_B}{4\pi} && (3.0.6)
\end{aligned}$$

Where a_i and b_i are the major and minor axes of the Tissot Intricatrix at random point x_i. The f and s are the flexion and skewness in a point and will be defined in this chapter. The $d_{ij,map}$ is the distance between two point on the map and $d_{ij,globe}$ is the distance between the same two points on the globe. L_B is the total length of the boundary cuts. The Root Mean Square (RMS) as described in Section 2.8 and the mean of x is indicated by $\langle X_i \rangle$. Goldberg and Gott computed these distortions by sampling 30.000 uniformly random points on the globe.
The natural logarithm is a good method for measuring this, because this means that with a scaling of one, the distortion will be zero. When using the natural logarithm in combination with the root mean square, a distortion that is two times bigger results in the same value as a distortion that is two times smaller. Which is what would be desired, because both are equally destructive for the quallity of the map. This goes for the area, isotropy and distance distortions.

3.1. Area

The area distortion is a measure for the distortion with the area surface, it measures the difference of the area surface on the map in comparison with the area surface on the globe. The area distortion is determined with Tissot Indicatrices, as described in Section 2.7. The definition of the area distortion is given by:

$$A = \text{RMS } (\ln\ a_i b_i - \langle \ln\ a_i b_i \rangle). \tag{3.1.1}$$

Looking more in depth at this definition, we can see a pleasant property:

$$\begin{aligned} A =& \text{RMS } (\ln\ a_i b_i - \langle \ln\ a_i b_i \rangle) \\ =& \sqrt{\langle (\ln\ a_i b_i - \langle \ln\ a_i b_i \rangle)^2 \rangle}, \end{aligned} \tag{3.1.2}$$

To make it easy, the squared area distortion is taken:

$$\begin{aligned} A^2 =& \langle (\ln\ a_i b_i - \langle \ln\ a_i b_i \rangle)^2 \rangle \\ =& \langle ((\ln\ a_i b_i)^2 - 2\ln\ a_i b_i \langle \ln\ a_i b_i \rangle + \langle \ln\ a_i b_i \rangle)^2 \rangle \\ =& \langle (\ln\ a_i b_i)^2 \rangle - \langle \ln\ a_i b_i \rangle^2 \end{aligned} \tag{3.1.3}$$

This is notable as a known formula from probability [15]:

$$\text{Var[X]} = E[X^2] - E[X]^2. \tag{3.1.4}$$

From this can be seen that the area distortion squared is the variance of $\ln(a_i b_i)$.

$$A^2 = \text{Var } (\ln\ a_i b_i), \tag{3.1.5}$$

$$A = \sqrt{\text{Var } (\ln\ a_i b_i)} = \text{SD } (\ln\ a_i b_i). \tag{3.1.6}$$

Therefore the area distortion is the standard deviation of $\ln(a_i b_i)$.
It is also important that the distortion is invariant under scaling of the map. This is important because otherwise the distortion is variable to an arbitrary value, which is not desired. To show that the area distortion is invariant under scaling of the map, the map is scaled by a scaling factor γ:

$$\begin{cases} x(\lambda,\phi) \to \tilde{x}(\lambda,\phi) = \gamma \cdot x(\lambda,\phi) \\ y(\lambda,\phi) \to \tilde{y}(\lambda,\phi) = \gamma \cdot x(\lambda,\phi) \end{cases}. \tag{3.1.7}$$

Knowing this, to show what this does to the area distortion. First has to be looked at what it does to the singular values a and b of the transformation matrix. Let $\tilde{T}$ be the transformation matrix under scaling by scaling factor γ,

$$\tilde{T} = \begin{bmatrix} \gamma \frac{\partial x}{\partial \lambda} \frac{1}{\cos\phi} & \gamma \frac{\partial x}{\partial \phi} \\ \gamma \frac{\partial y}{\partial \lambda} \frac{1}{\cos\phi} & \gamma \frac{\partial y}{\partial \phi} \end{bmatrix} = \gamma\ T, \tag{3.1.8}$$

$$|\det(\tilde{T})| = \frac{|\gamma^2 x_\lambda y_\phi - \gamma^2 y_\lambda x_\phi|}{\cos\phi} = \frac{\gamma^2 |x_\lambda y_\phi - y_\lambda x_\phi|}{\cos\phi} = \gamma^2\ |\det(T)|, \tag{3.1.9}$$

$$\text{Trace}(\tilde{T}^T \tilde{T}) = \frac{(\gamma x_\lambda)^2 + (\gamma y_\lambda)^2}{\cos^2\phi} + (\gamma x_\phi)^2 + (\gamma y_\phi)^2 = \gamma^2\ \text{Trace}(T^T T). \tag{3.1.10}$$

This gives the singular values, a' and b', that are the singular values of the scalled transformation matrix $\tilde{T}$:

$$\begin{aligned} \tilde{a} &= \frac{\sqrt{\text{Trace}(\tilde{T}^T \tilde{T}) + 2|\det(T')|} + \sqrt{\text{Trace}(\tilde{T}^T \tilde{T}) - 2|\det(\tilde{T})|}}{2} \\ &= \frac{\sqrt{\gamma^2 \text{Trace}(T^T T) + 2|\gamma^2 \det(T)|} + \sqrt{\gamma^2 \text{Trace}(T^T T) - 2|\gamma^2 \det(T)|}}{2} = \gamma a, \end{aligned} \tag{3.1.11}$$

$$\begin{aligned} \tilde{b} &= \frac{\sqrt{\text{Trace}(\tilde{T}^T \tilde{T}) + 2|\det(\tilde{T})|} - \sqrt{\text{Trace}(\tilde{T}^T \tilde{T}) - 2|\det(\tilde{T})|}}{2} \\ &= \frac{\sqrt{\gamma^2 \text{Trace}(T^T T) + 2|\gamma^2 \det(T)|} - \sqrt{\gamma^2 \text{Trace}(T^T T) - 2|\gamma^2 \det(T)|}}{2} = \gamma b. \end{aligned} \tag{3.1.12}$$

Now knowing that when a map is scaled with scaling factor γ the singular values are also multiplied with the scaling factor. With this information the area distortion of the scaled map can be determined:

$$\begin{aligned} \tilde{A} &= \text{RMS } (\ln(\tilde{a}_i \tilde{b}_i) - \langle \ln(\tilde{a}_i \tilde{b}_i) \rangle) \\ &= \text{RMS } (\ln(\gamma^2 \cdot a_i b_i) - \langle \ln(\gamma^2 \cdot a_i b_i) \rangle) \\ &= \text{RMS } (2\ln\gamma + \ln a_i b_i - \langle 2\ln\gamma + \ln a_i b_i \rangle) \\ &= \text{RMS } (2\ln\gamma + \ln\ a_i b_i - (2\ln\gamma + \langle \ln\ a_i b_i \rangle)) \\ &= \text{RMS } (\ln\ a_i b_i - \langle \ln\ a_i b_i \rangle) = A. \end{aligned} \tag{3.1.13}$$

Since the area distortion of the scaled map is the same as the area distortion of the original map, it can be concluded that the area distortion is invariant to scaling.
As equal area projections preserve the size of the area, the area distortion is zero for equal area map projections. Maps with low area distortion are mostly used for thematic maps, showing distributions such as population, farmland and forested area.

3.2. Isotropy

The isotropy distortion is a measure for the distortion of the angle, it measures the difference in the directions on the map in comparison with the directions on the globe. To determine this error, Tissot Indicatrices are used as described in Section 2.7. The definitoin of the isotropy distortion is:

$$I = \text{RMS}\left(\ln \frac{a_i}{b_i}\right). \tag{3.2.1}$$

The isotropy distortion can also be written out, but in this case it does do much:

$$I = \sqrt{\left\langle \left(\ln \frac{a}{b}\right)^2 \right\rangle} \quad \Rightarrow \quad I^2 = \left\langle \left(\ln \frac{a}{b}\right)^2 \right\rangle \tag{3.2.2}$$

To show that the isotropy distortion is invariant under scaling of the map, the same method is used as for the area distortion Section 3.1.

$$\begin{cases} x(\lambda,\phi) \to \tilde{x}(\lambda,\phi) = \gamma \cdot x(\lambda,\phi) \\ y(\lambda,\phi) \to \tilde{y}(\lambda,\phi) = \gamma \cdot x(\lambda,\phi) \end{cases} \tag{3.2.3}$$

The map is scaled with a scalar γ and as shown in Section 3.1 this results in that the singular values are multiplied with γ. This gives the isotropy distortion $\tilde{I}$ and the singular values $\tilde{a}$ and $\tilde{b}$ under scaling:

$$\tilde{I} = \text{RMS}\left(\ln \frac{\tilde{a}_i}{\tilde{b}_i}\right) = \text{RMS}\left(\ln \frac{\gamma \cdot a_i}{\gamma \cdot b_i}\right) = \text{RMS}\left(\ln \frac{a_i}{b_i}\right) = I. \tag{3.2.4}$$

Since $\tilde{a}$ is divided by $\tilde{b}$, the scaling factor γ disappears. Therefore the isotropy distortion under scaling is the same as the isotropy distortion of the original map. Thus can be concluded that scaling does not affect the isotropy distortion.
Conformal map projections preserve local shape, hence there is no angular distortion. This concludes in that they have a isotropy distortion of zero. Maps with a low isotropy are best used for topographic maps, navigation charts and weather maps.

3.3. Flexion

The flexion distortion measures the change in direction of a straight line on the globe to the map. A straight line on the surface of the Earth, might occur curved on the map. The flexion distortion is determined with the help of the velocity and acceleration vector. The acceleration vector in a two-dimensional map has two independent components: one perpendicular to the velocity vector and one parallel to its velocity vector, respectively $a_\perp$ and $a_\parallel$. For an individual point along a geodesic the flexion is defined, denoted by the local flexion distortion f:

$$f = \frac{a_\perp}{v} = \frac{dv_\perp}{ds}\frac{1}{v}. \tag{3.3.1}$$

Here ds is the arclength in radians. This equation can be rewritten with the definition of α which is the angle of rotation by the velocity vector.

$$d\alpha = \frac{dv_\perp}{v} \Rightarrow f = \frac{d\alpha}{ds}. \tag{3.3.2}$$

To determine the flexion distortion for the whole map projection, F, the average of the absolute value of the local flexion distortion is taken over the random points and all directions of α on the sphere. This is given by:

$$F = \langle |f_i| \rangle. \tag{3.3.3}$$

In Section 2.9 it has been shown how the acceleration and the velocity can be rewritten in terms of x and y and their respective derivatives. From this the following equation can be determined for the local flexion distortion:

$$f = \frac{a_\perp}{v} = \frac{\dot{x}\ddot{y} - \dot{y}\ddot{x}}{\dot{x}^2 + \dot{y}^2}. \tag{3.3.4}$$

Which means that the flexion distortion is given by:

$$F = \left\langle \left| \frac{\dot{x}\ddot{y} - \dot{y}\ddot{x}}{\dot{x}^2 + \dot{y}^2} \right| \right\rangle = \left\langle \frac{|\dot{x}\ddot{y} - \dot{y}\ddot{x}|}{\dot{x}^2 + \dot{y}^2} \right\rangle. \tag{3.3.5}$$

To see that the flexion is invariant to the scale of the map, the map is again scaled with scaling factor γ.

$$\begin{cases} x(\lambda,\phi) \to \tilde{x}(\lambda,\phi) = \gamma \cdot x(\lambda,\phi) \\ y(\lambda,\phi) \to \tilde{y}(\lambda,\phi) = \gamma \cdot x(\lambda,\phi) \end{cases}. \tag{3.3.6}$$

This results in the following

$$\tilde{F} = \left\langle \frac{|\dot{\tilde{x}}\ddot{\tilde{y}} - \dot{\tilde{y}}\ddot{\tilde{x}}|}{\dot{\tilde{x}}^2 + \dot{\tilde{y}}^2} \right\rangle = \left\langle \frac{|\gamma^2\dot{x}\ddot{y} - \gamma^2\dot{y}\ddot{x}|}{(\gamma\dot{x})^2 + (\gamma\dot{y})^2} \right\rangle = \left\langle \frac{\gamma^2|\dot{x}\ddot{y} - \dot{y}\ddot{x}|}{\gamma^2(\dot{x}^2 + \dot{y}^2)} \right\rangle = \left\langle \frac{|\dot{x}\ddot{y} - \dot{y}\ddot{x}|}{\dot{x}^2 + \dot{y}^2} \right\rangle = F. \tag{3.3.7}$$

Since the flexion distortion of the scaled map is equal to the flexion distortion of the original map. Thus can be concluded that the flexion is invariant under scaling of the map.
When looking at the flexion in a continuous manner, the flexion can be given by:

$$F = \frac{1}{8\pi^2} \int_{-\pi}^{\pi} \int_{-\frac{\pi}{2}}^{\frac{\pi}{2}} \int_{0}^{2\pi} \frac{|\det(\vec{v}\ \vec{a})|\cos\phi}{\vec{v}\cdot\vec{v}} d\alpha d\phi d\lambda. \tag{3.3.8}$$

The angle α represents the rotation of the unit vector, and $\cos\phi$ is derived from its projection onto the globe. If the flexion distortion is zero means that all geodesics will be straight lines, this is true for example for the gnomic projections. Maps with a low flexion are used for activities like navigation, surveying and planning.

3.4. Skewness

The skewness distortion measures the change in length between a straight line on the globe to the map. The map projection may makes things look lopsided on the map. For example, a line from the North Pole to the South Pole, on a map like the Mercator map, closer to the poles the line seems longer than it is supposed to be. For the skewness distortion the parallel component of the acceleration vector is of importance, skewness distortion in a random point is defined as, the local skewness distortion s:

$$s = \frac{a_\parallel}{v}. \tag{3.4.1}$$

To determine the skewness distortion, S, over a whole map, it is defined as the average of the absolute value of the local skewness distortion over the random points and all directions of α on the sphere. This is given by:

$$S = \langle |s_i| \rangle. \tag{3.4.2}$$

When writing the parallel acceleration in terms of x and y using the same method as that have been used for the Flexion and as shown in Section 2.9. The definition for the local skewness distortion can be written out in the following way:

$$s = \frac{a_\parallel}{v} = \frac{\vec{v}\cdot\vec{a}}{\vec{v}\cdot\vec{v}} = \frac{\dot{x}\ddot{x} + \dot{y}\ddot{y}}{\dot{x}^2 + \dot{y}^2}. \tag{3.4.3}$$

Which gives the definition for the skewness distortion:

$$S = \left\langle \left| \frac{\dot{x}\ddot{x} + \dot{y}\ddot{y}}{\dot{x}^2 + \dot{y}^2} \right| \right\rangle = \left\langle \frac{|\dot{x}\ddot{x} + \dot{y}\ddot{y}|}{\dot{x}^2 + \dot{y}^2} \right\rangle. \tag{3.4.4}$$

To see that the skewness is invariant to the scale of the map, the map is again scaled with scaling factor γ.

$$\begin{cases} x(\lambda,\phi) \to \tilde{x}(\lambda,\phi) = \gamma \cdot x(\lambda,\phi) \\ y(\lambda,\phi) \to \tilde{y}(\lambda,\phi) = \gamma \cdot x(\lambda,\phi) \end{cases}. \tag{3.4.5}$$

This result in the following

$$\tilde{S} = \left\langle \frac{|\dot{\tilde{x}}\ddot{\tilde{x}} + \dot{\tilde{y}}\ddot{\tilde{y}}|}{\dot{\tilde{x}}^2 + \dot{\tilde{y}}^2} \right\rangle = \left\langle \frac{|\gamma^2 \dot{x}\ddot{x} + \gamma^2 \dot{y}\ddot{y}|}{(\gamma\dot{x})^2 + (\gamma\dot{y})^2} \right\rangle = \left\langle \frac{\gamma^2 |\dot{x}\ddot{x} + \dot{y}\ddot{y}|}{\gamma^2(\dot{x}^2 + \dot{y}^2)} \right\rangle = \left\langle \frac{|\dot{x}\ddot{x} + \dot{y}\ddot{y}|}{\dot{x}^2 + \dot{y}^2} \right\rangle = S. \tag{3.4.6}$$

Since the skewness distortion of the scaled map is equal to the skewness distortion of the original map. Thus can be concluded that the skewness is invariant under scaling of the map.
When looking at the skewness in a continuous manner, the skewness distortion can be given by:

$$S = \frac{1}{8\pi^2} \int_{-\pi}^{\pi} \int_{-\frac{\pi}{2}}^{\frac{\pi}{2}} \int_{0}^{2\pi} \frac{|\vec{v} \cdot \vec{a}| \cos\phi}{\vec{v} \cdot \vec{v}} \, d\alpha d\phi d\lambda. \tag{3.4.7}$$

The angle α represents the rotation of the unit vector, and $\cos\phi$ is derived from its projection onto the globe. For conformal projections, the local skewness and the local flexion distortion are always equal in every point of the globe, which means that the flexion and skewness distortion are also equal. Unlike the flexion distortion, there is no known map projection with skewness zero.
Maps with a low skewness distortion are beneficial for tasks requiring precise distance measurements. They enable accurate estimation of travel distances and planning transportation routes.

3.5. Distance

The distance distortion measures the relationship between the path length on the globe in comparison with the path length on the map. The distance distortion is given by:

$$D = \text{RMS}\left(\ln \frac{d_{ij,map}}{d_{ij,globe}}\right). \tag{3.5.1}$$

Where $d_{ij,map}$ is the path length on the map measured olong a straight line along a geodesic between two point on the map, $((x_i, y_i), (x_j, y_j))$, and $d_{ij,globe}$ is the distance between the same two points on the globe, $((\lambda_i, \phi_i), (\lambda_j, \phi_j))$. This method uses the root mean square and the natural logarithm, this causes that the distance on the map is two times bigger than on the globe will give the same result as if it is two times smaller. The distance distortion written out gives:

$$D = \sqrt{\left\langle \left(\ln \frac{d_{ij,map}}{d_{ij,globe}}\right)^2 \right\rangle}. \tag{3.5.2}$$

When looking at it in a continuous manner, the distance distortion can be given by:

$$D = \sqrt{\left\langle \left(\ln\left(\frac{L(\lambda,\phi,\alpha,\beta)}{\beta}\right)\right)^2 \right\rangle}, \tag{3.5.3}$$

where $L(\lambda,\phi,\alpha,\beta)$ is the path length on the map and β the path length on the globe. With $\left\langle \ln\left(\frac{L(\lambda,\phi,\alpha,\beta)}{\beta}\right)\right\rangle$ defined as:

$$\begin{aligned} \left\langle \ln\left(\frac{L(\lambda,\phi,\alpha,\beta)}{\beta}\right)\right\rangle &= \frac{1}{4\pi} \int_{-\frac{\pi}{2}}^{\frac{\pi}{2}} \int_{0}^{2\pi} d\lambda d\phi \cos\phi \cdot \frac{1}{4\pi} \int_{0}^{\pi} \int_{0}^{2\pi} d\alpha d\beta \sin\beta \cdot \ln\left(\frac{L(\lambda,\phi,\alpha,\beta)}{\beta}\right) \\ &= \frac{1}{16\pi^2} \int_{-\frac{\pi}{2}}^{\frac{\pi}{2}} \int_{0}^{2\pi} \int_{0}^{\pi} \int_{0}^{2\pi} \cos\phi \sin\beta \ln \frac{L(\lambda,\phi,\alpha,\beta)}{\beta} \, d\alpha d\beta \, d\lambda d\phi. \end{aligned} \tag{3.5.4}$$

The path length on the map, $L(\lambda, \phi, \alpha, \beta)$, is defined as

$$L(\lambda, \phi, \alpha, \beta) = |r(\beta) - r(0)|, \tag{3.5.5}$$

with $r(\beta)$ as

$$\vec{r}(t) = \begin{bmatrix} \cos\lambda(t)\cos\phi(t) \\ \sin\lambda(t)\cos\phi(t) \\ \sin\phi(t) \end{bmatrix}, \tag{3.5.6}$$

with

$$\lambda(t) = \lambda_0 + \arcsin\left(\frac{\cos\alpha \sin t}{\cos\phi(t)}\right), \tag{3.5.7}$$

$$\phi(t) = \arcsin(\sin\phi_0 \cos t + \sin\alpha \cos\phi_0 \sin t). \tag{3.5.8}$$

The first double integral calculates the average value over the entire sphere, where the $\cos\phi$ is needed for the projection onto the globe. The second double integral calculates the average over all possible angels α and β, where the $\sin\beta$ is used to adjust. The $\vec{r}(t)$ represents the coordinates of a point on the surface. For a path along a geodesic, the $\lambda(t)$ and $\phi(t)$ are used, as defined as above. Where λ_0 and ϕ_0 are the the initial longitude and latitude and α determines the direction of the initial geodesic path. However, this definition does not clearly explain what happens when the points are close to a boundary cut.

3.6. Boundary cut

The boundary cut distortion is measured in the following way:

$$B = \frac{\text{length of the cut on the globe}}{4\pi}. \tag{3.6.1}$$

The length of the border on the globe is an difficult quantity to measure, therefore we categorise the maps into four different groups:

1. The non-interrupted projections, like the Azimuthal Equidistant, Gott-Mogolo Azimuthal and the Stereographic. These projection have a length of the cut on the globe of zero and therefore a boundary cut of
$$B = \frac{0}{4\pi} = 0.$$
2. The projections with a cut of length π on the globe, these are the most common map projections. Some examples of map projection with these boundary cuts are the Mercator, Equirectangular, Lambert Conic and Eckert VI. This results in a boundary cut of
$$B = \frac{\pi}{4\pi} = \frac{1}{4}.$$
3. The projections with a cut of length 2π on the globe, the map projections that result in a map consisting of two hemispheres are in this category. This results in a boundary cut of
$$B = \frac{2\pi}{4\pi} = \frac{1}{2}.$$
4. The projections that have multiple boundary cuts, for these map projections the boundary cut is difficult to determine and it depends on the specific projection. Some examples of these kind of map projections are the Boggs eumorphic, Fuller Projection and the Waterman butterfly projection.

The boundary cut distortion is also invariant to the scale of the map, because the measurement that this distortion is based on is measured on the globe and not on the map. And therefore the scale of the map does not effect this distortion at all.

3.7. Total distortion value

Knowing these different distortion, the best overall projection can be determined. To do this the different distortions need to be combined into one value. The method described in the article of Gott and Goldberg weights every distortion with normalisation constants. In the article the values of the distortions of the Equirectangular projection are chosen. This gives the following equation:

$$\sum_{\epsilon} = \left(\frac{A}{N_a}\right)^2 + \left(\frac{I}{N_i}\right)^2 + \left(\frac{F}{N_f}\right)^2 + \left(\frac{S}{N_s}\right)^2 + \left(\frac{D}{N_d}\right)^2 + \left(\frac{B}{N_b}\right)^2, \tag{3.7.1}$$

where N_a is the area distortion of the Equirectangular and similarly for the other normalisation constants. With $\sum_{\epsilon}$ being the total distortion value.

4 Data points

To determine the distortions as described in Chapter 3, can be done in two ways. The numerically or the continuous way. For the numerical method there need to be data points determined. There are numerous ways to select the data points of the coordinates (λ, ϕ) on the Earth. The two methods looked at here are randomly sampling data points and systematic generating data points. A few things need to be considered, one of which is how many data points are needed for an accurate mapping, which will be looked at with the area and isotropy distortions.

4.1. Systematic generating of points

During systematic generating of the data points, we take the range that we want to map and take a certain amount of points in between. We do this for the longitude, λ, and for the latitude, ϕ. In the case of a globe, the latitude ranges between $[-\frac{\pi}{2}, \frac{\pi}{2}]$ and the longitude ranges between $[-\pi, \pi)$.

4.2. Random sampling of points

In order to randomly sample points, we make use of the python function NumPy.random.uniform, which is a function from the NumPy package. It creates an array with uniformly distributed random values in between the boundaries that are given. For the longitude λ, it is clear that this needs to be between $-\pi$ and π. But for the latitude ϕ it involves a bit more thinking. The distribution on the globe is relevant should be uniformly. This means that we need to transform from spherical coordinates (λ, ϕ) to the coordinates on the map (x, y). To do this, we use:

$$\begin{aligned} &\lambda = \text{longitude} \Rightarrow \lambda \in [-\pi, \pi), \\ &\phi = \arcsin(\text{boundary}) \text{ with boundary } \in [-1, 1] \Rightarrow \phi \in [-\frac{\pi}{2}, \frac{\pi}{2}]. \end{aligned} \tag{4.2.1}$$

Where we randomly sample for λ in between $[-\pi, \pi)$ and for ϕ the boundary is in between $[-1, 1]$, where we apply the arcsin function, so that ϕ end in between $[-\frac{\pi}{2}, \frac{\pi}{2}]$. This comes from the idea that the area on the map has a relation to the map on the globe with the following:

$$dA = dy \cdot dx = \cos\phi \cdot d\phi \cdot d\lambda. \tag{4.2.2}$$

From with knowing how to go from the map to the globe, to get from the globe to the map, it has to be done the other way around.

$$\int_0^{2\pi} \int_{-\pi/2}^{\pi/2} f(\lambda, \phi) \cos\phi \; d\phi d\lambda = \int_0^{2\pi} \int_{-1}^{1} f(\lambda, \arcsin(s)) ds d\lambda. \tag{4.2.3}$$

Plotting this onto a 2D frame, a randomly generated set of data points is presented in Figure 4.1. From this figure it can be seen that around a latitude of zero there are more points and when going to $-\frac{\pi}{2}$ and $\frac{\pi}{2}$ there are less points and the amount of points is consistent with the change of λ. Which was what was expected since it represents the points on the globe.

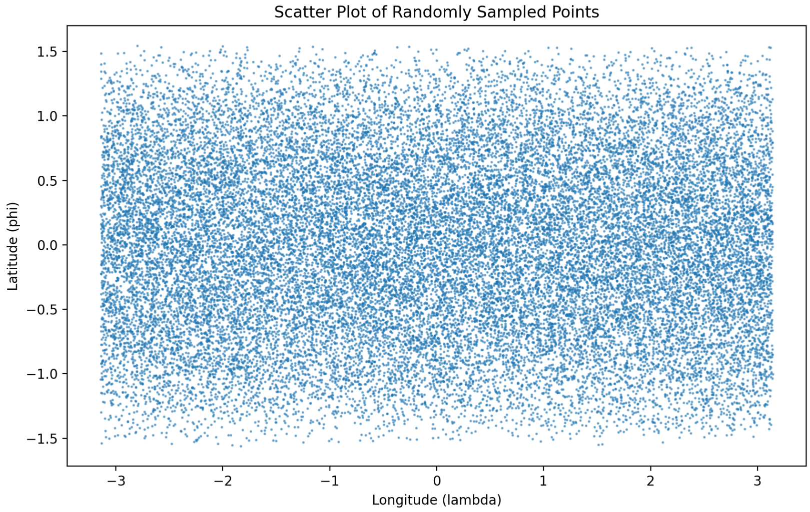

Figure 4.1: A visual representation of 30000 random sampled points.

4.3. Number of data points

It is also important to look at the number of points necessary to have a sufficiently homogeneous covering on the globe and a stable solution for the distortion. For this we have looked at different map projections and the results of the area and isotropy distortion for different amount of points. The results for the area distortions are plotted in Figure 4.2 and the results for the isotropy distortion are plotted in Figure 4.3.
Looking at the results for the area distortions, it is can be seen that for all projection after 20.000 points the result does not further improve. It does depend on the map projection itself. As can be seen the Equirectanglura is more stable that the Mercator. While the Azimuthal equidistant with two hemispheres is a lot more accurate from the start. With most map projections there are still big outliers at times, results that are further away from the mean. Therefore the mean is also a great way to find the area distortion. This gives a more stable solution every time, but it takes longer to compute because not only does the area distortion need to be computed for the biggest amount of values, but every value below that.
Looking at the results for the isotropy distortion, after 20.000 points the result is mostly stable with the couple outliers.
There has also been attempts to try and look at this kind of plots for the flexion and the skewness distortion, but due to a longer running time this would have taken days for one figure.

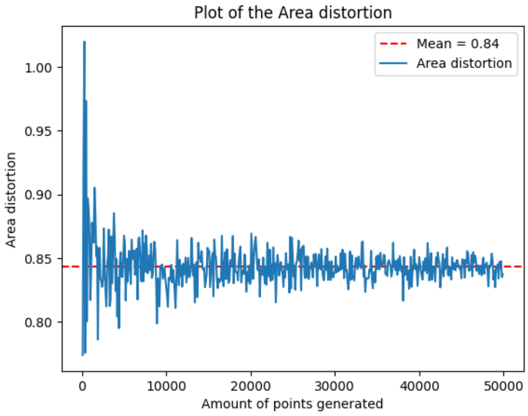

(a) The area distortion of the Mercator for all different amount of points generated up until 50.000 point.

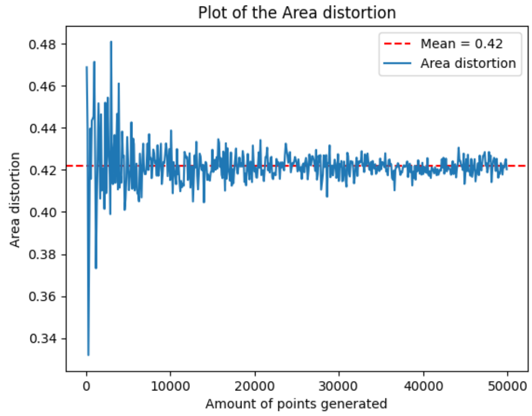

(b) The area distortion of the equirectangular for all different amount of points generated up until 50.000 point.

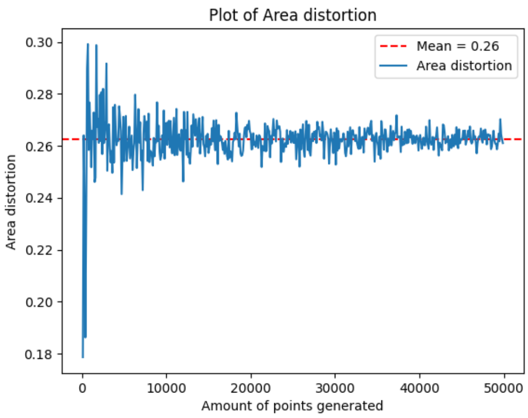

(c) The area distortion of the Winkel Tripel for all different amount of points generated up until 50.000 point.

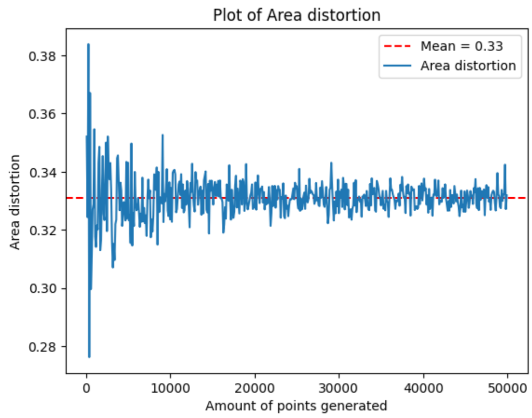

(d) The area distortion of the Gott Wagner for all different amount of points generated up until 50.000 point.

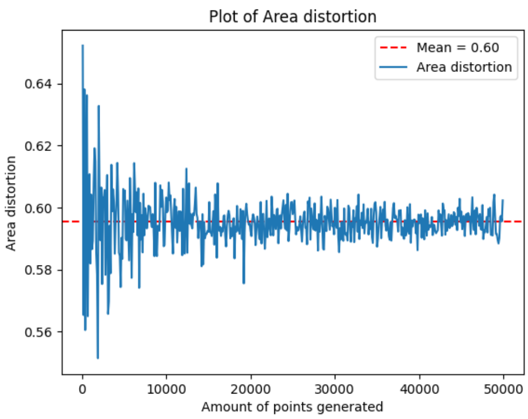

(e) The area distortion of the Azimuthal equidistant for all different amount of points generated up until 50.000 point.

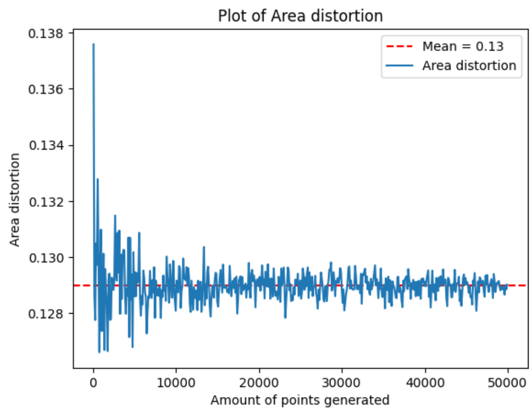

(f) The area distortion of the Azimuthal equidistant with two hemispheres for all different amount of points generated up until 50.000 point.

Figure 4.2: The area distortion for six different map projections for different amounts of generated data points up until 50.000. From these plots can be seen how many data points are needed to find a stable solution. This can be said from 20.000 points, with a couple outliers.

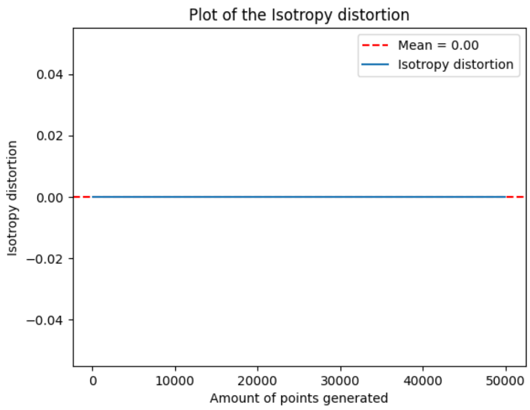

(a) Mercator

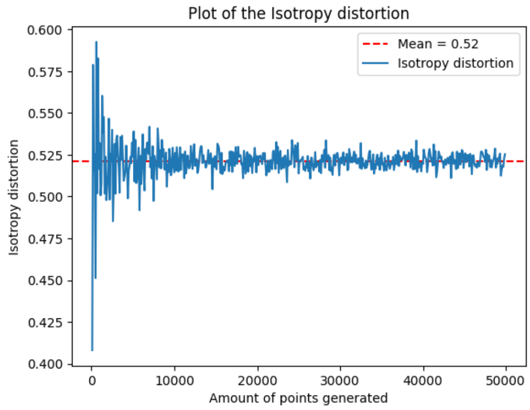

(b) Equi

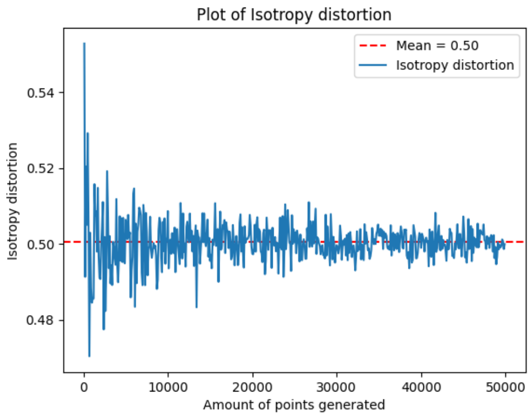

(c) Winkel Tripel

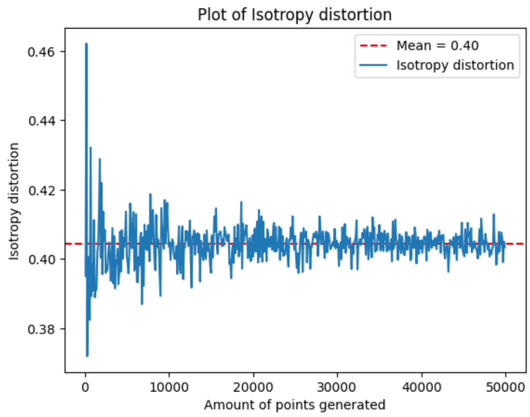

(d) Gott Wagner

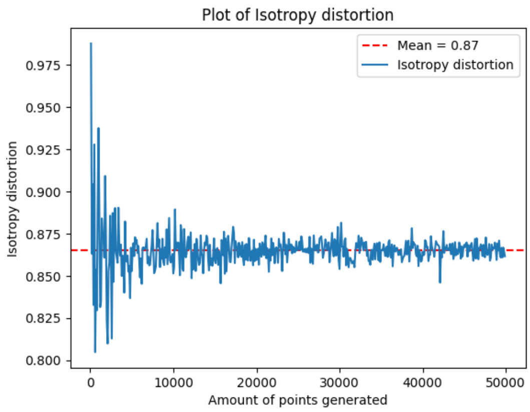

(e) Azimuthal

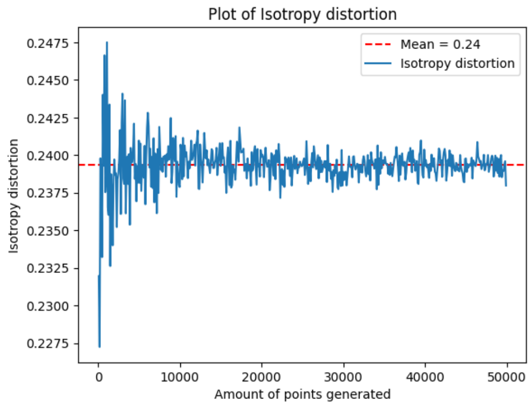

(f) Subfigure 6

Figure 4.3

5

Different map projections

5.1. Mercator

The Mercator projection has been widely used map around the world for a long time. It was presented by Gerardus Mercator in 1569. The Mercator map is a cylindrical conformal map, where the meridians are equally spaced straight lines. The parallels are straight lines that are spaced disproportionately. [11]

(a) Mercator map plotted with the inverse transformation function.

(b) Mercator map plotted without the inverse transformation function.

Figure 5.1: The Mercator projection plotted twice, first with the help of the inverse equation and second with only the forward transformation formulas. The Mercator map is a conformal map, with equally spaced meridians and disproportional spaced parallels.

The transformation formulas of the Mercator are given by:

$$x(\lambda,\phi) = \lambda, \tag{5.1.1}$$

$$y(\lambda,\phi) = \ln\left(\tan(\frac{\pi}{4} + \frac{\phi}{2})\right). \tag{5.1.2}$$

The inverse transformation formulas are:

$$\lambda = \frac{x}{R}, \tag{5.1.3}$$

$$\phi = \frac{\pi}{2} - 2\arctan(e^{-y}). \tag{5.1.4}$$

The range of the transformation of the Mercator is $\{(x,y)|\ x \in [-\pi,\pi], y \in \mathbb{R}\}$.
For the computation of the distortions the derivatives of the transformation formulas with respect to both λ and ϕ need to be determined. The derivatives for the Mercator projection are:

$$\frac{\partial x}{\partial \lambda} = 1, \tag{5.1.5}$$

$$\frac{\partial x}{\partial \phi} = 0, \tag{5.1.6}$$

$$\frac{\partial y}{\partial \lambda} = 0, \tag{5.1.7}$$

$$\frac{\partial y}{\partial \phi} = \frac{1}{\cos\phi}. \tag{5.1.8}$$

Knowing the partial derivatives, the results for the area distortion and isotropy distortion, as defined in Section 3.1 and Section 3.2, can be approximated. The area distortion and isotropy distortion of the Mercator are $A = 0.84$, $I = 0$. In Figure 5.2 the area and isotropy distortion are determined for different amounts of generated points and also the mean of these distortions. In Figure 5.3 a contour plot of the area distortion of the Mercator is plotted. It shows that around the Equator the area distortion is below zero, which means that the $\ln\ a_i b_i$ in those points is smaller than the average. And when going to the poles, the area distortion increases rapidly.

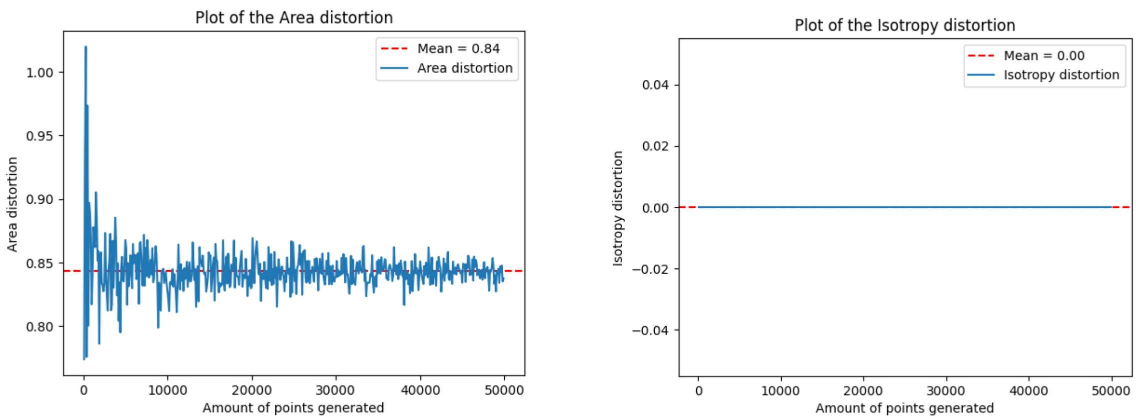

(a) The area distortion determined for different amount of generated points of the Mercator, with also showing the mean of 0.84.

(b) The isotropy distortion determined for different amount of generated points of the Mercator, with also showing the mean of 0.

Figure 5.2: The area and isotropy distortion for different amounts of generated points of the Mercator.

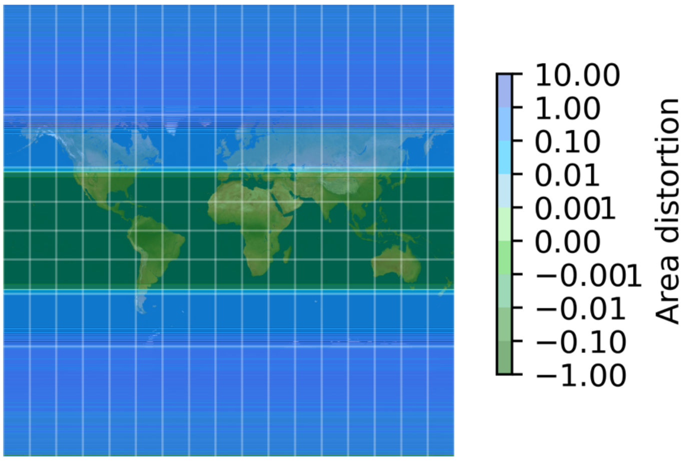

Figure 5.3: The contour plot of the area distortion on the Mercator. It shows that around the Equator the area distortion is below zero, which means that the $\ln(a_i b_i)$ in those points is smaller than the average. And when going to the poles, the area distortion increases rapidly. The area distortion is also not depended on the longitude, as the lines area all straight.

For the Mercator projection the flexion and skewness can be determined analytically [14]. To do this we use the definitions of the flexion and skewness when looking in continuous manner as defined in Sections 3.3 and 3.4. These are the following equations:

$$F = \frac{1}{8\pi^2} \int_{-\pi}^{\pi} \int_{-\frac{\pi}{2}}^{\frac{\pi}{2}} \int_{0}^{2\pi} \frac{|\vec{v_\perp} \cdot \vec{a}| \cos\phi}{\vec{v} \cdot \vec{v}} d\alpha d\phi d\lambda, \tag{5.1.9}$$

$$S = \frac{1}{8\pi^2} \int_{-\pi}^{\pi} \int_{-\frac{\pi}{2}}^{\frac{\pi}{2}} \int_{0}^{2\pi} \frac{|\vec{v} \cdot \vec{a}| \cos\phi}{\vec{v} \cdot \vec{v}} d\alpha d\phi d\lambda. \tag{5.1.10}$$

To determine the velocity and acceleration the method described in Section 2.9 is used. The Hessian matrices need to be determined, both with respect to x and y. For the Mercator these are easily computed, denoted by H_x and H_y:

$$H_x = \begin{bmatrix} x_{\lambda\lambda} & x_{\phi\lambda} \\ x_{\lambda\phi} & x_{\phi\phi} \end{bmatrix} = \begin{bmatrix} 0 & 0 \\ 0 & 0 \end{bmatrix}, \tag{5.1.11}$$

$$H_y = \begin{bmatrix} y_{\lambda\lambda} & y_{\phi\lambda} \\ y_{\lambda\phi} & y_{\phi\phi} \end{bmatrix} = \begin{bmatrix} 0 & 0 \\ 0 & \tan(\phi)\frac{1}{\cos\phi} \end{bmatrix}. \tag{5.1.12}$$

From the previous determination of the derivatives the jacobian is given by:

$$J = \begin{bmatrix} \frac{\partial x}{\partial \lambda} & \frac{\partial x}{\partial \phi} \\ \frac{\partial y}{\partial \lambda} & \frac{\partial y}{\partial \phi} \end{bmatrix} = \begin{bmatrix} 1 & 0 \\ 0 & \frac{1}{\cos\phi} \end{bmatrix}, \tag{5.1.13}$$

Knowing the K matrix from Section 2.7:

$$K = \begin{bmatrix} \frac{1}{\cos\phi} & 0 \\ 0 & 1 \end{bmatrix}. \tag{5.1.14}$$

As shown in Section 2.9, the velocity parallel to the globe can be determined as followed:

$$\vec{v} = \begin{bmatrix} \dot{x} \\ \dot{y} \end{bmatrix} = J\,u, \tag{5.1.15}$$

with u being given from Section 2.9:

$$u = \begin{bmatrix}\dot{\lambda}\\ \dot{\phi}\end{bmatrix} = K\begin{bmatrix}\cos\alpha\\ \sin\alpha\end{bmatrix} = \begin{bmatrix}\frac{\cos\alpha}{\cos\phi}\\ \sin\alpha\end{bmatrix}. \tag{5.1.16}$$

This gives the velocity vector for the Mercator:

$$\vec{v} = \begin{bmatrix}\dot{x}\\ \dot{y}\end{bmatrix} = \begin{bmatrix}1 & 0\\ 0 & \frac{1}{\cos\phi}\end{bmatrix}\begin{bmatrix}\frac{\cos\alpha}{\cos\phi}\\ \sin\alpha\end{bmatrix} = \begin{bmatrix}\frac{\cos\alpha}{\cos\phi}\\ \frac{\sin\alpha}{\cos\phi}\end{bmatrix}. \tag{5.1.17}$$

For the velocity perpendicular to the globe the same can be done, from Section 2.9:

$$\vec{v_\perp} = \begin{bmatrix}\dot{x}\\ \dot{y}\end{bmatrix} = J\,u_\perp, \tag{5.1.18}$$

with $u_\perp$ being given from Section 2.9:

$$u_\perp = K\begin{bmatrix}-\sin\alpha\\ \cos\alpha\end{bmatrix} = \begin{bmatrix}\frac{-\sin\alpha}{\cos\phi}\\ \cos\alpha\end{bmatrix}. \tag{5.1.19}$$

This gives the perpendicular velocity vector for the Mercator:

$$\vec{v_\perp} = \begin{bmatrix}\dot{x}\\ \dot{y}\end{bmatrix} = \begin{bmatrix}1 & 0\\ 0 & \frac{1}{\cos\phi}\end{bmatrix}\begin{bmatrix}\frac{-\sin\alpha}{\cos\phi}\\ \cos\alpha\end{bmatrix} = \begin{bmatrix}\frac{-\sin\alpha}{\cos\phi}\\ \frac{\cos\alpha}{\cos\phi}\end{bmatrix}. \tag{5.1.20}$$

To determine the acceleration for the Mercator projection, the equation from Section 2.9 is used:

$$\vec{a} = \begin{bmatrix}\ddot{x}\\ \ddot{y}\end{bmatrix} = Jw + \begin{bmatrix}u^T H_x u\\ u^T H_y u\end{bmatrix}, \tag{5.1.21}$$

with w being given from Section 2.9:

$$w = \begin{bmatrix}\ddot{\lambda}\\ \ddot{\phi}\end{bmatrix} = K\begin{bmatrix}\sin 2\alpha\\ -\cos^2\alpha\end{bmatrix}\cdot\tan\phi = \begin{bmatrix}\frac{\tan\phi\sin 2\alpha}{\cos\phi}\\ -\tan\phi\cos^2\alpha\end{bmatrix}. \tag{5.1.22}$$

For the Mercator these components are all know and this gives:

$$\begin{aligned}\vec{a} = \begin{bmatrix}\ddot{x}\\ \ddot{y}\end{bmatrix} &= \begin{bmatrix}1 & 0\\ 0 & \frac{1}{\cos\phi}\end{bmatrix}\begin{bmatrix}\frac{\tan\phi\sin 2\alpha}{\cos\phi}\\ -\tan\phi\cos^2\alpha\end{bmatrix} + \begin{bmatrix}0\\ \frac{\sin^2\alpha\tan\phi}{\cos\phi}\end{bmatrix}\\ &= \begin{bmatrix}\frac{\tan\phi\sin 2\alpha}{\cos\phi}\\ \frac{-\tan\phi\cos\alpha}{\cos\phi}\end{bmatrix}.\end{aligned} \tag{5.1.23}$$

This gives the following calculations for value of the Flexion:

$$\begin{aligned}F &= \frac{1}{8\pi^2}\int_{-\pi}^{\pi}\int_{-\frac{\pi}{2}}^{\frac{\pi}{2}}\int_{0}^{2\pi}\frac{|\vec{v_\perp}\cdot\vec{a}|\cos\phi}{\vec{v}\cdot\vec{v}}\,d\alpha d\phi d\lambda\\ &= \frac{1}{8\pi^2}\int_{-\pi}^{\pi}\int_{-\frac{\pi}{2}}^{\frac{\pi}{2}}\int_{0}^{2\pi}\frac{|\frac{-\cos\alpha\tan\phi}{\cos^2\phi}|\cos\phi}{\frac{1}{\cos^2\phi}}\,d\alpha d\phi d\lambda.\end{aligned} \tag{5.1.24}$$

The integral can be split up and solved:

$$\begin{aligned}F &= \frac{1}{8\pi^2}\int_{-\pi}^{\pi}1\,d\lambda\int_{-\frac{\pi}{2}}^{\frac{\pi}{2}}\frac{|\frac{\tan\phi}{\cos^2\phi}|\cos\phi}{\frac{1}{\cos^2\phi}}\,d\phi\int_{0}^{2\pi}|-\cos\alpha|\,d\alpha\\ &= \frac{1}{8\pi^2}\int_{-\pi}^{\pi}1\,d\lambda\int_{-\frac{\pi}{2}}^{\frac{\pi}{2}}|\sin\phi|\,d\phi\int_{0}^{2\pi}|\cos\alpha|\,d\alpha\\ &= \frac{1}{8\pi^2}\cdot 2\pi\cdot 2\cdot 4 = \frac{2}{\pi}.\end{aligned} \tag{5.1.25}$$

The calculation of the skewness can be done in the same way:

$$
\begin{aligned}
S &= \frac{1}{8\pi^2}\int_{-\pi}^{\pi}\int_{-\frac{\pi}{2}}^{\frac{\pi}{2}}\int_{0}^{2\pi}\frac{|\vec{v}\cdot\vec{a}|\cos\phi}{\vec{v}\cdot\vec{v}}\,d\alpha d\phi d\lambda \\
&= \frac{1}{8\pi^2}\int_{-\pi}^{\pi}\int_{-\frac{\pi}{2}}^{\frac{\pi}{2}}\int_{0}^{2\pi}\frac{|\frac{\sin\alpha\tan\phi}{\cos^2\phi}|\cos\phi}{\frac{1}{\cos^2\phi}}\,d\alpha d\phi d\lambda.
\end{aligned}
\tag{5.1.26}
$$

This can be split up for each integral and solved:

$$
\begin{aligned}
S &= \frac{1}{8\pi^2}\int_{-\pi}^{\pi} 1\,d\lambda \int_{-\frac{\pi}{2}}^{\frac{\pi}{2}}\frac{|\frac{\tan\phi}{\cos^2\phi}|\cos\phi}{\frac{1}{\cos^2\phi}}\,d\phi\int_{0}^{2\pi}|\sin\alpha|\,d\alpha \\
&= \frac{1}{8\pi^2}\int_{-\pi}^{\pi} 1\,d\lambda \int_{-\frac{\pi}{2}}^{\frac{\pi}{2}}|\sin\phi|\,d\phi\int_{0}^{2\pi}|\sin\alpha|\,d\alpha \\
&= \frac{1}{8\pi^2}\cdot 2\pi\cdot 2\cdot 4 = \frac{2}{\pi}.
\end{aligned}
\tag{5.1.27}
$$

The analytical method gives the following results for the flexion and the skewness, $F = \frac{2}{\pi}$ and $S = \frac{2}{\pi}$, which is within close range of the result that followed from of the numerical approach, $F = 0.64$ and $S = 0.64$. In Figure 5.4 and Figure 5.5 the flexion and skewness are plotted. Because the Mercator is an conformal map, the flexion and skewness result in the same plot as they are equal to each other. The plots of the flexion distortion and the skewness distortion show that the local flexion distortion is the closest to zero at the Equator. When going towards the poles the flexion increases. The flexion is also independent of the longitude, as the lines are all straight.

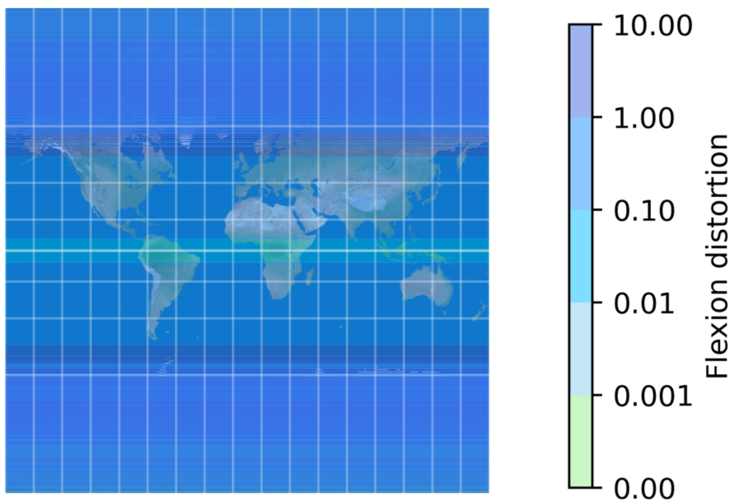

Figure 5.4: The contour plot of the flexion distortion on the Mercator. The local flexion distortion is the closest to zero at the Equator. When going towards the poles the flexion increases. The flexion is also independent of the longitude, as the lines are all straight.

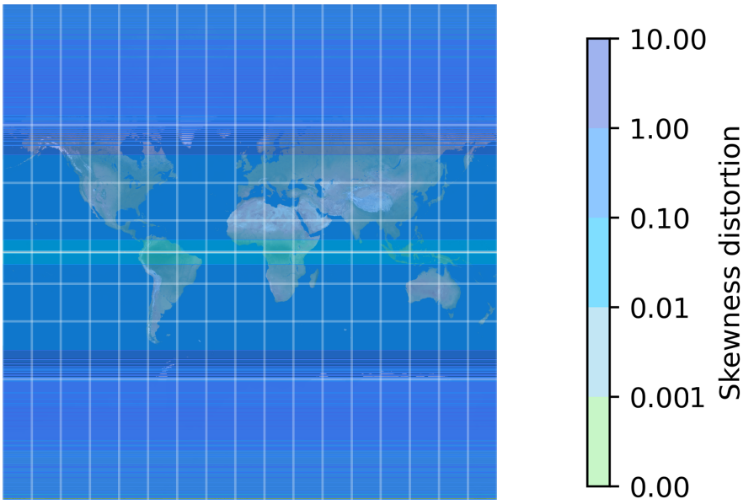

Figure 5.5: The contour plot of the flexion distortion on the Mercator. The local flexion distortion is the closest to zero at the Equator. When going towards the poles the flexion increases. The flexion is also independent of the longitude, as the lines are all straight.

The distance distortion is obtained by the numerical approximation with randomly generating the data points, in figure 5.6 the distance distortion is determined for different amount of generated points and plotted. The distance distortion for the Mercator is $D = 0.44$.

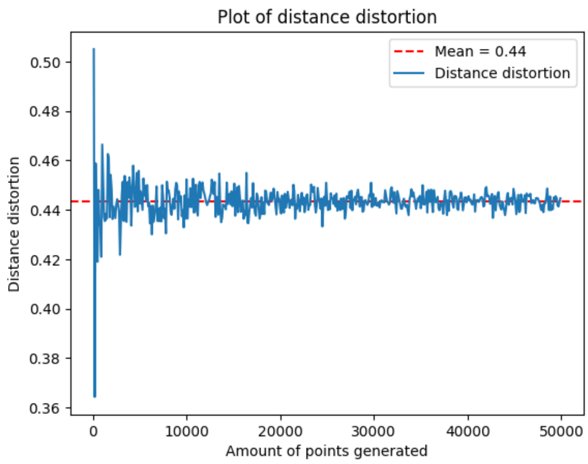

Figure 5.6: The distance distortion determined for different amount of randomly generated points of the Mercator, with also showing the mean of 0.44.

The Mercator projection has a cut of length π on the globe, and thus from the definition from Section 3.6 the boundary cut distortion of the Mercator projection is $B = \frac{\pi}{4\pi} = \frac{1}{4}$.

5.2. Equirectangular

The Equirectangular projection is a quite simple map projection. The projection maps meridians to equally spaced vertical straight lines and the lines of latitude to horizontal equally spaced straight lines. The Equirectangular projection in neither conformal nor equal area [16].

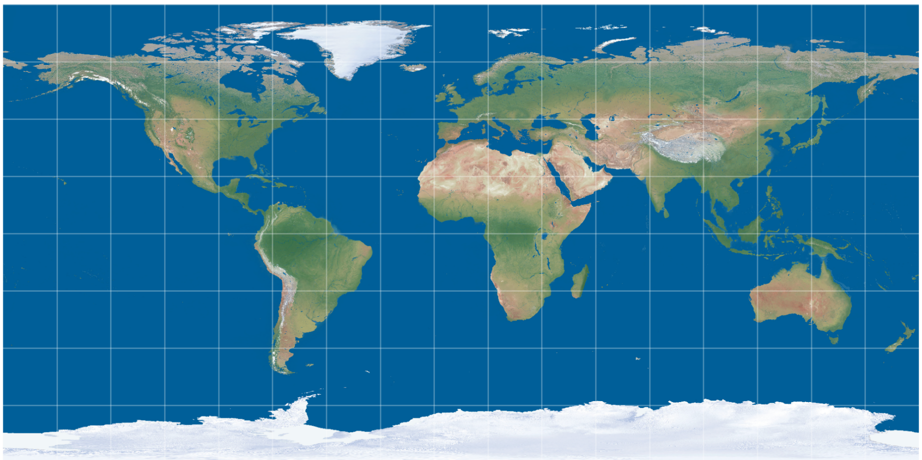

Figure 5.7: The Equirectangular projection with $\phi_1 = 0, \phi_0 = 0$ and $\lambda_0 = 0$. The meridians are equally spaced vertical straight lines and the parallels are equally spaced horizontal lines. The Equirectangular projection is neither conformal nor equal area.

The transformation formulas of the Equirectangular are given by:

$$x(\lambda,\phi) = (\lambda - \lambda_0)\cos(\phi_1), \tag{5.2.1}$$

$$y(\lambda,\phi) = \phi - \phi_0. \tag{5.2.2}$$

Where ϕ_1 is the standard parallels (north and south of the Equator), this is where the scale of the projection is true. The central parallel of the map is given by ϕ_0 and λ_0 is the central meridian of the map. The inverse transformation formulas are

$$\lambda(x,y) = \frac{x}{\cos\phi_1} + \lambda_0, \tag{5.2.3}$$

$$\phi(x,y) = y + \phi_0. \tag{5.2.4}$$

The range of transformation of the Equirectangular is $\{(x,y)|\ x \in [-\pi,\pi], y \in [-\frac{\pi}{2},\frac{\pi}{2}]\}$.
For the computation of the distortions the derivatives of the transformation formulas with respect to both λ and ϕ need to be determined. The derivatives for the Equirectangular projection are:

$$\frac{\partial x}{\partial \lambda} = \cos\phi_1, \tag{5.2.5}$$

$$\frac{\partial x}{\partial \phi} = 0, \tag{5.2.6}$$

$$\frac{\partial y}{\partial \lambda} = 0, \tag{5.2.7}$$

$$\frac{\partial y}{\partial \phi} = 1. \tag{5.2.8}$$

Knowing the partial derivatives, the results for the area distortion and isotropy distortion, as defined in Section 3.1 and Section 3.2, can be approximated. The area distortion and isotropy distortion of the Equirectangular are $A = 0.416$, $I = 0.514$. In figure 5.8 the area and isotropy distortion are determined for different amounts of generated points and also the mean of these distortions. In Figure 5.9 a contour plot of the area distortion of the Equirectangular is plotted and in Figure 5.10 a contour plot of the isotropy distortion of the Equirectangular is plotted. Figure 5.9 shows that near the Equator the area distortion is under zero, which means that the $\ln(a_i b_i)$ in those points is smaller than the average. Figure 5.9 shows that close to the Equator the isotropy distortion is zero, which is a result of the ϕ_1 and ϕ_0. Going closer to the poles, the isotropy distortion increases.

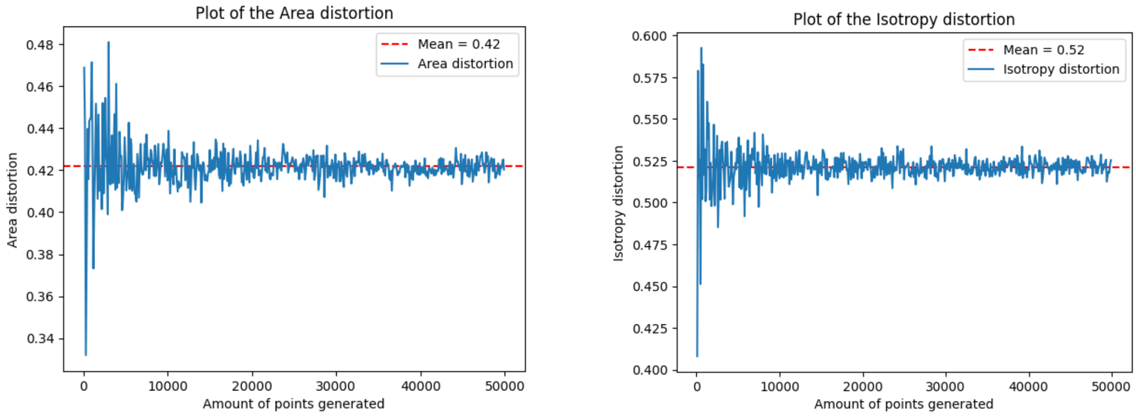

(a) The Area distortion determined for different amounts of generated points up till 50.000 for the Equirectangular, with also showing the mean of 0.26.

(b) The isotropy distortion determined for different amount of generated points for the Equirectangular, with also showing the mean of 0.50.

Figure 5.8: The area and isotropy distortion for different amounts of generated points of the Equirectangular.

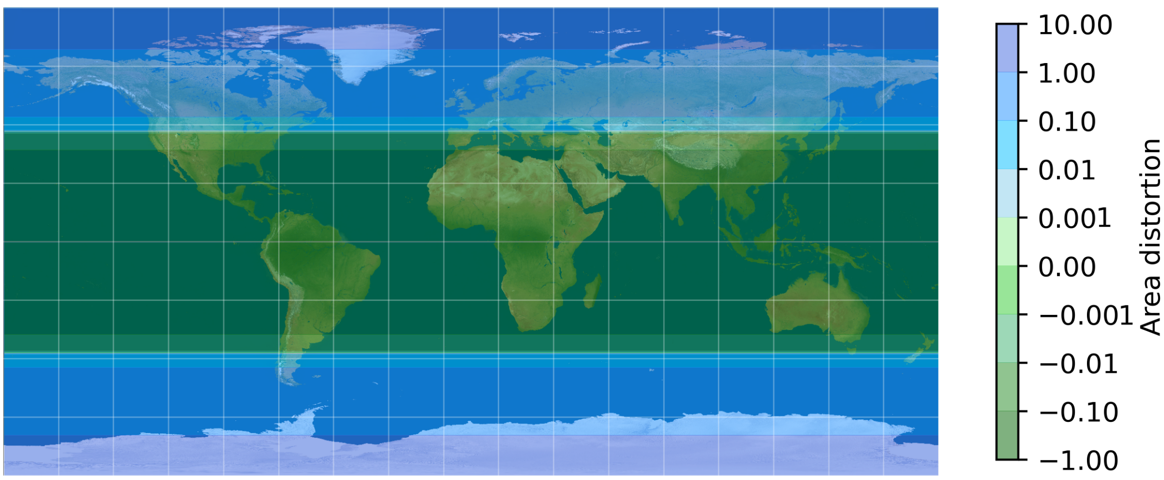

Figure 5.9: The contour plot of the area distortion on the Equirectangular (with $\phi_1 = 0, \phi_0 = 0$ and $\lambda_0 = 0$). It shows that near the Equator the area distortion is under zero, which means that the $\ln(a_i b_i)$ in those points is smaller than the average. The area distortion is independent of the longitude, as the lines are all straight.

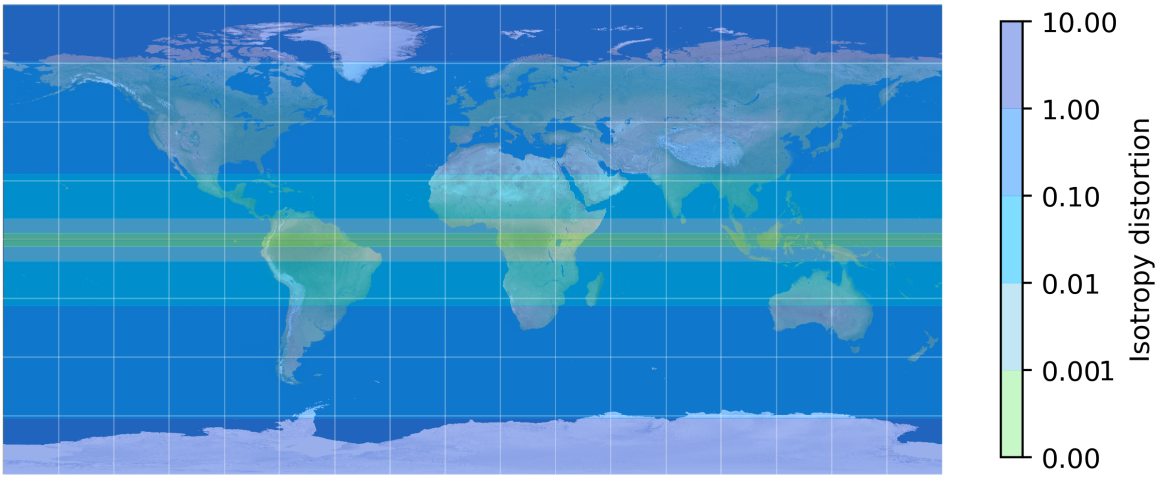

Figure 5.10: The contour plot of the isotropy distortion on the Equirectangular (with $\phi_1 = 0, \phi_0 = 0$ and $\lambda_0 = 0$). It shows that close to the Equator the isotropy distortion is zero, which is a result of the ϕ_1 and ϕ_0. Also going to the poles, the isotropy distortion increases. The isotropy is also independent of the longitude, as the lines are all straight.

For the calculation of the flexion and skewness distortion, the method explained in Sections 3.3 and 3.4 is carried out. These distortions are numerically approached and for this the Hessian matrix is needed, both with respect to x and y. For the Equirectangular these are easily computed, denoted by H_x and H_y:

$$H_x = \begin{bmatrix} x_{\lambda\lambda} & x_{\phi\lambda} \\ x_{\lambda\phi} & x_{\phi\phi} \end{bmatrix} = \begin{bmatrix} 0 & 0 \\ 0 & 0 \end{bmatrix}, \tag{5.2.9}$$

$$H_y = \begin{bmatrix} y_{\lambda\lambda} & y_{\phi\lambda} \\ y_{\lambda\phi} & y_{\phi\phi} \end{bmatrix} = \begin{bmatrix} 0 & 0 \\ 0 & 0 \end{bmatrix}. \tag{5.2.10}$$

Knowing these matrices, the flexion and skewness distortion are determined. The results from the numerical approach for the flexion and skewness distortion for the Equirectangular projection are: $F = 0.636$ and $S = 0.626$. In Figure 5.11 and Figure 5.12 the flexion distortion and skewness distortion is plotted, both distortions are close to zero around the Equator and are independent of the longitude. It can also be seen that the flexion increases quicker when going to the poles in comparison with the skewness.

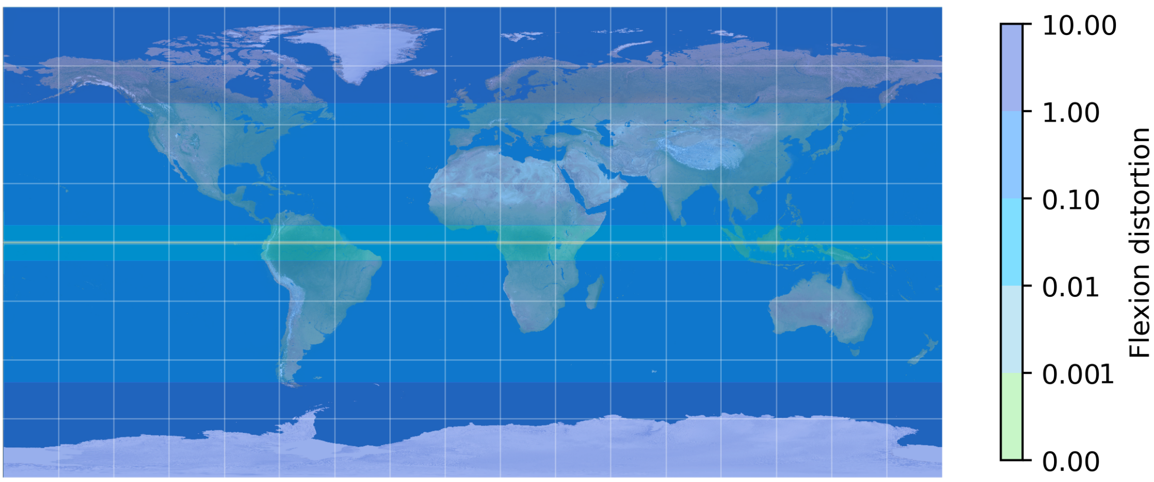

Figure 5.11: The contour plot of the flexion distortion on the Equirectangular projection. The local flexion distortion is close to zero around the Equator. When going towards the poles the flexion increases. The flexion is also independent of the longitude, as the lines are all straight.

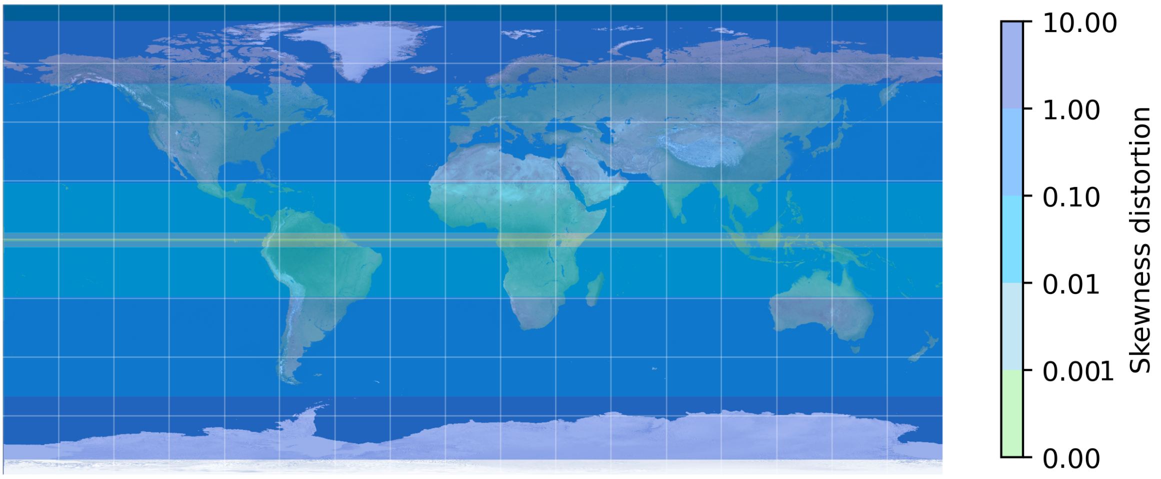

Figure 5.12: The contour plot of the skewness distortion on the Equirectangular projection. The local skewness distortion is close to zero around the Equator. When going towards the poles the skewness increases. The skewness is also independent of the longitude, as the lines are all straight.

The distance distortion is obtained by the numerical approximation with randomly generating the data points, in Figure 5.13 the distance distortion is determined for different amount of generated points and plotted. The distance distortion for the Equirectangular is $D = 0.45$.

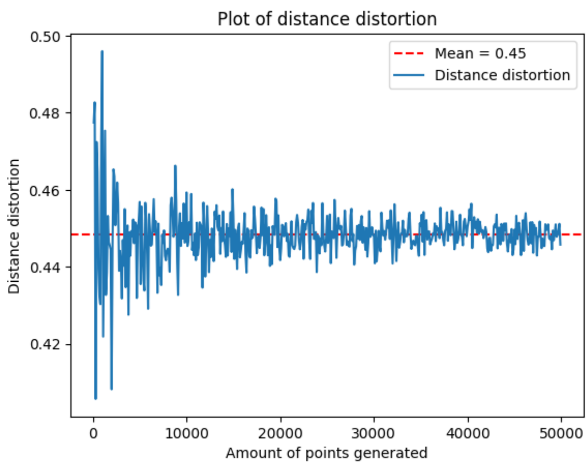

Figure 5.13: The distance distortion determined for different amount of randomly generated points of the equirectangular, with also showing the mean of 0.45.

The Equirectangular projection has a cut of length π on the globe, and thus from the definition from Section 3.6 the boundary cut distortion of the Equirectangular projection is $B = \frac{\pi}{4\pi} = \frac{1}{4}$.

5.3. Winkel Tripel

The Winkel Tripel projection was developed by Oswald Winkel in 1921. The Tripel follows the ideology that it is a compromise between the properties of three elements, namely the area, angle and distance. The winkel Tripel tries to obtain in a lower distortion distribution overall with this[17]. The Winkel Tripel projection is the map that is used by the National Geographic Society since 1995, when it replaced the Robinson projection [18].

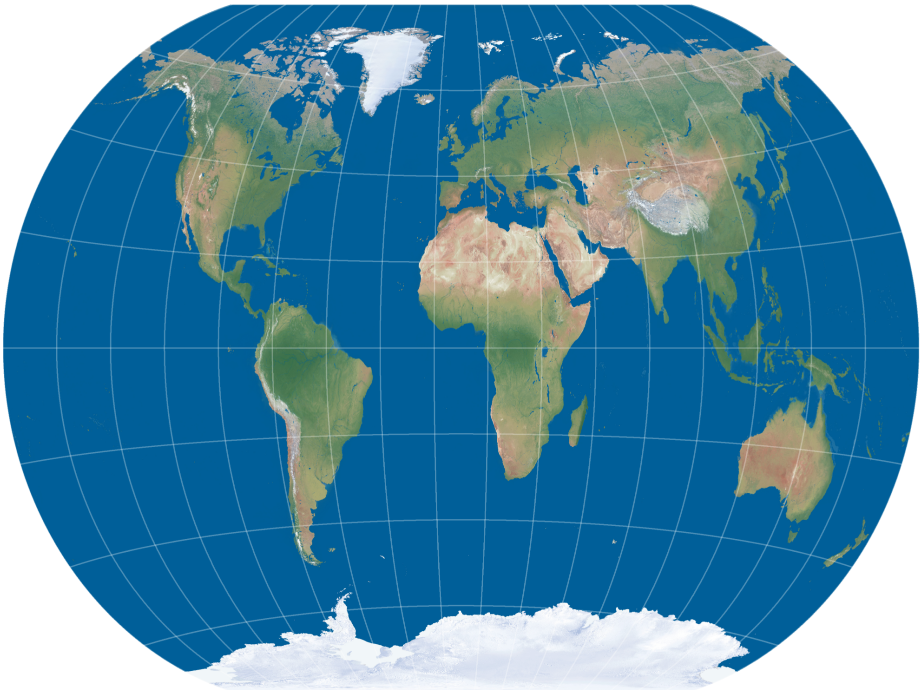

Figure 5.14: The Winkel Tripel is neither a conformal nor equal area map projection. But it tries to minimise three properites: area, angle and distance.

The transformation formulas are given by:

$$x(\lambda,\phi) = \frac{1}{2}\left(\frac{2\arccos(\cos\phi\cos\frac{\lambda}{2})}{\sqrt{1-\cos^2\phi\cos^2\frac{\lambda}{2}}}\cos\phi\sin\frac{\lambda}{2} + \lambda\cos\phi_0\right), \tag{5.3.1}$$

$$y(\lambda,\phi) = \frac{1}{2}\left(\frac{\arccos(\cos\phi\cos\frac{\lambda}{2})}{\sqrt{1-\cos^2\phi\cos^2\frac{\lambda}{2}}}\sin\phi + \phi\right). \tag{5.3.2}$$

The range of the transformation of the Winkel Tripel is $\{(x,y)|\ x\in[-\pi,\pi], y\in[-\frac{3\pi}{4},\frac{3\pi}{4}]\}$.
For the computation of the distortions of the Winkel Tripel projection, the derivatives of the transformation formulas with respect to both λ and ϕ need to be determined first. The derivative for the Winkel Tripel projection are:

$$\frac{\partial x}{\partial\lambda} = \frac{1}{2}\left(\frac{2\cos^2\phi\cos^2\frac{\lambda}{2}-\cos^2\phi-1}{-C} + \frac{(\cos^3\phi-\cos\phi)D\cos\frac{\lambda}{2}}{-C^{\frac{3}{2}}}\right), \tag{5.3.3}$$

$$\frac{\partial x}{\partial\phi} = \frac{\sin\frac{\lambda}{2}\sin\phi\big(D-\cos\frac{\lambda}{2}\cos\phi\sqrt{C}\big)}{\sqrt{C}*-C}, \tag{5.3.4}$$

$$\frac{\partial y}{\partial\lambda} = \frac{\cos\phi\sin\phi\sin\frac{\lambda}{2}}{4C} - \frac{\cos^2\phi\sin\phi D\cos\frac{\lambda}{2}\sin\frac{\lambda}{2}}{4C^{\frac{3}{2}}}, \tag{5.3.5}$$

$$\frac{\partial y}{\partial\phi} = \frac{(\cos\frac{\lambda}{2}+1)\Big((\cos\frac{\lambda}{2}-1)\cos\phi D + (\cos\frac{\lambda}{2}\cos^2\phi-1)\sqrt{C}\Big)}{-2C^{\frac{3}{2}}}, \tag{5.3.6}$$

with

$$C = 1-\cos^2\phi\ \cos^2\frac{\lambda}{2}, \tag{5.3.7}$$

$$D = \arccos\big(\cos\phi\cos\frac{\lambda}{2}\big). \tag{5.3.8}$$

Knowing the partial derivatives, the results for the Area and the Isotropy distortion, as defined in Section 3.1 and Section 3.2, can be approximated. The Area distortion and Isotropy distortion for the Winkel Tripel are $A = 0.26$ and $I = 0.50$. In Figure 5.15 the area and isotropy distortion are determined for different amounts of generated points and also the mean of these distortions. In Figure 5.16 a contour plot of the area distortion of the Winkel Tripel is plotted and in Figure 5.17 a contour plot of the isotropy distortion of the Winkel Tripel is plotted. Figure 5.16 shows that around the Equator the values are negative, which means that the ln $a_i b_i$ in those points is smaller than the average. Also it shows that closer to the prime meridian the area distortion is even smaller. Close to the poles it has the most area distortion. Figure 5.17 shows that around the crossing of the Equator and the prime meridian the isotropy distortion is the closest to zero. while going further from this point the isotropy distorting increases.

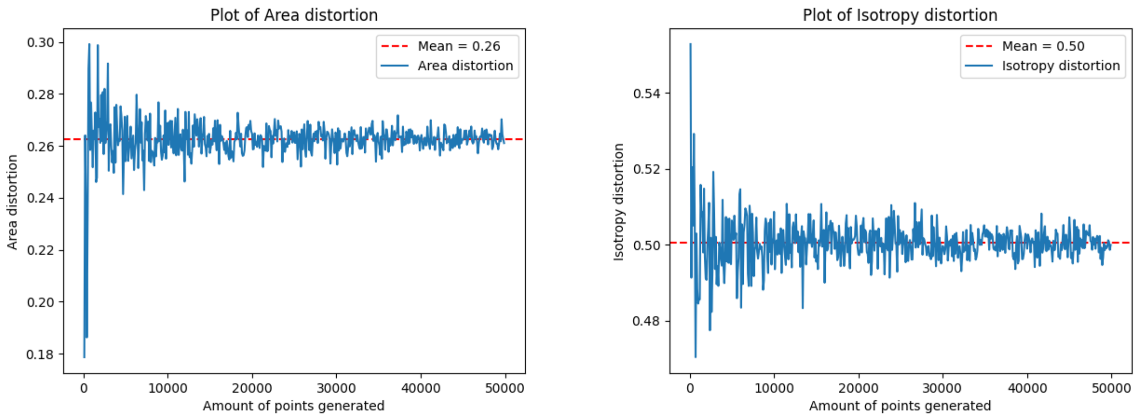

(a) The area distortion determined for different amount of generated points for the Winkel Tripel, with also showing the mean of 0.26.

(b) The isotropy distortion determined for different amount of generated points for the Winkel Tripel, with also showing the mean of 0.50.

Figure 5.15: The area and isotropy distortion for the Winkel Tripel.

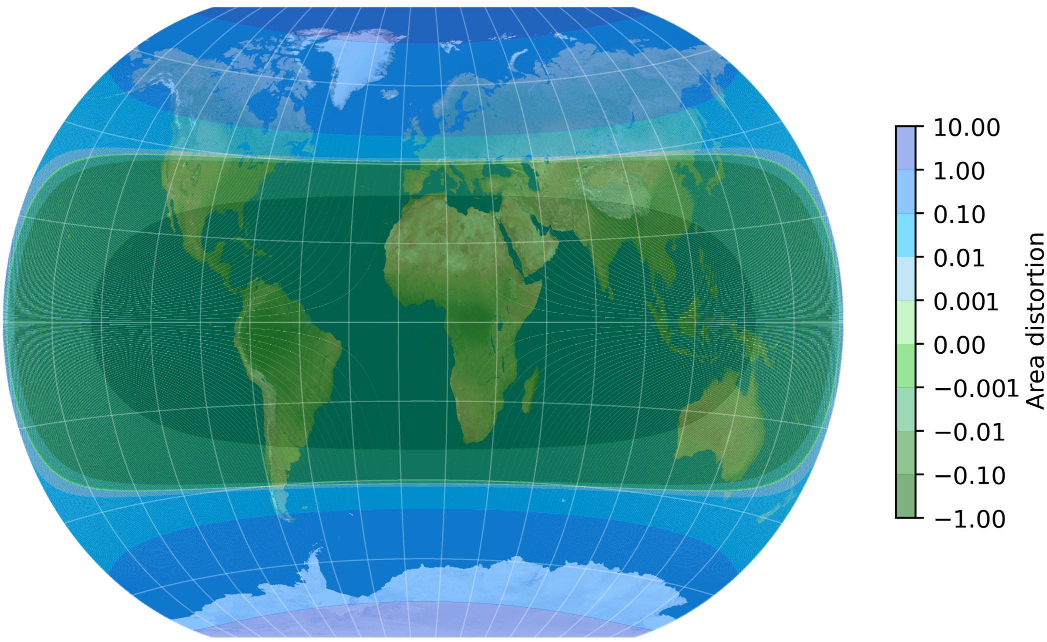

Figure 5.16: The contour plot of the area distortion on the Winkel Tripel. It shows that around the Equator the values are negative, which means that the ln $a_i b_i$ in those points is smaller than the average. Also it shows that closer to the prime meridian the area distortion is even smaller. Close to the poles it has the most area distortion.

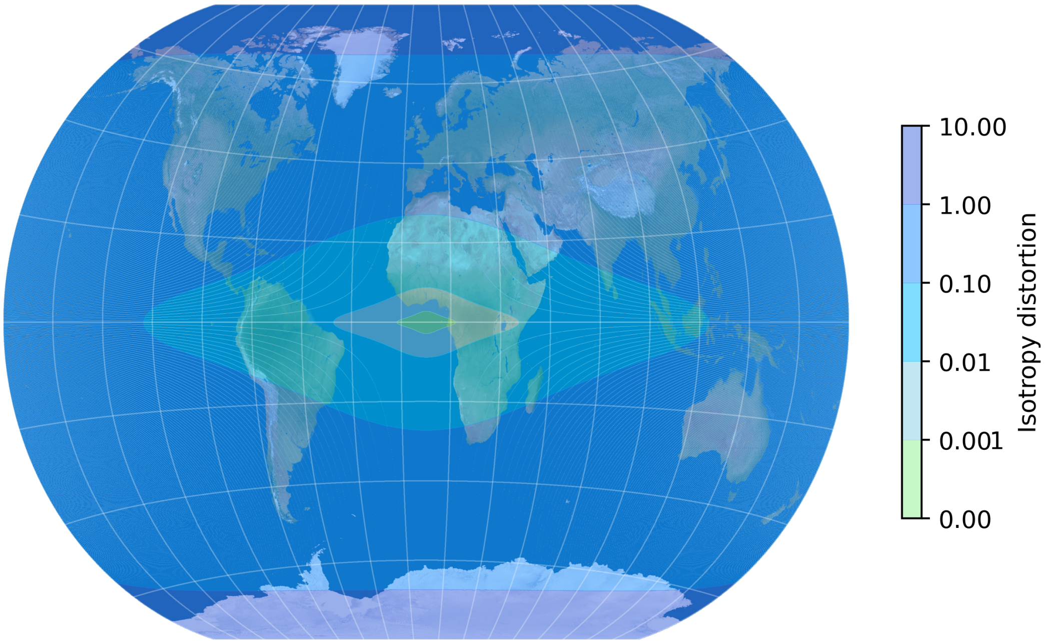

Figure 5.17: The contour plot of the isotropy distortion on the Winkel Tripel. It shows that around the crossing of the Equator and the prime meridian the isotropy distortion is the closest to zero. while going further from this point the isotropy distorting increases.

For the calculation of the Flexion and Skewness distortion, the method explained in Sections 3.3 and 3.4 is carried out. These distortions are numerically approached and for this the Hessian matrix is needed, both with respect to x and y. For the Winkel Tripel the second order partial derivatives are:

$$x_{\lambda\lambda} = \frac{\left(4\cos^2\phi\cos^2\frac{\lambda}{2}D - 3\cos\phi\cos\frac{\lambda}{2}\sqrt{-2E} + 2D\right)\sqrt{-2E}\ \sin^2\phi\sin\frac{\lambda}{2}\cos\phi}{(\cos^4\phi\cos^4\frac{\lambda}{2} - 2\cos^2\phi\cos^2\frac{\lambda}{2} + 1)\cdot 8E}, \tag{5.3.9}$$

$$x_{\phi\phi} = -\frac{\left(\left(\left(4\cos^3\phi - 6\cos\phi\right)\cos^2\frac{\lambda}{2} + 2\cos\phi\right)D + \cos\frac{\lambda}{2}\left(\cos^2\phi\cos^2\frac{\lambda}{2} - 3\cos^2\phi 2\right)\sqrt{-2E}\right)\sin\frac{\lambda}{2}}{\sqrt{-2E}\left(\cos^4\phi\cos^4\frac{\lambda}{2} - 2\cos^2\phi\cos^2\frac{\lambda}{2} + 1\right)}, \tag{5.3.10}$$

$$x_{\lambda\phi} = -\frac{\left(\left(\left(\cos^3(\phi) - 3\cos\phi\right)\cos^2\frac{\lambda}{2} + 2\cos\phi\right)\sqrt{-2E} + 4\left(\cos^2\phi\cos^2\frac{\lambda}{2} - \frac{3\cos^2\phi}{2} + \frac{1}{2}\right)\cos\frac{\lambda}{2}D\right)\sin\phi}{\sqrt{-2E}\left(2\cos^4\phi\cos^4\frac{\lambda}{2} - 4\cos^2\phi\cos^2\frac{\lambda}{2} + 2\right)}, \tag{5.3.11}$$

with

$$D = \arccos\left(\cos\phi\cos\frac{\lambda}{2}\right), \tag{5.3.12}$$

$$E = \cos^2(\phi)\cos(\lambda) + \cos^2(\phi) - 2. \tag{5.3.13}$$

This gives the Hessian matrix of variable x:

$$H_x = \begin{bmatrix} x_{\lambda\lambda} & x_{\phi\lambda} \\ x_{\lambda\phi} & x_{\phi\phi} \end{bmatrix}, \tag{5.3.14}$$

where $x_{\lambda\lambda}$ is the second derivative of x with respect to λ, the similarly for $x_{\phi\lambda}, x_{\lambda\phi}$ and $x_{\phi\phi}$.

$$y_{\lambda\lambda} = \frac{2\left(\left(-\cos^4\frac{\lambda}{2}\cos^3\phi - 2\cos\phi\cos^2\frac{\lambda}{2}\sin^2\phi + \cos\phi\right)D + \sqrt{-2E}\left(\cos^2\phi\cos^2\frac{\lambda}{2} - \frac{3(\cos^2\phi)}{2} + \frac{\lambda}{2}\right)\cos\frac{\lambda}{2}\right)\cos\phi\sin\phi}{\sqrt{-2E}\left(8\cos^4\phi\cos^4\frac{\lambda}{2} - 16\cos^2\phi\cos^2\frac{\lambda}{2} + 8\right)}, \tag{5.3.15}$$

$$y_{\phi\phi} = \frac{\left(-4\cos^2\phi\cos^2\frac{\lambda}{2}D + 3\cos\phi\cos\frac{\lambda}{2}\sqrt{-2E} - 2D\right)\sin^2\frac{\lambda}{2}\sin\phi}{\sqrt{-2E}\left(2\cos^4\phi\cos^4\frac{\lambda}{2} - 4\cos^2\phi\cos^2\frac{\lambda}{2} + 2\right)}, \tag{5.3.16}$$

$$y_{\lambda\phi} = \frac{\left(\left(\cos^4\phi\cos^2\frac{\lambda}{2} + 2\cos^2\phi\sin^2\frac{\lambda}{2} - 1\right)\sqrt{-2E} + 2D\cos\phi\cos\frac{\lambda}{2}\left(\cos^2\phi\cos^2\frac{\lambda}{2} - 3\cos^2\phi + 2\right)\right)\sin\frac{\lambda}{2}}{\sqrt{-2E}\left(4\cos^4\phi\cos^4\frac{\lambda}{2} - 8\cos^2\phi\cos^2\frac{\lambda}{2} + 4\right)}, \tag{5.3.17}$$

with D and E defined as:

$$D = \arccos(\cos\phi\cos\frac{\lambda}{2}), \tag{5.3.18}$$

$$E = \cos^2(\phi)\cos(\lambda) + \cos^2(\phi) - 2. \tag{5.3.19}$$

This gives the hessian matrix of variable y:

$$H_y = \begin{bmatrix} y_{\lambda\lambda} & y_{\phi\lambda} \\ y_{\lambda\phi} & y_{\phi\phi} \end{bmatrix}, \tag{5.3.20}$$

where $y_{\lambda\lambda}$ is the second derivative of y with respect to λ, the similarly for $y_{\phi\lambda}, y_{\lambda\phi}$ and $y_{\phi\phi}$.
Knowing these matrices, the flexion and skewness distortion can be determined. The results from the numerical approach for the flexion and skewness distortion for the Winkel Tripel projection are: $F = 0.70$ and $S = 0.44$. In Figure 5.18 and Figure 5.19 the local flexion distortion and the local skewness distortion are plotted. It can be seen that with distortions are the closes to zero at the origin of the map, where the prime meridian and the Equator intersect. When going further from this point the it increases. When compared, the skewness increases more slowly than the flexion.

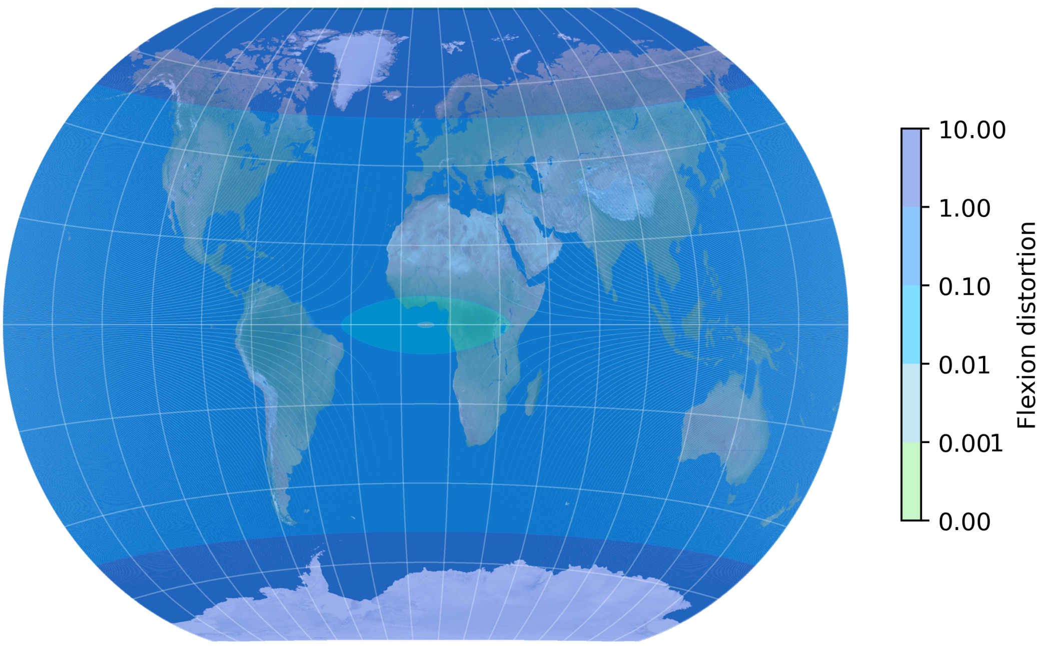

Figure 5.18: The contour plot of the flexion distortion on the Winkel-Tripel. The local flexion distortion is the closes to zero at the origin of the map, where the prime meridian and the Equator intersect. When going further from this point the local flexion distortion increases.

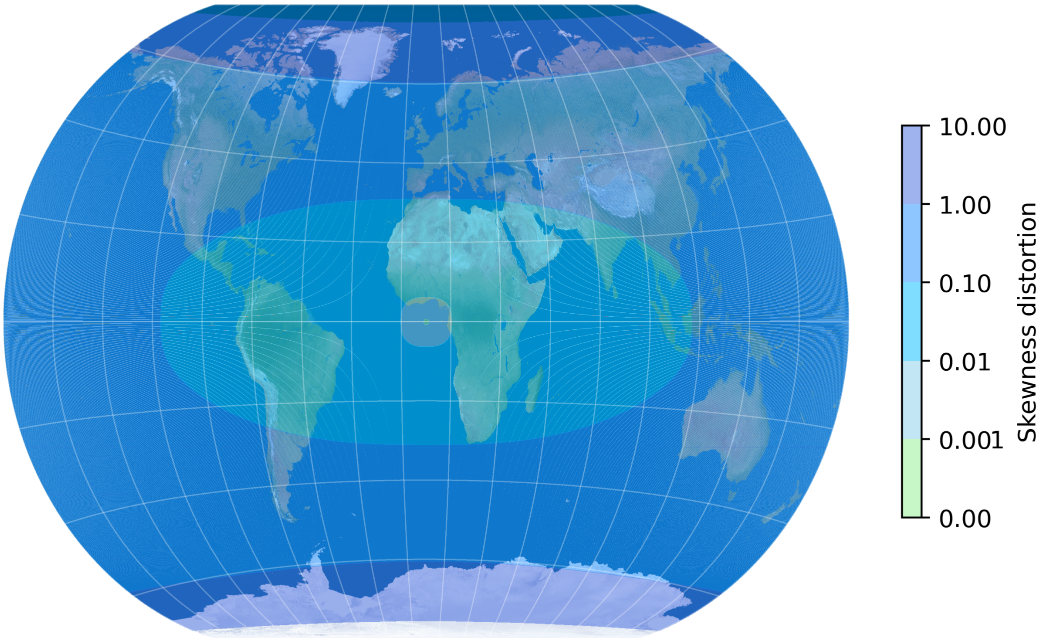

Figure 5.19: The contour plot of the skewness distortion on the Winkel-tripel. The local skewness distortion is the closest to zero at the origin of the map, where the prime meridian and the Equator intersect. When going further from this point the local flexion distortion increases.

The distance distortion is obtained by the numerical approximation with randomly generating the data points, in Figure 5.20 the distance distortion is determined for different amount of generated points and plotted. The distance distortion for the Winkel Tripel is $D = 0.37$.

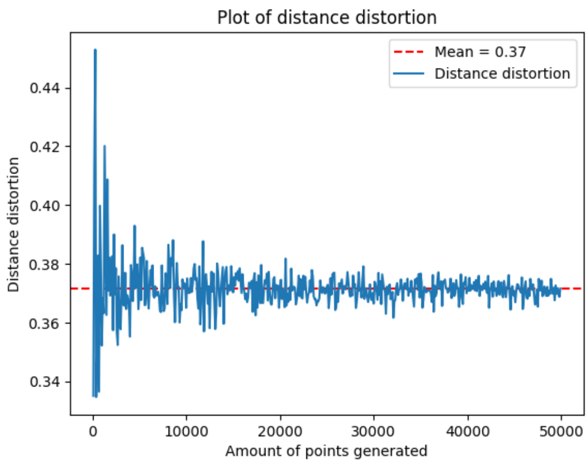

Figure 5.20: The distance distortion determined for different amount of randomly generated points of the Winkel Tripel, with also showing the mean of 0.37.

The Winkel Tripel projection has a cut of length π on the globe, and thus from the definition from Section 3.6 the boundary cut distortion of the Winkel Tripel projection is $B = \frac{\pi}{4\pi} = \frac{1}{4}$.

5.4. Gott-Wagner

The Gott-Wagner projection is developed with the idea to try to minimise the overall distortion, measured by the distortion values presented by Gott and Goldberg in 2007. Gott started with the Aitoff-Wagner projection, but added a curved pole line. The parameters were chosen to have a curved pole line a bit longer than the Winkel-Tripel to try to lessen flexion in longitude lines, and leave Africa less squashed than it some map projections.[19]

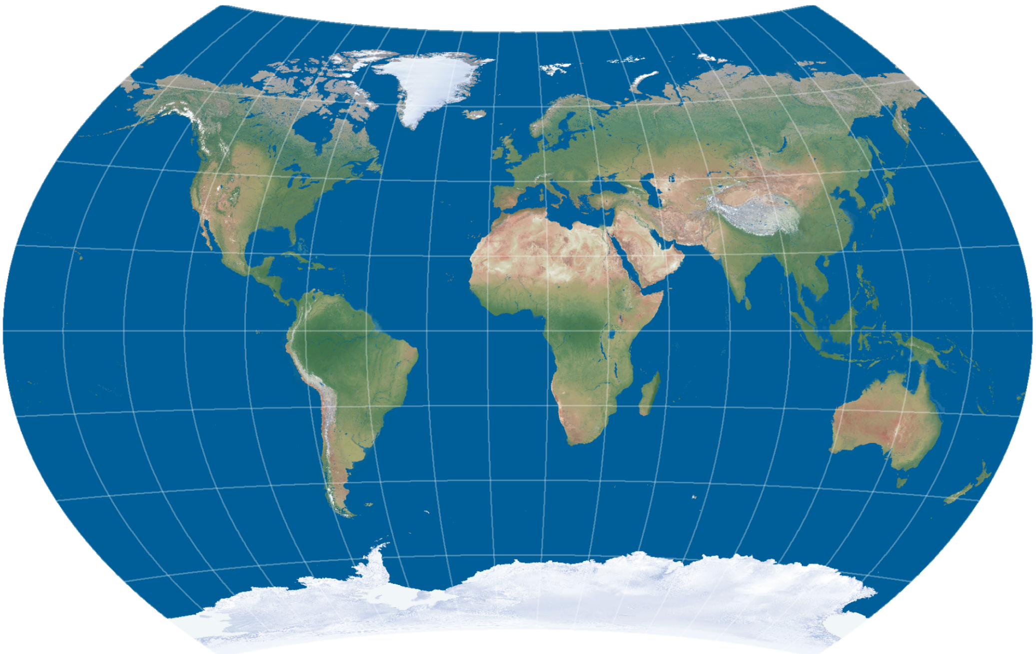

Figure 5.21: The Gott Wagner Projection is neither conformal nor equal-area. This projection tries to minimise the overall distortion, mainly focusing on the distortions presented by Gott and Goldberg in 2007. It has curved pole lines to lessen flexion.

The transformation formulas of Gott-Wagner are given by:

$$x(\lambda,\phi) = \frac{2z\cos\frac{2\phi}{3}\sin\frac{\lambda}{2\sqrt{3}}}{\sin z}, \tag{5.4.1}$$

$$y(\lambda,\phi) = \frac{z\sin\frac{2\phi}{3}}{\sin z}, \tag{5.4.2}$$

with z defined as:

$$z = \arccos\big(\cos\frac{2\phi}{3}\cos\frac{\lambda}{2\sqrt{3}}\big). \tag{5.4.3}$$

The range of the transformation of the Gott-Wagner is

$$\{(x,y)|\ x \in \big[-\frac{\pi}{\sqrt{3}},\frac{\pi}{\sqrt{3}}\big], y \in \Big[-\arccos\Big(\frac{1}{2}\cos\Big(\frac{\pi}{2\sqrt{3}}\Big)\Big)\sqrt{\frac{6}{7-\cos(\frac{\pi}{\sqrt{3}})}}, \arccos\Big(\frac{1}{2}\cos\Big(\frac{\pi}{2\sqrt{3}}\Big)\Big)\sqrt{\frac{6}{7-\cos(\frac{\pi}{\sqrt{3}})}}\Big]\}.$$

For the computation of the distortions of the Gott-Wagner projection, the derivatives of the transformation formulas with respect to both λ and ϕ need to be determined first. The derivative for the Gott-Wagner projection are:

$$\frac{\partial x}{\partial \phi} = \frac{4\left(\cos\frac{\lambda\sqrt{3}}{6}\cos\frac{2\phi}{3}\sqrt{w} - z\right)\sin\frac{\lambda\sqrt{3}}{6}\sin\frac{2\phi}{3}}{3(w)^{\frac{3}{2}}}, \tag{5.4.4}$$

$$\frac{\partial x}{\partial \lambda} = \frac{\left(\cos\frac{2\phi}{3}\sin^2\frac{\lambda\sqrt{3}}{6}\sqrt{w} + \sin^2\frac{2\phi}{3} z\cos\frac{\lambda\sqrt{3}}{6}\right)\sqrt{3}\cos\frac{2\phi}{3}}{3(w)^{\frac{3}{2}}}, \tag{5.4.5}$$

$$\frac{\partial y}{\partial \phi} = \frac{2\left(\sin^2\frac{\lambda\sqrt{3}}{6} z\cos\frac{2\phi}{3} + \sin^2\frac{2\phi}{3}\cos\frac{\lambda\sqrt{3}}{6}\sqrt{w}\right)}{3(w)^{\frac{3}{2}}}, \tag{5.4.6}$$

$$\frac{\partial y}{\partial \lambda} = \frac{1}{6}\left(\sqrt{3}\sin\frac{\lambda\sqrt{3}}{6}\sin\frac{2\phi}{3}\left(\frac{\cos\frac{2\phi}{3}}{w} - \frac{z\cos^2\frac{2\phi}{3}\cos\frac{\lambda\sqrt{3}}{6}}{w^{\frac{3}{2}}}\right)\right), \tag{5.4.7}$$

with z and w defined as:

$$z = \arccos\left(\cos\frac{2\phi}{3}\cos\frac{\lambda}{2\sqrt{3}}\right), \tag{5.4.8}$$

$$w = -\cos^2\frac{2\phi}{3}\cos^2\frac{\lambda\sqrt{3}}{6} + 1. \tag{5.4.9}$$

Knowing the partial derivatives, the results for the Area and the Isotropy distortion, as defined in Section 3.1 and Section 3.2, can be approximated. The Area distortion and Isotropy distortion for the Gott-Wagner are $A = 0.32$ and $I = 0.40$. In Figure 5.22 the area and isotropy distortion are determined for different amounts of generated points and also the mean of these distortions. In Figure 5.23 a contour plot of the area distortion of the Gott-Wagner is plotted and in Figure 5.24 a contour plot of the isotropy distortion of the Gott-Wagner is plotted. Figure 5.23 shows that the area distortion is in an area around the Equator with a curved line under zero, which means that the ln $a_i b_i$ in those points is smaller than the average. Closer to the North and South pole increases the area distortion. Figure 5.24 shows that the isotropy distortion is the closed to zero at two separate places, where it branches out around those point with increasing isotropy distortion.

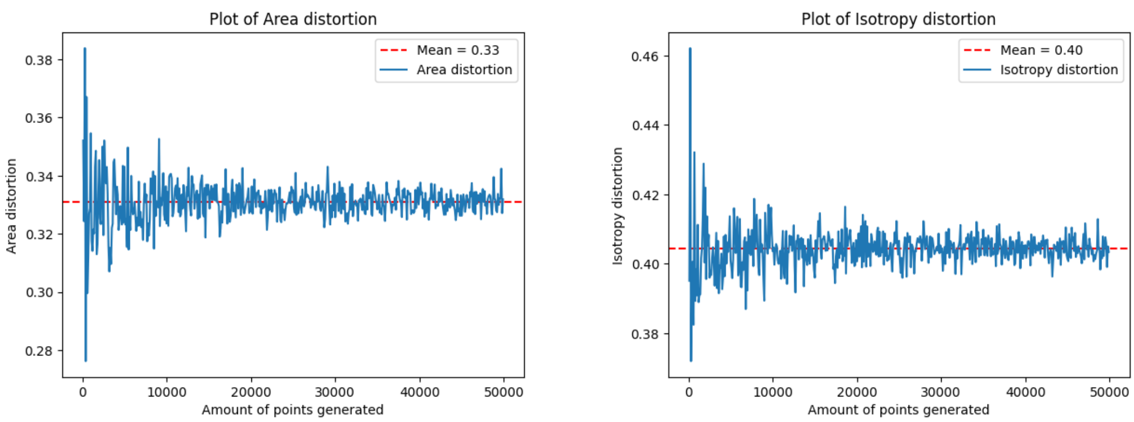

(a) The Area distortion determined for different amount of generated points for the Gott-Wagner, with also showing the mean of 0.33.

(b) The Isotropy distortion determined for different amount of generated points for the Gott-Wagner, with also showing the mean of 0.40.

Figure 5.22: The area and isotropy distortion for the Gott-Wagner.

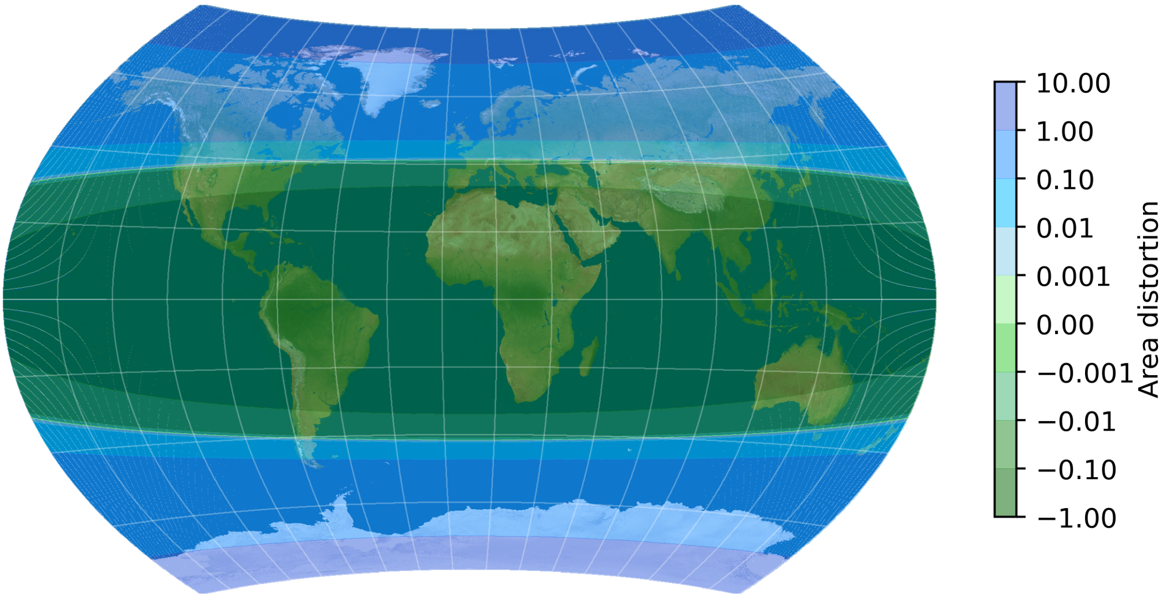

Figure 5.23: The contour plot of the area distortion on the Gott Wagner. The area distortion is in an area around the Equator with a curved line under zero, which means that the ln $a_i b_i$ in those points is smaller than the average. Closer to the North and South pole increases the area distortion.

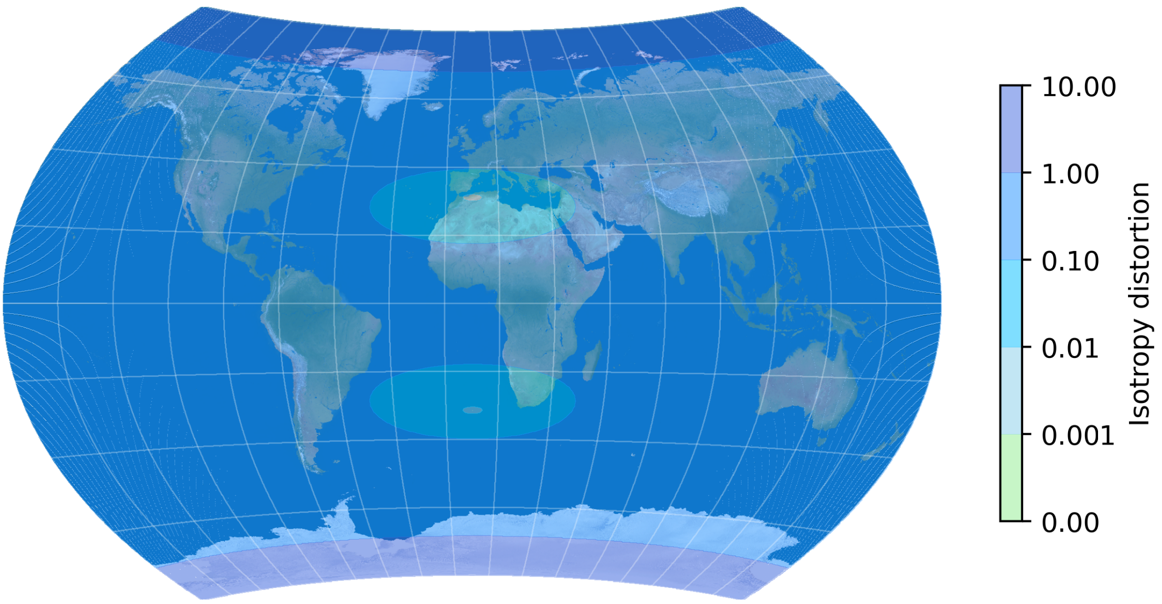

Figure 5.24: The contour plot of the isotropy distortion on the Gott Wagner. The isotropy distortion is the closed to zero at two separate places, where it branches out around those point with increasing isotropy distortion.

For the calculation of the Flexion and Skewness distortion, the method explained in Sections 3.3 and 3.4 is carried out. These distortions are numerically approached and for this the Hessian matrix is needed, both with respect to x and y. For the Gott-Wagner the second order partial derivatives are:

$$x_{\lambda\lambda} = \frac{\sin^2\frac{2\phi}{3}\left(-2z(1-w)+3\cos\frac{\lambda\sqrt{3}}{6}\cos\frac{2\phi}{3}\sqrt{w}-z\right)\sin\frac{\lambda\sqrt{3}}{6}\cos\frac{2\phi}{3}}{6w^{\frac{5}{2}}}, \tag{5.4.10}$$

$$x_{\phi\phi} = -\frac{16\sin\frac{\lambda\sqrt{3}}{6}\left(\frac{1}{2}\left(\cos\frac{\lambda\sqrt{3}}{6}\left((1-w)-3\cos^2\frac{2\phi}{3}+2\right)\sqrt{w}\right)+D\left(\frac{1}{2}+\left(\cos^2\frac{2\phi}{3}-\frac{3}{2}\right)\cos^2\frac{\lambda\sqrt{3}}{6}\right)\cos\frac{2\phi}{3}\right)}{9w^{\frac{5}{2}}}, \tag{5.4.11}$$

$$x_{\lambda\phi} = -\frac{2\left(\left(\left(\cos^3\frac{2\phi}{3}-3\cos\frac{2\phi}{3}\right)\cos^2\frac{\lambda\sqrt{3}}{6}+2\cos\frac{2\phi}{3}\right)\sqrt{w}+2\left((1-w)-\frac{3}{2}\cos^2\frac{2\phi}{3}+\frac{1}{2}\right)z\cos\frac{\lambda\sqrt{3}}{6}\right)\sqrt{3}\sin\frac{2\phi}{3}}{9w^{\frac{5}{2}}}, \tag{5.4.12}$$

with z and w defined as:

$$z = \arccos\left(\cos\frac{2\phi}{3}\cos\frac{\lambda}{2\sqrt{3}}\right), \tag{5.4.13}$$

$$w = -\cos^2\frac{2\phi}{3}\cos^2\frac{\lambda\sqrt{3}}{6}+1. \tag{5.4.14}$$

This gives the Hessian matrix of variable x:

$$H_x = \begin{bmatrix} x_{\lambda\lambda} & x_{\phi\lambda} \\ x_{\lambda\phi} & x_{\phi\phi} \end{bmatrix}. \tag{5.4.15}$$

where $x_{\lambda\lambda}$ is the second order derivative of x with respect to λ, the similarly for $x_{\phi\lambda}, x_{\lambda\phi}$ and $x_{\phi\phi}$.

$$y_{\lambda\lambda} = \frac{\left(-z\cos\frac{2\phi}{3}\left(\cos^2\frac{2\phi}{3}\cos^4\frac{\lambda\sqrt{3}}{6}+2\sin^2\frac{2\phi}{3}\cos^2\frac{\lambda\sqrt{3}}{6}-1\right)+\sqrt{w}\cos\frac{\lambda\sqrt{3}}{6}\left(3-2w-3\cos^2\frac{2\phi}{3}\right)\right)\cos\frac{2\phi}{3}\sin\frac{2\phi}{3}}{12w^{\frac{5}{2}}}, \tag{5.4.16}$$

$$y_{\phi\phi} = \frac{4\sin^2\frac{\lambda\sqrt{3}}{6}\left(-2z(1-w)+3\cos\frac{\lambda\sqrt{3}}{6}\cos\frac{2\phi}{3}\sqrt{w}-z\right)\sin\frac{2\phi}{3}}{9w^{\frac{5}{2}}}, \tag{5.4.17}$$

$$y_{\lambda\phi} = \frac{\sqrt{3}\sin\frac{\lambda\sqrt{3}}{6}\left(\left(\cos^4\frac{2\phi}{3}\cos^2\frac{\lambda\sqrt{3}}{6}+1-2w\right)\sqrt{w}+z\cos\frac{2\phi}{3}\cos\frac{\lambda\sqrt{3}}{6}\left(3-w-3\cos^2\frac{2\phi}{3}\right)\right)}{9w^{\frac{5}{2}}}, \tag{5.4.18}$$

with z and w defined as:

$$z = \arccos(\cos\frac{2\phi}{3}\cos\frac{\lambda}{2\sqrt{3}}), \tag{5.4.19}$$

$$w = -\cos^2\frac{2\phi}{3}\cos^2\frac{\lambda\sqrt{3}}{6}+1. \tag{5.4.20}$$

This gives the Hessian matrix of variable y:

$$H_y = \begin{bmatrix} y_{\lambda\lambda} & y_{\phi\lambda} \\ y_{\lambda\phi} & y_{\phi\phi} \end{bmatrix}, \tag{5.4.21}$$

where $y_{\lambda\lambda}$ is the second order derivative of y with respect to λ, the similarly for $y_{\phi\lambda}, x_{\lambda\phi}$ and $y_{\phi\phi}$.
Knowing these matrices, the flexion and skewness distortion can be determined. The results from the numerical approach for the flexion and skewness distortion for the Gott-Wagner projection are: $F = 0.683$ and $S = 0.409$. In Figure 5.25 a contour plot of the flexion distortion of the Gott-Wagner is plotted and in Figure 5.26 a contour plot of the skewness distortion. Figure 5.25 shows that the local flexion distortion is the closest to zero at the origin of the map, where the prime meridian and the Equator intersect. When going further from this point the local flexion distortion increases. Figure 5.26 shows that for the skewness distortion it is also close to zero around the intersection of the prime meridian and the Equator, but it is distributed a bit different in comparison with the flexion distortion as shown in the figure.

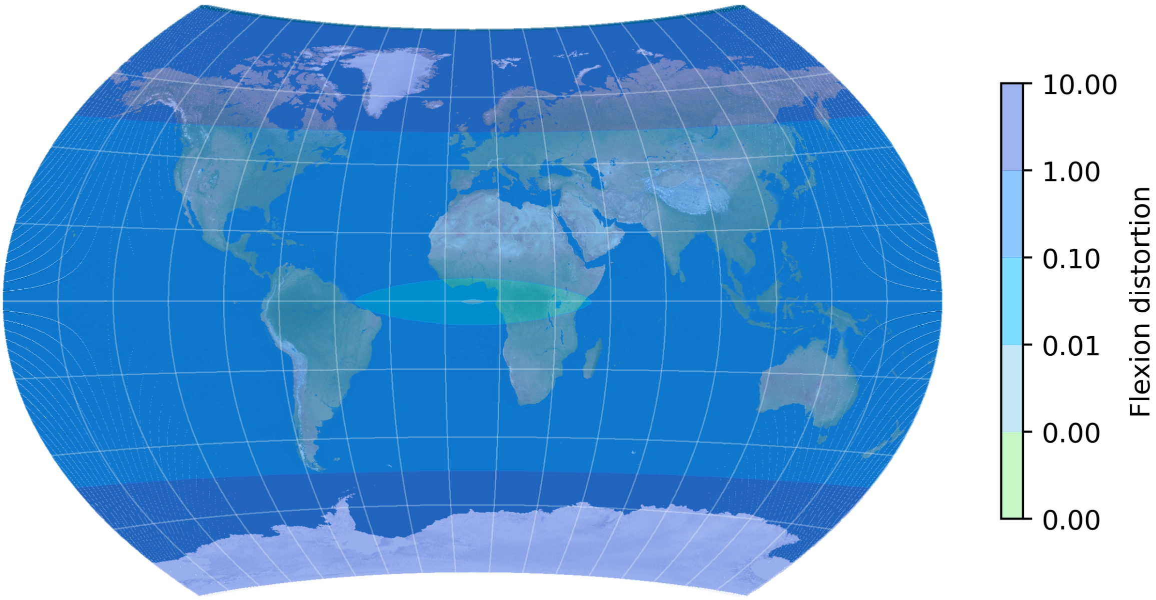

Figure 5.25: The contour plot of the flexion distortion on the Gott-Wagner. The local flexion distortion is the closest to zero at the origin of the map, where the prime meridian and the Equator intersect. When going further from this point the local flexion distortion increases.

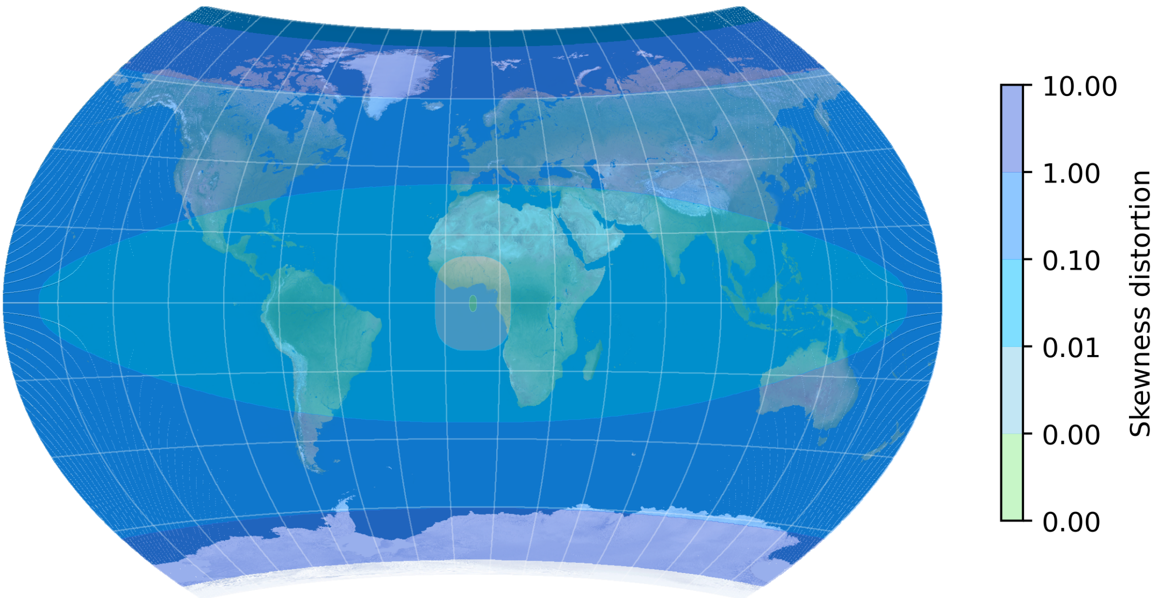

Figure 5.26: The contour plot of the skewness distortion on the Gott-Wagner. The local skewness distortion is the closest to zero at the origin of the map, where the prime meridian and the Equator intersect. When going further from this point the local flexion distortion increases.

The distance distortion is obtained by the numerical approximation with randomly generating the data points, in Figure 5.27 the distance distortion is determined for different amount of generated points and plotted. The distance distortion for the Gott-Wagner is $D = 0.40$.

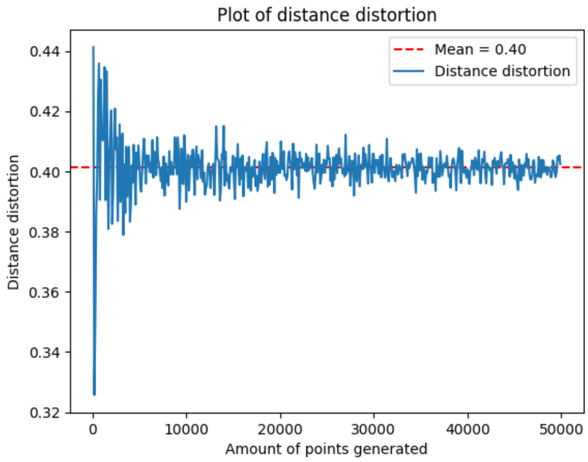

Figure 5.27: The distance distortion determined for different amount of randomly generated points of the Gott-Wagner, with also showing the mean of 0.40.

The Gott-Wagner projection has a cut of length π on the globe, and thus from the definition from Section 3.6 the boundary cut distortion of the Gott-Wagner projection is $B = \frac{\pi}{4\pi} = \frac{1}{4}$.

5.5. Azimuthal Equidistant

The Azimuthal Equidistant projection is an equidistant projection, meaning that distances measured from the centre are accurate. This projection is neither equal-area nor conformal. When considering the Azimuthal Equidistant with a polar aspect the meridians are equally spaces straight lines intersecting at the central pole. The parallels are equally spaced circle, centred at the pole. This map is sometimes used by people who belief the Earth is flat to support their beliefs, as it shows the entire globe in a circular format [20].

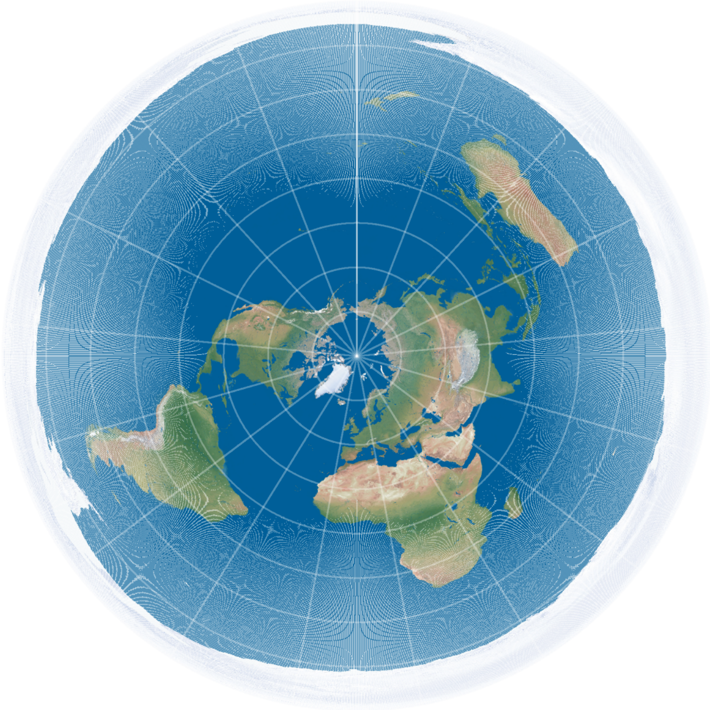

Figure 5.28: Azimuthal Equidistant with $\phi_1 = \frac{\pi}{2}$, so that the North Pole is in the middle. The distances that are measured from the centre are true. This projection is neither equal-area nor conformal. The meridians are straight lines. And the South pole is the whole circle.

The transformation formulas of the Azimuthal Equidistant are given by:[11]

$$x = k' \cos\phi \sin(\lambda - \lambda_0), \tag{5.5.1}$$
$$y = k'(\cos\phi_1 \sin\phi - \sin\phi_1 \cos\phi \cos(\lambda - \lambda_0)), \tag{5.5.2}$$

with

$$k' = \frac{c}{\sin c}. \tag{5.5.3}$$

Here (ϕ_1, λ_0) being the latitude and longitude of the centre of projection and origin and c defined as:

$$\cos c = \sin\phi_1 \sin\phi + \cos\phi_1 \cos\phi \cos(\lambda - \lambda_0). \tag{5.5.4}$$

The inverse transformation formulas for the Azimuthal Equidistant are given by:

$$\phi = \arcsin(\cos c \sin\phi_1 + (y \sin c \cos \frac{\phi_1}{\rho})), \tag{5.5.5}$$

with

$$\rho = \sqrt{x^2 + y^2} \tag{5.5.6}$$

The inverse formula for the λ is depended on the centre of the projection. If ϕ_1 is $-\frac{\pi}{2}$, the centre is the South Pole:

$$\lambda = \lambda_0 + \arctan\left(\frac{x}{-y}\right). \tag{5.5.7}$$

If ϕ_1 is $\frac{\pi}{2}$, the centre is the North pole:

$$\lambda = \lambda_0 + \arctan\left(\frac{x}{y}\right). \tag{5.5.8}$$

And otherwise λ is given by:

$$\lambda = \lambda_0 + \arctan\left(\frac{x \sin c}{\rho \cos\phi_1 \cos c - y \sin\phi_1 \sin c}\right), \tag{5.5.9}$$

with

$$\rho = \sqrt{x^2 + y^2}, \tag{5.5.10}$$

$$c = \rho. \tag{5.5.11}$$

Let's take the North pole as the centre of the projection, this means that $\phi_1 = \frac{\pi}{2}$ and λ is arbitrary, the transformation formulas are:

$$x = (\frac{\pi}{2} - \phi) \sin(\lambda - \lambda_0), \tag{5.5.12}$$

$$y = -(\frac{\pi}{2} - \phi) \cos(\lambda - \lambda_0), \tag{5.5.13}$$

with the inverse equations for the North pole:

$$\lambda = \lambda_0 + \arctan\left(\frac{x}{-y}\right), \tag{5.5.14}$$

$$\phi = \arcsin(\cos c \sin\phi_1 + (y \sin c \cos\frac{\phi_1}{\rho})), \tag{5.5.15}$$

with

$$\rho = \sqrt{x^2 + y^2} \tag{5.5.16}$$

For the computation of the area distortion and isotropy distortion the derivatives of the transformation formulas with respect to both λ and ϕ need to be determined. For the computation of the distortions, the north pole is taken as focus point, hence $\phi_1 = \frac{\pi}{2}$ and $\lambda_0 = 0$. The derivatives for the Azimuthal Equidistant with the North pole as focus point are:

$$\frac{\partial x}{\partial \lambda} = (\frac{\pi}{2} - \phi) \cos\lambda, \tag{5.5.17}$$

$$\frac{\partial x}{\partial \phi} = -\sin\lambda, \tag{5.5.18}$$

$$\frac{\partial y}{\partial \lambda} = (\frac{\pi}{2} - \phi) \sin\lambda, \tag{5.5.19}$$

$$\frac{\partial y}{\partial \phi} = \cos\lambda. \tag{5.5.20}$$

Knowing the partial derivatives, the results for the area and the isotropy distortion, as defined in Section 3.1 and Section 3.2, can be approximated. The area distortion and isotropy distortion for the Azimuthal Equidistant are $A = 0.60$ and $I = 0.87$. In Figure 5.29 the area and isotropy distortion are determined for different amounts of generated points and also the mean of these distortions. In Figure 5.30 a contour plot of the area distortion of the Azimuthal equidistant is plotted and in Figure 5.31 a contour plot of the isotropy distortion of the Azimuthal equidistant is plotted. Figure 5.30 shows that in the norther hemisphere the area distortion is zero, which means that the $\ln a_i b_i$ in this region is smaller that the average. At the Equator it is closest to zero and going from the Equator to the South Pole the area distortion increases. Figure 5.31 shows that the isotropy distortion is the closest to zero around the North Pole and increases while going to the South Pole.

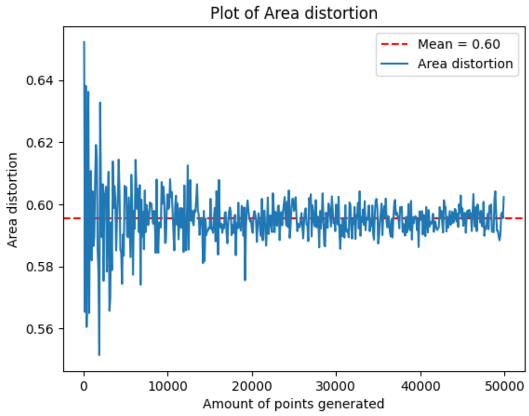

(a) The Area distortion determined for different amount of generated points for the Azimuthal Equidistant, with also showing the mean of 0.60.

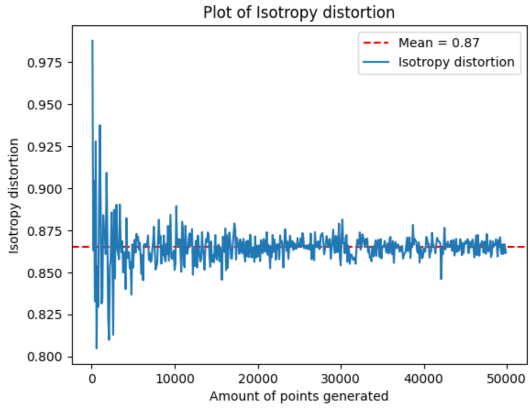

(b) The isotropy distortion determined for different amount of generated points for the Azimuthal Equidistant, with also showing the mean of 0.87.

Figure 5.29: The area and isotropy distortion for the Azimuthal Equidistant.

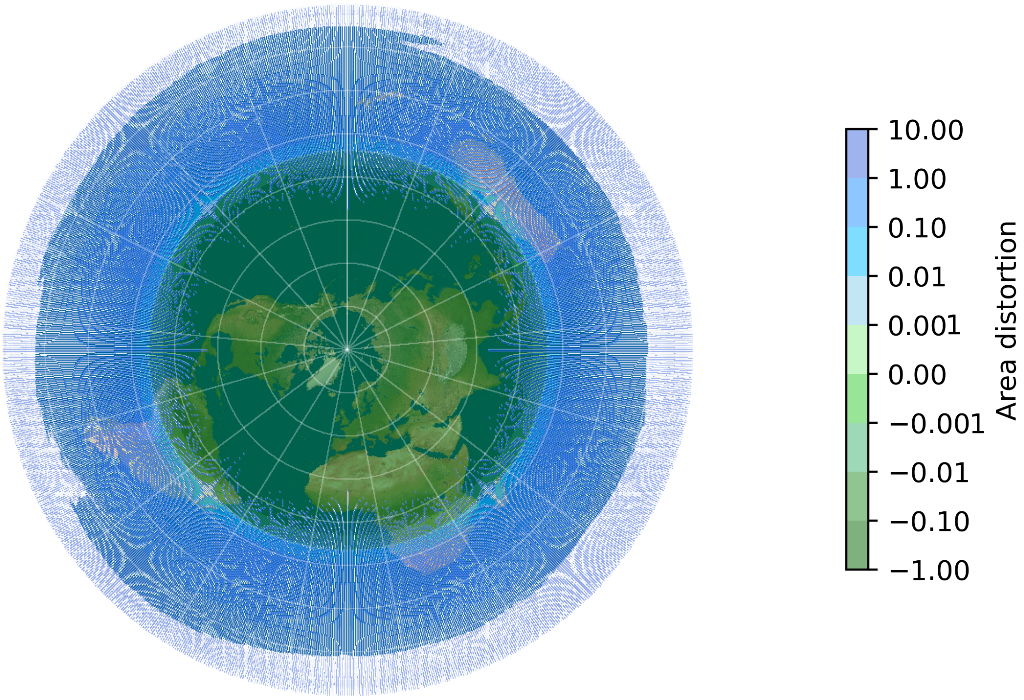

Figure 5.30: The contour plot of the area distortion on the Azimuthal Equidistant, with $\phi_1 = \frac{\pi}{2}$. The area distortion is in the norther hemisphere zero, which means that the $\ln a_i b_i$ in this region is smaller that the average. At the Equator it is closest to zero and going from the Equator to the South Pole the area distortion increases.

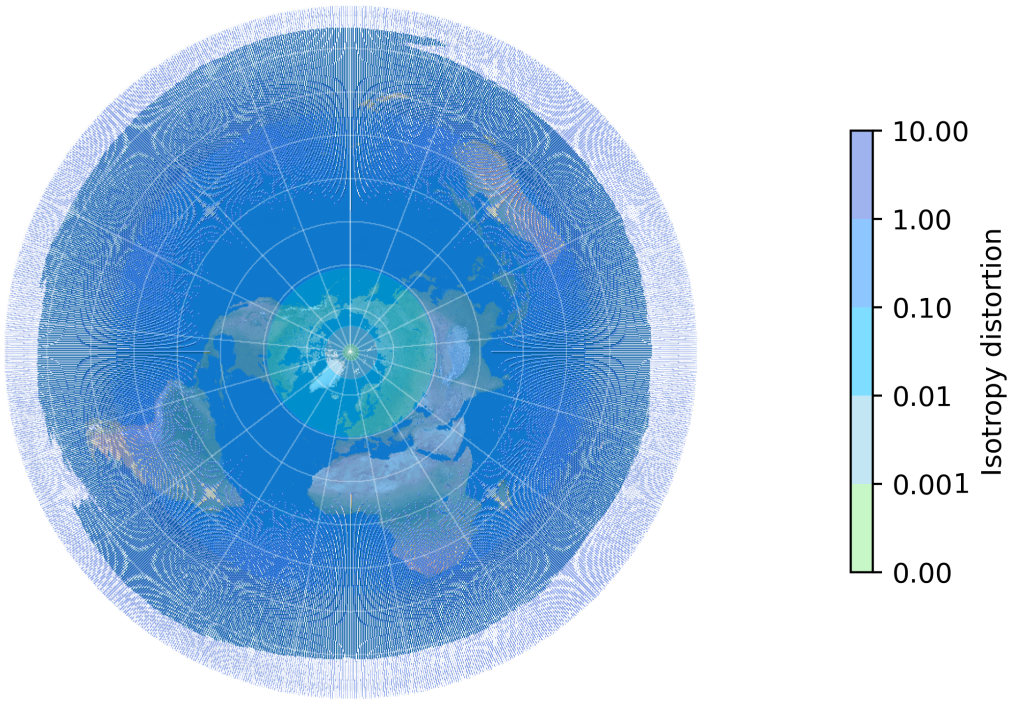

Figure 5.31: The contour plot of the isotropy distortion on the Azimuthal equidistant, with $\phi_1 = \frac{\pi}{2}$. The isotropy distortion is the closest to zero around the North Pole and increases while going to the South Pole.

For the calculation of the flexion and skewness distortion, the method explained in Sections 3.3 and 3.4 is carried out. These distortions are numerically approached and for this the Hessian matrix is needed, both with respect to x and y. For the Azimuthal Equidistant the second order partial derivatives are:

$$x_{\lambda\lambda} = -(\frac{\pi}{2} - \phi)\cos\lambda, \tag{5.5.21}$$

$$x_{\phi\phi} = 0, \tag{5.5.22}$$

$$x_{\lambda\phi} = \sin\lambda. \tag{5.5.23}$$

This gives the Hessian matrix of variable x:

$$H_x = \begin{bmatrix} x_{\lambda\lambda} & x_{\phi\lambda} \\ x_{\lambda\phi} & x_{\phi\phi} \end{bmatrix} = \begin{bmatrix} -(\frac{\pi}{2} - \phi)\cos\lambda & \sin\lambda \\ \sin\lambda & 0 \end{bmatrix}, \tag{5.5.24}$$

where $x_{\lambda\lambda}$ is the second order derivative of x with respect to λ, the similarly for $x_{\phi\lambda}, x_{\lambda\phi}$ and $x_{\phi\phi}$.

$$y_{\lambda\lambda} = (\frac{\pi}{2} - \phi)\sin\lambda, \tag{5.5.25}$$

$$y_{\phi\phi} = 0, \tag{5.5.26}$$

$$y_{\lambda\phi} = \cos\lambda. \tag{5.5.27}$$

This gives the hessian matrix of variable y:

$$H_y = \begin{bmatrix} y_{\lambda\lambda} & y_{\phi\lambda} \\ y_{\lambda\phi} & y_{\phi\phi} \end{bmatrix} = \begin{bmatrix} (\frac{\pi}{2} - \phi)\sin\lambda & \cos\lambda \\ \cos\lambda & 0 \end{bmatrix}, \tag{5.5.28}$$

where $y_{\lambda\lambda}$ is the second order derivative of y with respect to λ, the similarly for $y_{\phi\lambda}, x_{\lambda\phi}$ and $y_{\phi\phi}$.
Knowing these matrices, the flexion and skewness distortion can be determined. The results from the numerical approach for the flexion and skewness distortion for the Azimuthal Equidistant projection are: $F = 0.996$ and $S = 0.569$. In Figure 5.32 a contour plot of the flexion distortion of the Azimuthal Equidistant is

plotted and in Figure 5.33 a contour plot of the skewness distortion. Figure 5.32 shows that the local flexion distortion is the lowest at the North Pole and increases while going to the South Pole. Figure 5.33 shows that for the local skewness distortion is the also lowest at the North Pole and increases while going to the South Pole. When comparing the two distortions, it can be seen that the skewness local distortion increases more slowly than the flexion distortion.

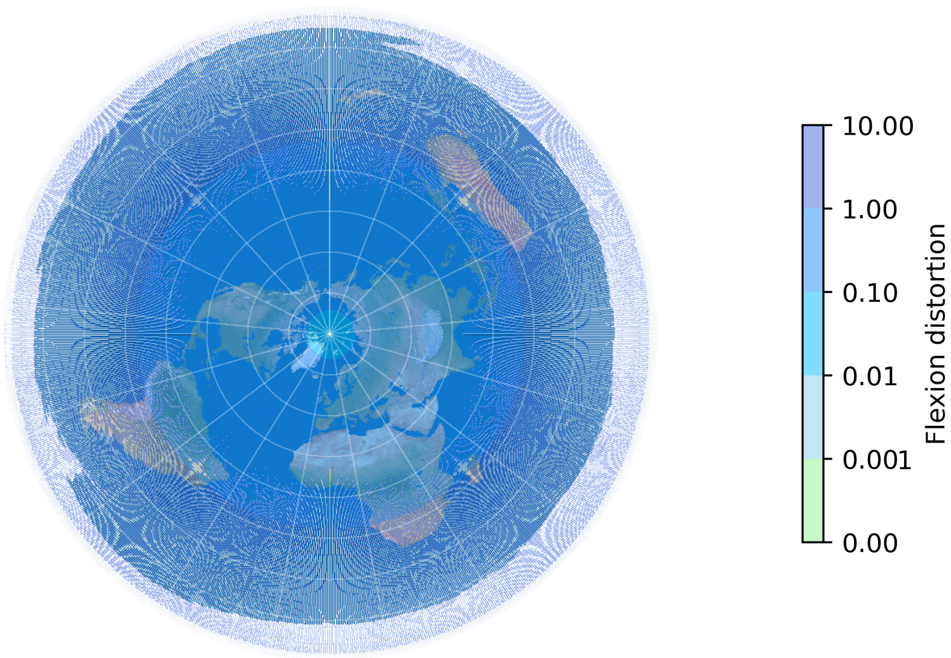

Figure 5.32: The contour plot of the flexion distortion on the Azimuthal Equidistant. The local flexion distortion is the lowest at the North Pole and increases while going to the South Pole.

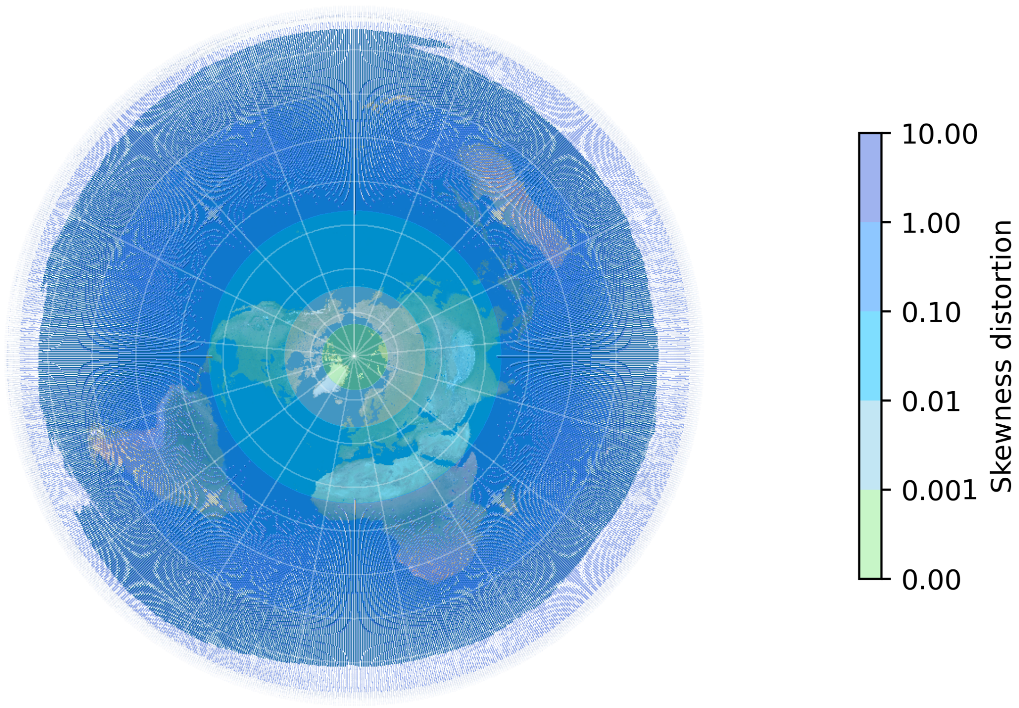

Figure 5.33: The contour plot of the skewness distortion on the Azimuthal Equidistant. The local skewness distortion is the lowest at the North Pole and increases while going to the South Pole.

The distance distortion is obtained by the numerical approximation with randomly generating the data points, in Figure 5.34 the distance distortion is determined for different amount of generated points and plotted. The distance distortion for the Azimuthal Equidistant is $D = 0.36$.

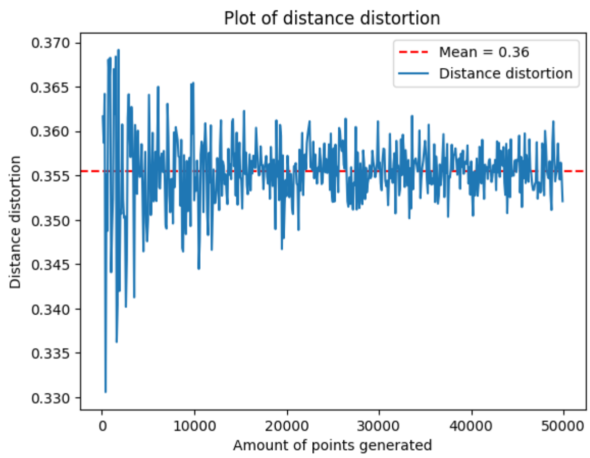

Figure 5.34: The distance distortion determined for different amount of randomly generated points of the Azimuthal Equidistant, with also showing the mean of 0.40.

The Azimuthal Equidistant projection has a cut of length 0 on the globe, and thus from the definition from Section 3.6 the boundary cut distortion of the Azimuthal Equidistant projection is $B = \frac{0}{4\pi} = 0$.

5.5.1. Azimuthal Equidistant split into two-hemispheres

A common technique to make azimuthal projections more accurate is to split the projection from one circle into two disks. This results in less distortion overall in general. This is seen shown in figure 5.35

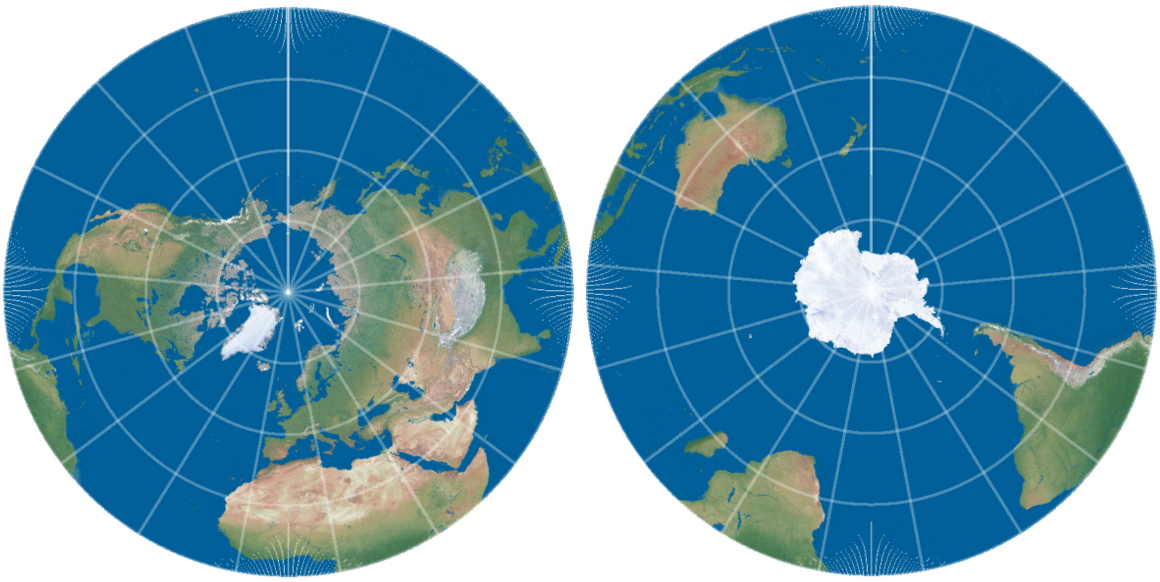

Figure 5.35: The Azimuthal Equidistant split into two-hemispheres with the North and South Poles int the centre of the two circles. The Equator is the edge on both disks and the meridians are straight lines, while the parallels are circles with the South and North Pole in the centre.

The area distortion and isotropy distortion are $A = 0.129$ and $I = 0.239$. In Figure 5.36 the area and isotropy distortion are determined for different amounts of generated points and also the mean of these distortions. In Figure 5.37 a contour plot of the area distortion of the Azimuthal Equidistant split into two-hemispheres is plotted and in Figure 5.38 a contour plot of the isotropy distortion of the the Azimuthal Equidistant split into two-hemispheres is plotted. Figure 5.37 shows that the area distortion is zero to close the North and South Pole zero, which means that the $\ln a_i b_i$ in this region is smaller that the average. Closer to the Equator the area distortion increases. Figure 5.38 shows that the isotropy distortion is close to the North and South Pole zero and going to the Equator the area distortion increases. The area and isotropy distortions for the Azimuthal Equidistant is significantly improved by splitting it in two hemispheres, which was the intended purpose.

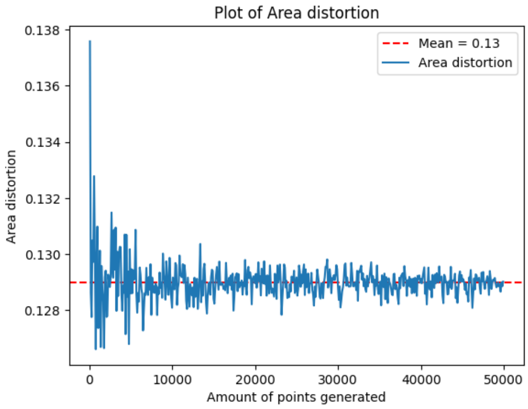

(a) The area distortion determined for different amount of generated points for the Azimuthal Equidistant split into two-hemisphere, with also showing the mean of 0.13.

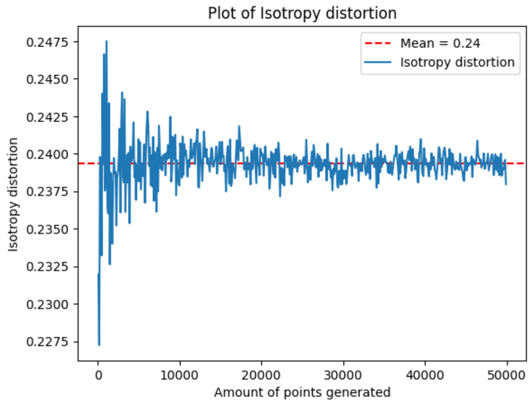

(b) The isotropy distortion determined for different amount of generated points for the Azimuthal Equidistant split into two-hemispheres, with also showing the mean of 0.24.

Figure 5.36: The area and isotropy distortion for the Azimuthal Equidistant split into two-hemispheres.

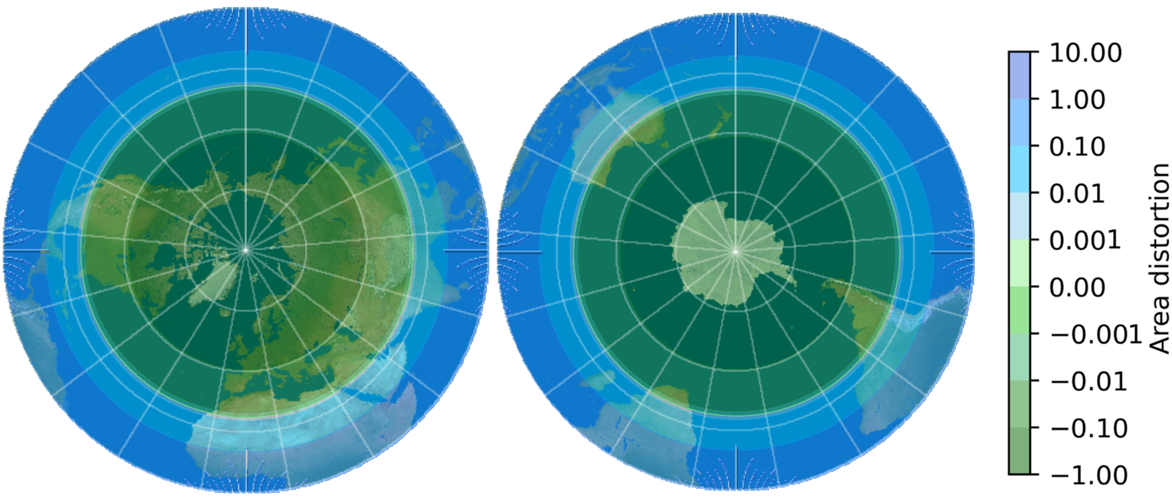

Figure 5.37: The contour plot of the area distortion on the Azimuthal Equidistant split into two-hemispheres, with the North and South Pole in the centre. The area distortion is zero close to the North and South Pole, which means that the $\ln a_i b_i$ in this region is smaller that the average. Closer to the Equator the area distortion increases.

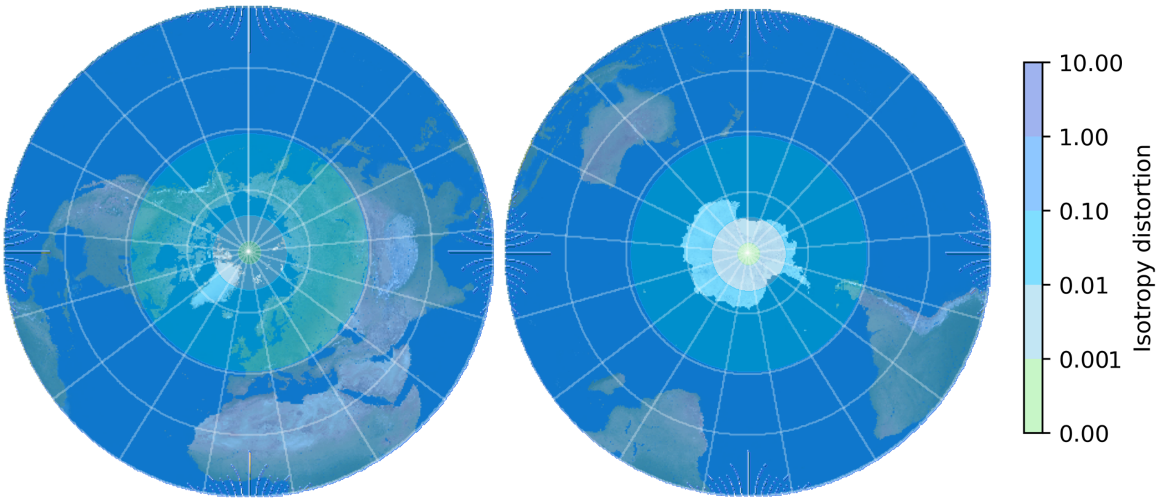

Figure 5.38: The contour plot of the isotropy distortion on the Azimuthal Equidistant split into two-hemispheres, with the North and South Pole in the centre. The isotropy distortion is close to the North and South Pole zero and going to the Equator the area distortion increases.

The results from the numerical approach for the flexion and skewness distortion are: $F = 0.47$ and $S = 0.47$. In Figure 5.32 a contour plot of the flexion distortion of the Azimuthal Equidistant is plotted and in Figure 5.33 a contour plot of the skewness distortion.

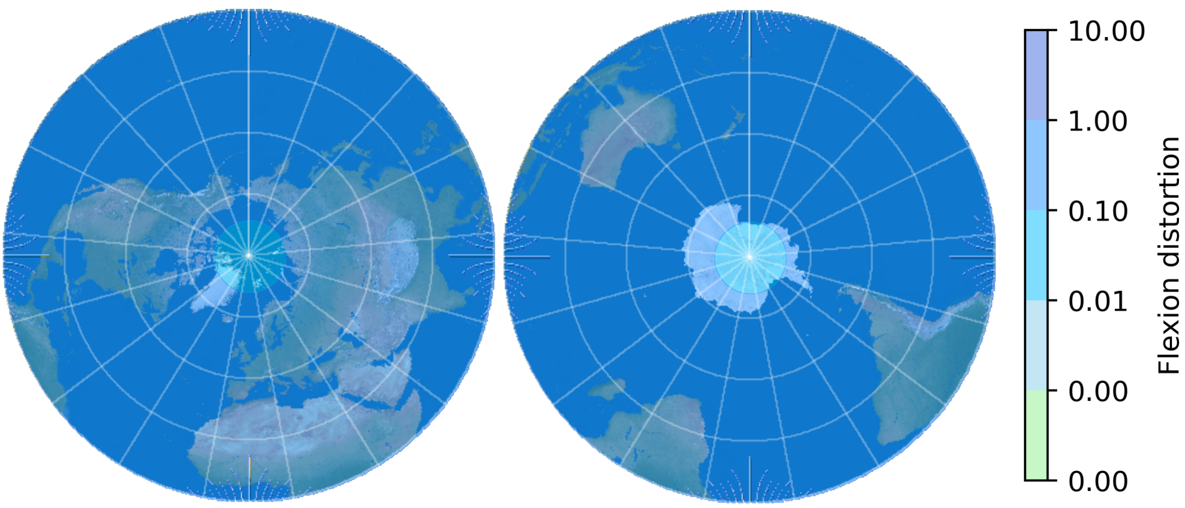

Figure 5.39: The contour plot of the local flexion distortion on the Azimuthal Equidistant split into two-hemispheres, with the North and South Pole in the centre. The local flexion distortion is zero close to the North and South Pole and it increases while going to the equator.

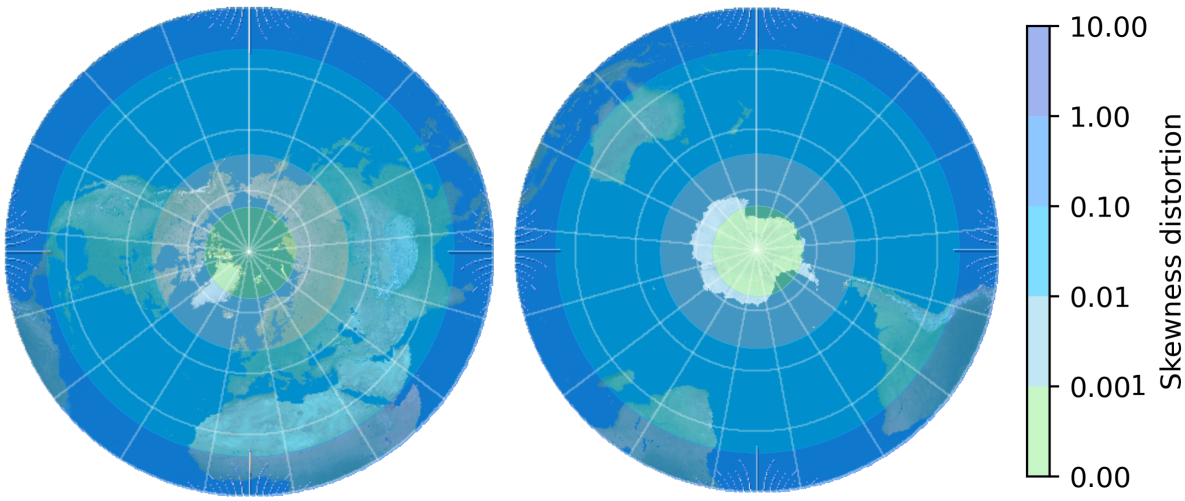

Figure 5.40: The contour plot of the local skewness distortion on the Azimuthal Equidistant split into two-hemispheres, with the North and South Pole in the centre. The local skewness distortion is zero close to the North and South Pole and it increases while going to the equator.

5.6. Results

An overview of the results for the six different distortions for the different maps determined in this chapter:

Map Projection	Area	Isotropy	Flexion	Skewness	Distance	Boundary cut
Mercator	0.84	0	0.64	0.64	0.44	0.25
Equirectangular	0.42	0.52	0.64	0.63	0.45	0.25
Winkel Tripel	0.26	0.5	0.70	0.44	0.37	0.25
Gott-Wagner	0.32	0.40	0.68	0.41	0.40	0.25
Azimuthal Equidistant	0.60	0.87	0.996	0.57	0.36	0
Azimuthal Equidistant split into two-hemispheres	0.13	0.24	0.46	0.06	0.062	0.5

Table 5.1: An overview of all the distortion values. The distance distortion of the Azimuthal Equidistant split into two-hemispheres could not be determined as the definition is not clear what to do with boundary cuts, therefore the distance distortion value is from the article by Gott and Goldberg (2007).

To determine the total distortion values, $\sum_\epsilon$, the method from Section 3.7 is used. In this method the distortions are normalised with respect to the distortions of the Equirectangular, with the following equation:

$$\sum_\epsilon = \left(\frac{A}{N_a}\right)^2 + \left(\frac{I}{N_i}\right)^2 + \left(\frac{F}{N_f}\right)^2 + \left(\frac{S}{N_s}\right)^2 + \left(\frac{D}{N_d}\right)^2 + \left(\frac{B}{N_b}\right)^2, \tag{5.6.1}$$

where $N_a = 0.42$, $N_i = 0.45$, $N_f = 0.64$, $N_s = 0.63$, $N_d = 0.45$ and $N_b = 0.25$. This gives the following normalised overview, with the total distortion value:

Map Projection	Area	Isotropy	Flexion	Skewness	Distance	Boundary cut	Total
Mercator	2.00	0	1.01	1.02	0.98	1	8.02
Equirectangular	1	1	1	1	1	1	6
Winkel Tripel	0.62	0.96	1.10	1.12	0.82	1	5.45
Gott-Wagner	0.76	0.77	0.91	0.92	0.89	1	4.65
Azimuthal Equidistant	1.42	1.67	1.57	1.59	0.80	0	10.46
Azimuthal Equidistant split into two-hemispheres	0.31	0.46	0.72	0.73	0.14	2	5.39

Table 5.2: An overview of the normalised distortion values, with the total distortion value. The distance distortion of the Azimuthal Equidistant split into two-hemispheres could not be determined as the definition is not clear what to do with boundary cuts, therefore the distance distortion value is from the article by Gott and Goldberg (2007).

6
Conclusion

In this thesis, the area, isotropy, flexion, and skewness distortions are defined and determined for multiple different map projections. These include the Mercator, Equirectangular, Winkel Tripel, Gott-Wagner, Azimuthal Equidistant and the Azimuthal Equidistant split into two-hemispheres. By applying these distortions identified by Gott and Goldberg, the projections were numerically determined and compared. The different map projections ranked by the final distortion value are:

1. Gott-Wagner (4.65)
2. Azimuthal Equidistant (5.39)
3. Winkel Tripel (5.45)
4. Equirectangular (6)
5. Mercator (8.02)
6. Azimuthal Equidistant (10.46)

The Gott-Wagner projection emerges as the best option based on the final distortion value. While having a general list of the best map projection is useful, it is also important to consider which distortions are most important to minimise for specific purposes.
Each type of distortion corresponds to a different optimal map projection for specific purposes. For instance, maps with minimal area distortion are mostly used for thematic maps showing distributions such as population, farmland and forested area. Therefore, the Azimuthal Equidistant projection with two hemispheres is the best choice out of the six for this purpose. Projections with a low isotropy are best for topographic maps, navigation charts and weather maps. The map projection with the lowest isotropy distortion is the Mercator. Meanwhile, the Azimuthal Equidistant split into two-hemispheres has the lowest flexion is therefore best suitable for navigation, surveying and planning. A map with low skewness maintains the length accuracy and they are best used for accurate estimation of travel distances and planning transportation routes. For these purposes, the Gott-Wagner is the most suitable with the lowest skewness.
To conclude, the Gott-Wagner projection strikes the best balance by minimising overall distortion, making it more suitable for general-purpose mapping. But selecting the best map projection depends on minimising the distorting specific to its needs, whether for navigation, thematic mapping, or precise measurements. Each distortion criterion leads to a different ideal projection, this leads to maps that are tailored for their intended use.

7

Discussion

In this thesis, we follow the distortions defined in the article by Gott and Goldberg from 2007. These distortions are intriguing but can be improved. The distortions can be categorised into pairs of two, that are of similar type.
The area and isotropy distortion are distortions that are used to determine the area and angular distortions, with some variation these are more known. The exact definition of the area and isotropy distortions are particularly useful, as they are invariant to the scale of the map and are constructed such that an error twice as large will result in the same distortion as an error half as large. It was shown that the area distorting is the standard deviation is of $\ln(ab)$, while the isotropy distortion is the root mean square of $\ln(\frac{a}{b})$. For isotropy distortion, the standard deviation is not necessary to have a distortion invariant to the scale. However, it might be beneficial to treat both distortions equally. When the isotropy distortion is given by the standard deviation of $\ln(\frac{a}{b})$, the sum of the squares of these distortions are as follows:

$$\begin{aligned}(\mathrm{SD}(\ln\frac{a}{b}))^2 + (\mathrm{SD}(\ln(ab))^2 &= \langle(\ln ab)^2 - \langle \ln ab\rangle^2\rangle + \langle(\ln\frac{a}{b})^2 - \langle\ln\frac{a}{b}\rangle^2\rangle \\ &= \langle(\ln a + \ln b)^2 - \langle\ln a + \ln b\rangle^2\rangle + \langle(\ln a - \ln b)^2 - \langle\ln a - \ln b\rangle^2\rangle \\ &= 2\langle(\ln a)^2 + (\ln b)^2 - \langle\ln a\rangle^2 - \langle\ln b\rangle^2\rangle \\ &= 2\langle(\ln a)^2\rangle + 2\langle(\ln b)^2\rangle - 2\langle\ln a\rangle^2 - 2\langle\ln b\rangle^2\rangle \\ &= 2(\mathrm{SD}(\ln a))^2 + 2(\mathrm{SD}(\ln b))^2.\end{aligned} \tag{7.0.1}$$

The flexion and skewness distortions are new introduced distortion by Gott and Goldberg, so there is not a lot of research on this beside this article. The idea is to examine how geodesics are deformed, adding an additional element to the calculation. These add an extra depth to the determination of the distortion of an map, that as said before has not been done before.
The distance distortion and the boundary cut distortion are both designed to penalise interruptions in the map, as multiple interruptions are generally detrimental for most purposes. The distance distortion measures the relationship between the path length on the globe in comparison with the path length on the map. The flaw with this distortion is that it is not clear about what happens when the points are close to a boundary cut and this definitions is not invariant to the scaling, at least not how defined in this thesis. However, when taking the standard deviation of the $\ln \frac{d_{ij,map}}{d_{ij,globe}}$ instead of the root mean square, the distortion would be defined by:

$$D = \sqrt{\left\langle\left(\ln\frac{d_{ij,map}}{d_{ij,globe}} - \left\langle\ln\frac{d_{ij,map}}{d_{ij,globe}}\right\rangle\right)^2\right\rangle} \tag{7.0.2}$$

Then scaling the map by scaling factor γ gives that the distance on the map is multiplied with γ. This results in the following for the definition of the distance distortion:

$$\begin{aligned}
\tilde{D} &= \sqrt{\left\langle \left(\ln \frac{\gamma d_{ij,map}}{d_{ij,globe}} - \left\langle \ln \frac{\gamma d_{ij,map}}{d_{ij,globe}} \right\rangle \right)^2 \right\rangle} \\
&= \sqrt{\left\langle \left(\ln\gamma + \ln \frac{d_{ij,map}}{d_{ij,globe}} - \left\langle \ln\gamma + \ln \frac{d_{ij,map}}{d_{ij,globe}} \right\rangle \right)^2 \right\rangle} \\
&= \sqrt{\left\langle \left(\ln\gamma + \ln \frac{d_{ij,map}}{d_{ij,globe}} - \left(\ln\gamma + \left\langle \ln \frac{d_{ij,map}}{d_{ij,globe}} \right\rangle \right) \right)^2 \right\rangle} \\
&= \sqrt{\left\langle \left(\ln \frac{d_{ij,map}}{d_{ij,globe}} - \left\langle \ln \frac{d_{ij,map}}{d_{ij,globe}} \right\rangle \right)^2 \right\rangle} = D
\end{aligned} \tag{7.0.3}$$

Therefore this definition of the distance distortion would be a better choice as it is invariant under scaling.
The boundary cut distortion is a great concept introduced in this article, where the length of the border on the globe is divided with 4π. The length of the border on the globe is difficult to determine precisely. It would beneficial to have a formula or clearer definition to determine this distortion, this is something to be looked at with further research.
Furthermore, the most troublesome aspect is the computation of the total distortion value. For this value, all distortion values are normalised in relation to the Equirectangular projection. This method is not the most elegant solution and there should be looked into other options. An idea to explore is the beneficial properties the different distortions have with each other as shown for A and I in equation 7.0.1.
The distortion values obtained closely match those reported in the article, with minor discrepancies possibly due to the computational method. The distortions are determined via numerical approximation using 30,000 randomly generated points on the globe, which is the same method as used in the article. Since random point are chosen to determine the distortions, the variations in these points could contribute to slight differences in results. As discussed in Chapter 4, increasing the number of points does not necessarily improve accuracy beyond a certain number of points, however there will still be some variability in the result. Chapter 3 demonstrates that while analytically computing distortions offers a promising alternative, it comes with complexity and computational challenges. In spite of that, it would be a great method that would definitely result in a more accurate solution and should be looked into further.
The list of projections discussed in this thesis is quite limited. Therefore, saying that the best map is the one following from this report is a bit simplistic. However, this list can be expanded to create a more comprehensive list. To compute the distortion values, the transformation formulas and the first and second derivatives need to be determined, as well as the boundary cut. By comparing it with more map projections, it can be concluded which map projection is the best map overall.

References

[1] R. Kunzig. "A Tale of two obsessed archeologists, one ancient city, and nagging doubts about whether science can ever hope to reveal the past". In: Discover Magazine (1999).

[2] Axis maps. Cartography guide - map projections. URL: https://www.axismaps.com/guide/map-projections (visited on 07/11/2024).

[3] M. Lampaine and E. Lynn Usery. Choosing a Map Projection. 8th ed. Cham, Switzerland: Springer International Publishing, 2017.

[4] C.F. Gauss and P. Pesic. General Investigations of Curved Surfaces. New York: Dover publications, 2005.

[5] R. N. Velotta. "Get a first look at MSG Sphere construction in Las Vegas". In: Las Vegas Review-Journal. (2019).

[6] R.N. Velotta. A big basketball and a mammoth moon: For Sphere, what's next? 2023. URL: https://www.reviewjournal.com/local/the-strip/a-big-basketball-and-a-mammoth-moon-for-sphere-whats-next-2874219/ (visited on 07/08/2020).

[7] A. Giardina and A. Weprin. The Las Vegas Sphere Is a "Mind-Boggling" Vision of the Future of Entertainment. 2023. URL: https://www.hollywoodreporter.com/business/business-news/las-vegas-sphere-design-technology-led-screens-1235594308/ (visited on 07/08/2020).

[8] GIS by ESRI. Understanding Map Projections. United States of America: Environmental Systems Research Institute, Inc, 1994.

[9] E. Ghaderpour. "Some Equal-area, Conformal and Conventional Map Projections: A Tutorial Review". In: Journal of Applied Geodesy 10.3 (Sept. 2016), pp. 197–209. ISSN: 1862-9016. DOI: 10.1515/jag-2015-0033. URL: http://dx.doi.org/10.1515/jag-2015-0033.

[10] V. Mittal. Geometric phase and its applications: topological phases, quantum walks and non-inertial quantum systems. 2022. arXiv: 2209.04810 [quant-ph].

[11] J.P. Snyder. Map Projections - A Working Manual. Washington: U.S. Geological Survey professional paper, 1926.

[12] Wikipedia. Indicatrix van Tissot. 2000. URL: https://nl.wikipedia.org/wiki/Indicatrix_van_Tissot (visited on 06/21/2024).

[13] E.W. Weisstein From Mathworld. Root-Mean-Square. URL: https://mathworld.wolfram.com/Root-Mean-Square.html (visited on 06/06/2024).

[14] D.M. Goldberg and J. Richard Gott III. Flexion and Skewness in Map Projections of the Earth. 2007. arXiv: astro-ph/0608501 [astro-ph].

[15] G. Grimmett and D. Welsh. Probability an introduction. 2th ed. Oxford University Press, 2014.

[16] P.A. Longley et al. Geographic Information Systems and Science. John Wiley Sons, 2005.

[17] C. Ipbüker and I.Ö. Bildirici. "A General Algorithm for the Inverse Transformation of Map Projections Using Jacobian Matrices". In: Proceedings of the Third International Symposium Mathematical Computational Applications 4.6 (2002), pp. 175–182.

[18] National Geographic Society. Selecting a Map Projection – National Geographic Education. URL: https://web.archive.org/web/20121201125546/http://education.nationalgeographic.com/education/media/selecting-map-projection/?ar_a=1 (visited on 05/28/2024).

[19] J. Richard Gott III, D.M. Goldberg, and R.J. Vanderbei. Flat Maps that improve on the Winkel Tripel. 2021. arXiv: 2102.08176 [astro-ph.IM].

[20] J.P Snyder and P.M. Voxland. An Album of Map Projections. Denver: Professional Paper 1453, 1989.